

Republic of Iraq

Ministry of Higher Education and

Scientific Research

University of Babylon

College of Science

Department of Physics



Investigating of Some Dye- Organic Structures for Solar Cells Application

**A Thesis Submitted to the College of Science, University of Babylon in
Partial Fulfillment of the Requirements for the Degree of Master of
Science in Physics**

by

Sadiq Abbas Subuh Fayhan Almurshidy

Supervised by

Dr. Nidhal M. AL-Shareefi

Assistant Professor

Dr. Mohsin K. Al-Khaykane

Assistant Professor

2023 A.D

1445 H.D

بِسْمِ اللَّهِ الرَّحْمَنِ الرَّحِيمِ
الْحَمْدُ لِلَّهِ رَبِّ الْعَالَمِينَ
الرحمن الرحيم
مالك يوم الدين
إياك نعبدُ وإياك نستعينُ
إهدنا الصراطَ المُستقيمَ
صراطَ الَّذِينَ أَنْعَمْتَ عَلَيْهِمْ غَيْرِ الْمَغْضُوبِ
عَلَيْهِمْ وَلَا الضَّالِّينَ
صَدَقَ اللَّهُ الْعَلِيُّ الْعَظِيمُ

(سورة الفاتحة)

Supervisors Certification

We certify that this thesis entitled (**Investigation of Some Organic Nanostructures for Solar Cell Application**) was prepared by (**Sadiq Abbas Subuh Fayhan**) under our supervision at the Department of Physics in the Collage of Sciences, University of Babylon, as a partial fulfillment of requirements for Master Degree of Sciences of Physics .

Signature:

Signature:

Supervisor: Dr. Nidhal M. Al-Shareefi

Supervisor: Dr. Mohsin K. Al-Khaykane

Title: Assistant Professor

Title: Assistant Professor

Address: Department of Physics-College
of Science-University of Babylon.

Address: Department of Physics-College
of Science-University of Babylon.

Data: //2023

Data: //2023

Certification of The Head of The Department

In view of the available recommendation , I forward this plan for debate by the examination committee .

Signature :

Name : Dr. Samira Adnan Mahdi

Title : Asst. Prof

Address : Head of The Department of Physics , College of Sciences, University of
Babylob

Date : / / 2023

Acknowledgments

Praise be to God alone, he fulfilled his promise, dearest his soldiers, defeated the parties alone, may Allah's blessings be upon the best of his creation, Muhammad and his pure family.

Many thanks and gratitude to my supervisors, Dr. Nidal Muhammad Obaid Al-Sharifi and D. Mohsin Kadhim Abed Al-Khaykane for their guidance and follow-up they gave me throughout the research period.

Many thanks and appreciation to the honorable head of the department of Physics for the guidance she provided. Many thanks and appreciation to all professors and staff in the department of Physics.

Many thanks and appreciation to all colleagues who helped me.

Many thanks and appreciation to the respected dean of the faculty of science and his respected assistants .

Sadiq- almurshidy

Dedication

I dedicate this simple effort to the soul of my father, may God have mercy on him, who wished me all the best. I dedicate it to my dear mother, who always urged me to study and strive. I dedicate it to my brothers and sisters for the support they gave me. I dedicate it to my dear wife and children.

Sadiq- almurshidy

Summary

The current study deals with the nanostructures of 24 chemical compounds that were proposed to use in photovoltaic applications. The work contains two parts based on the same working principle, the first part deals with 11 compounds based on the **anthracene** molecule, and the second part deals with the 13 compounds based on the **benzobisthiadiazole (BBT)** molecule, with subcompounds consisting of three compounds (one acceptor and two donor compounds) for the purpose of creating secondary energy levels between the occupied upper molecular orbital (**HOMO**) and the virtual molecular orbital (**LUMO**) levels of the two major compounds to facilitate electron transfer, through this work. The electronic and spectroscopic properties were examined and better results were obtained than some previous studies.

The compounds were built from scratch by using (**Gauss View 5.0.8**) software, then the (**Becke,3-Parameter, Lee-Yang- Parr**) (**B3LYP**) hybrid function from density functional theory (**DFT**) was applied together with the base functions (**6-31G**) in the Gaussian software package to study and analyze the properties of the ground state of the proposed compounds, also we calculated the lengths of bonds between the atoms and angles between the bonds were calculated, through these calculations it is possible to know the geometric shape of each compound .

The program (**Gauss Sum**) was used to study the properties of the excited state after using the time-dependent density functional theory (**TD-DFT**) and finding the absorption spectra of the compounds.

By using the (**DFT**) theory, the energy gap for each compound was calculated to find the energy difference between the (**LUMO**) level and the (**HOMO**) level. relatively small energy gaps were obtained consistent with the previous studies also, one of the important calculations that we got from studying the ground state of each compound is the calculation of the electronic affinity as well as the chemical hardness and softness, as well as the electrophilic index. All these parameters depend on the knowledge of (**HOMO**) and (**LUMO**).

The lowest energy gap is obtained in compounds 12 and 13, the two compounds depended on the benzobisthiadia (**BBT**) molecule, while the lowest energy gap for the anthracene-based compounds.

By using the time-dependent density functional theory (TD-DFT) and(Gauss Sum) program, the absorption spectra for each compound are studied and electronic transitions were identified, where each compound had direct and indirect transitions, and each transition occurred at a specific wavelength, and the knowledge of the wavelength at which had the electronic transition to calculate the electronic injection process for each compound, and the light harvesting for each compound was also calculated by studying the excited state of each compound.

List of Contents

Subject		PageNo.
Absract		I
List of contents		III
List of Figures		VII
List of Tables		VIII
List of Symbols and Abbreviations		IX
Chapter One		
Introduction and Literature Review		
Sections	Subject	Page No.
1.1	Introduction	1
1.2	Anthracen ($C_{14}H_{10}$)	3
1.3	Benzobisthiadiazole ($C_6H_2N_4S_2$) (BBT)	4
1.4	Solar Cell	4
1.5	Types of Solar Cells	5
1.5.1	Organic Solar Cells (OSCs)	6
1.6	Solar Cell Efficiency (η)	6
1.7	Previous Studies	7
1.8	Aims of The Study	10
Chapter Two		
Theoretical Background		
Sections	Subject	PageNo.
2.1	Introduction	11

Subject		PageNo.
2.2	Schrödinger Equation	11
2.3	Wave Function	13
2.4	Hartree - Fock (HF) Approximation	14
2.5	Density Functional Theory(DFT)	15
2.6	Time-Dependent Density Functional Theory (TD-DFT)	15
2.7	Exchange-Correlation Functional	17
2.7.1	The Local Spin Density Approximation LDA (LSDA)	17
2.7.2	The Generalized Gradient Approximation (GGA)	18
2.8	Kohn-Sham Equations	19
2.9	Hybrid Functional	20
2.10	Basis Sets	21
2.10.2	Split-Valence Basis Sets	23
2.11	Minimal Basis Sets and Split-Valence	22
2.12	Slater-type Orbitals (STO)	24
2.13	Gaussian-type Orbitals (GTO)	23
2.14	Polarization and Diffuse Functions	23
2.15	Computations Properties	24
2.15.1	Energy of HOMO, LUMO and Band Gap	24
2.15.2	Total Energy, Ionization Potential and Electron Affinity	25
2.15.3	Chemical Potential Chemical Hardness and Softness	26
2.15.4	Electrophilic Index and Electronegativity	27
2.15.5	Molecular Polarizability and Total Dipole Moment	28

Subject		PageNo.
2.16	Fermi Energy	28
2.17	Geometrical Structures Optimization	29
2.18	Open-Circuit Voltages	29
2.19	Electron Injection Process	30
2.20	Light Harvesting Efficiency (LHF)	31
2.21	Electronic Transitions	31
2.21.1	Infrared IR-Spectrum	32
2.21.2	UV- Visible Radiation	33
2.22	The Software	33
2.22.1	Gaussian 09 (G09) Program	33
2.22.2	Gauss View Program	34
2.22.3	Gauss Sum 3.0	34
2.22.4	Avogadro Software	35
Chapter Three		
Results and Discussion		
3.1	Introduction	35
3.2	Molecular Structure of the Proposed Compounds	38
3.3	Electronic Properties	49
3.3.1	Energy Gap	49

Subject		PageNo.
3.3.2	The HOMO and LUMO Levels	52
3.4	Some Electronic Variables	58
3.4.1	Ionization Energy and Electron Affinity	58
3.4.2	The Hardness and Softness	62
3.4.3	The light Harvesting Efficiency (LHE)	66
3.4.4	Electronegativity (En)	68
3.4.5	Open Circuit Voltage (Voc)	70
3.4.6	Electron Injection Process (DGinj)	71
3.4.7	Density of State	73
3.4.8	Ultraviolet and VisibleSpectrum (UV-Vis)	80
3.4.9	General Comparison	90
Chapter four		
Conclusions and Future Works		
4.1	Conclusions	93
4.2	The Future Works	95
	References	96

List of Figures

Figure No.	Subject	Page No.
1.1	Anthracene Molecule	3
1.2	Benzobizthiadiazol Molecule	4
2.1	The electronic Transitions of p, s, and n Electrons	35
3.1	Chemical Designs of the Proposed Compounds	35-33
3.2	WorkSteps Chart	36
3.3	The Nanostructure of Suggested Compounds	40-37
3.4	E_{gap} for the Compounds	49
3.5	The HOMO And LUMO Levels of Suggested Compounds	56
3.6	The HOMO and LUMO for the Compounds	57
3.7	The Diagram of Ionization Potential of the Compounds	60
3.8	The Diagram of Electric Affinity of the Compounds	61
3.9	The Diagram of IE and EA of Compounds	62
3.10	The Chemical Hardness and Softness for the Studied Compounds.	64
3.11	Electrophilic index of the Studied Compounds	66
3.12	Harvesting Efficiency (LHE) of the Studied Compounds	69
3.13	The diagram of Electronegativity of the Studied Compounds	71
3.14	The diagram of Electron Injection of the Compounds	75
3.15	Density of State Spectrum of The Suggested Compounds	76-82

Figure No.	Subject	Page No.
3.16	The UV-Vis. Spectrum of the Suggested Compounds	84- 89
3.17	Electronic Transitions- Wavelength Max (nm)	93

List of Tables

Table No.	Subject	Page No.
3.1	The geometrical parameters for each compound	42
3.2	The HOMO, LUMO, E_{gap} for the compounds	48
3.3	The Ionization Energy(IE) and Electron Affinity(E A) for the compounds	58
3.4	The Values of Chemical Hardness and Softness for the Studied Compounds	62
3.4	The Electrophilicity of the Compounds	65
3.5	Values of Light-Harvesting Efficiency (LHE) for the Studied Compounds	67
3.6	Values Electronegativity for the Studied Compounds	70
3.7	The Open Circuit Voltage Values for the Proposed Compounds	71
3.8	The Electron Injection Process (DG_{inj}) of Compounds	73
3.9	Wavelength and Osc. Strength and λ Max and Major and Contris of Compounds	90
3.10	General Comparison Between Properties of Compounds	94

List of Symbols and Abbreviations

<i>Symbol</i>	Description
E	Total Energy
BBT	Benzobisthiadiazole Compound
HOMO	Highest Occupied Molecular Orbital
LUMO	Lowest Unoccupied Molecular Orbitals
B3LYP	Hybrid Function (Becke, 3-Parameter, Lee-Yang- Parr)
DFT	Density Functional Theory
TD-DFT	Time Dependent Density Functional Theory
6-31G	Base Functions
eV	Electron-Volt ($1\text{eV} = 1.6023 \times 10^{-19} \text{ c}$)
nm	Nano Meter (10^{-9} m)
μm	Micrometer (10^{-6} m)
CYN	Cyanoacrylic acidCompound
(OSCs)	Organic Solar Cells
η	Solar Cell Efficiency
V_{max}	The Maximum Voltage Value
I_{max}	Maximum Value of the Current
P_{max}	Maximum Value for Power
P_{in}	Input Power
$\alpha(\text{E})$	Absorption Spectrum
(OPV)	Organic Photovoltaic
(PCEs)	Power Conversion Efficiencies
(DSSCs)	Dye-Sensitized Solar Cells
(ΔG_{inj})	Electron Injection

(LHE)	Light-Harvesting Efficiency
(IR)	Infrared
(UV)	Ultraviolet
(SE)	Semi-Empirical
E	Total Energy
KE	kinetic energy
PE	potential energy
Ze	Field of Charge
\hbar	Reduce Planck Constant ($h/2\pi$)
Ψ	Wave Function of an Electron
∇^2	The Laplacian Operator
\hat{H}	Hamiltonian Operator
M_A	Mass of Nucleus (A)
Z_A, Z_B	Charges on Nuclei A and B
r_{pd}	Distance Between p and d Electrons
R_{AB}	Distance Between Nuclei A and B
$[\Psi]^2$	Probability Density
Π	Multiplication
Σ	Sumation
ρ	Numerical Density
$\hat{V}_{ext.}$	External Potential Operator
$\hat{V}_{elec. elec.}$	Coulomb Operator
\hat{T}	kinetic Energy Operator
E_X^{B88}	Exchange Functional
STO's	Slater-type Orbitals

GTOs	Gaussian-type Orbitals
ξ	Orbital exponent
l, m	Orbital and Magnetic Quantum Numbers, Respectively
C_{ij}	Orbital Expansion Coefficients
ECPs	Effective-Core Potentials
KT	Koopmans Theorem
I_E	Ionization Energy
E_A	Electron Affinity
H	Hardness Chemical
S	Softness Chemical
ω	Electrophilic Index
E_N	Electronegativity
$\langle \alpha \rangle$	polarizability
E_F	Fermi Energy
Voc	Open-Circuit Voltages
f	Oscillation Strength Associated
Vis	Visible
DOS	Density of States
VSEPR	Valence Shell Electron Paire Repulsion Theory

Chapter one

**Introduction and
Literature Review**

Introduction and Literature Review

1. 1 Introduction

Energy is one of the biggest and most important problems faced by the inhabitants of the earth since the beginning of industrial development in the eighteenth century and to the present day, and fossil fuels have been the main source of energy, and it is known that fossil fuels are a stored form of solar energy that has been stored for millions of years and that it is about to run out due to the excessive use of the increased demand for energy.

The consumption of these sources has led to damage to the environment on the planet as a whole. Solar energy is the most important alternative source to fossil sources and as a result of continuous research and development, tangible and significant progress is currently taking place in the use of this energy, so it is expected that the sun's energy will be the main source of energy in the coming years[1].

After 1970, silicon solar cells were used to power small devices such as watches. Usually, amorphous silicon solar cells convert between (3-6)% of the energy of light reaching the ground into electricity (this percentage represents the conversion efficiency of the solar cells at that time). It is of low efficiency. Thin-film solar cells have been used as a new type of solar cell in order to improve efficiency, and the possibility of manufacturing it according to the required specifications, such as light weight, flexibility and other characteristics [2].

Clean energy production requires new methods and has a good future, as well as a new chemical composition that differs from the old formulas to manufacture more effective photoelectric conversion devices, collecting, converting and transporting energy into its various forms [3]. Many organic and inorganic semiconductors have been used to make solar cells. The selection was mostly based

on known materials as, till lately, experimental data was the main source for screening materials for solar cell [4].

Second generation solar cells include of thin films of materials like formless silicon, cadmium telluride and copper indium (gallium) diselenide[5]. A solar cell is a device that converts photons of specific wavelengths into electricity [6].

Research in this area has continued and technology has been developed to produce many types and structures of materials currently used in photovoltaics. technology. The first and second generation photovoltaics are mainly made of semiconductors including crystalline silicon, 8- compounds, cadmium telluride, and indium copper/sulfide.

Serious research in photovoltaic technology requires finding solutions that overcome the difficulties and make photovoltaic energy an economically viable alternative from a low-cost solution that provides high efficiency.

Some of the technological goals of current solar cell research and manufacturing are represented in the use of less semiconductor materials through the adoption of thin structures and the use of less expensive conductive materials and improve the performance of solar cells and increase the absorption of the solar spectrum and simplify processing and reduce the cost of manufacturing[7].

Despite the low efficiency of organic cells when compared with silicon photovoltaic cells, organic photovoltaic cells show great promise due to the low cost of solar energy, and there is still a lot of work aimed at improving its performance[5]. In our study, Two main molecules are adopted, namely the anthracene molecule and the benzobisthiadiazole (BBT) molecule.

1.2 Anthracene (C₁₄H₁₀)

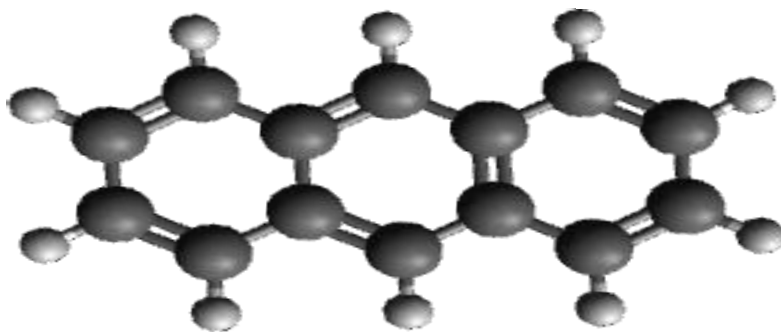


Figure (1.1): Anthracene molecule.

Figure (1.1) was designed by Avogadro program. As for anthracene, it was chosen because it has the following characteristics :Good light harvesting, good efficiency, improved electron injection, and from these characteristics it appears that anthracene represents a promising link in the applications of organic solar cells[6]. Anthracene is a solid hydrocarbon compound containing three rings of benzene. It is used in the production of red alizarin dyes. It is also used in the manufacturing of chemicals used in wood preservation, insecticides and packaging materials. Anthracene has no color, but it shows a blue color when exposed to ultraviolet light[7].

Two chemical compounds can be derived from anthracene, all of which are from the hydroxyl group, namely **1- hydroxy anthracene**, or what is also called anthrol or anthrasnol **2- second hydroxy anthracene**, and these derivatives are used in the production of some medicines. Anthracene is also used in the manufacturing of devices sensitive to alpha rays , photon and electron sensors. It is also used in the manufacturing of plastics. The highest reading of the emission spectrum of anthracene is between the two wavelengths of 400 and 440 nm [8].

1.3 Benzobisthiadiazole ($C_6H_4N_4S_2$) (BBT)

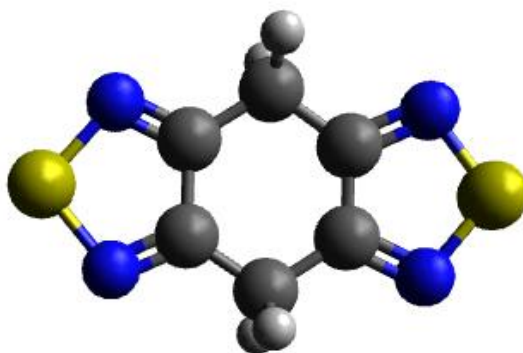


Figure (1.2) : Benzobisthiadiazole molecule.

The benzobisthiadiazole (BBT) group is a strong electron withdrawing group and a promising molecule, which is been widely applied in organic photovoltaics, nonlinear optics, organic field-effect transistors and organic light-emitting diodes, due to its charge carrier mobilities and low bandgap value. These materials are used as organic electrodes for supercapacitor application[9-12].

Also, the use of thiadiazole compounds in solar cells does not constitute a danger. When organic materials interact with sunlight or with other external factors, it leads to the generation of new compounds that may be toxic or cause some types of cancer, so from a chemical point of view the use of this substance is considered security [13].

1.4 Solar Cells

Solar cells are solid devices in which the sun's energy is converted into electrical energy, the base is a part made of p-type with a little boron added to it, less than 1 nm thick, and a highly doped n-type part silicon with a thickness of less than (1 μm) is created by doping with phosphorus at a much higher concentration [14],

The result of the high voltage of the p-n junction, electrons move to the n-type region and generate energy an electric similar to that generated by any electrochemical battery.

Depending on the principle of transformations, radiation interacts with the semiconductor, where an amount of energy can be absorbed that is greater than the

energy gap of the material that makes up the solar cell. An electron-hole pair is formed, then this pair is separated from the other, and an amount of energy is emitted that is approximately equal to the energy gap in the semiconductor that is formed. From the solar cell [15], The probability of the two processes occurring is equivalent.

The type of energy gap formed also has an impact on the efficiency of the solar cell, depending on the relative position of the upper part of the valence band and the lower part of the conduction band in the wave vector space [16].

There are two types of energy gaps in all semiconductors, they are either direct or indirect. For a direct gap semiconductor a photon elevates the energy level of an electron directly from the valence band to the conduction band, but for an indirect gap semiconductor there is no alignment between the top of the valence band and the bottom of the conduction band in the wave vector space, and excitation occurs as a result of the mediation of a photon, or in other words, a lattice vibration [17].

1.5 Types of Solar Cells.

The first generation of solar cells is produced on silicon wafers. It is the oldest and most popular technology due to its high energy efficiencies. Silicon wafer-based technology is categorized into two subgroups named Monocrystalline / Monocrystalline Silicon Solar Cell • Poly / Polycrystalline Silicon Solar Cell.

Most of the thin film solar cells are second generation solar cells, and are more economical as compared to the first generation silicon wafer solar cells. Silicon-wafer cells have light absorbing layers up to 350 μm thick, while thin-film solar cells have a very thin light absorbing layers, generally of the order of 1 μm thickness .

Third generation cells are the new promising technologies but are not commercially investigated in details. Most of the developed 3rd generation solar cell types are [18]:

- 1) Nano crystal based solar cells.
- 2) Polymer based solar cells.
- 3) Dye sensitized solar cells.
- 4) Concentrated solar cells.

1.5.1 Organic Solar Cells(OSCs)

Interest in organic solar cells stems of ease of processing. This is because, many organic solar cell devices have used polymers as an essential part of their construction. For example, conjugated polymers often contribute as electron donors and hole conductors in the active layer of organic solar cells. Since the science of polymer processing is well developed, it is hoped that conventional processing steps will be used one day. That such flexible cells can be used in countless ways, from portable electronics to commercial power production [19].

1.6 Solar Cell Efficiency (η)

It is the ratio between the output power to the input power, It is directly proportional to the output power and inversely proportional to the input [20].

The photovoltaic cells (PV) power conversion efficiency, η , can be given by :

$$\eta = \frac{V_{max}I_{max}}{P_{in}} = \frac{P_{max}}{P_{in}} = \frac{V_{oc} J_{sc} FF}{P_{in}} \dots\dots\dots(1.1)[21].$$

where P_{max} is maximum power

P_{in} is input power, $P= VI$, V_{oc} is Open -circuit voltage, FF is Fill factor, J_{sc} is Short -circuit current density

Solar cell efficiency is the most common parameter that is used to compare the performance of solar cells. Therefore, the improvement ratio of the solar cell efficiency is given by the equation [21].

$$\Delta\eta = \frac{(\eta\%)_{LSC} - (\eta\%)_{bare}}{(\eta\%)_{bare}} \times 100\% \dots\dots\dots (1.2)$$

Where $(\eta\%)_{LSC}$ is the conversion efficiency when pure solar concentrator on the solar cell and $(\eta\%)_{bare}$ is the bare solar cell efficiency [22].

1.7 Previous Studies

Christian B.Nielsen et al. in (2015)[23]. The properties of the active layer have been studied in the organic photovoltaic device based on a donor semiconductor that absorbs the energy of the sun, and work has been done to modify the absorption properties of the donor materials, in this study, the fullerene acceptors were replaced due to the lack of flexibility in the structure, and this causes difficulty in changing the energy levels, as well as the lack of absorption ranges in the solar spectrum range, Perylene acceptors have been used as aromatic compounds. The issue of avoiding the crystallization of these materials was also studied in order to obtain a homogeneous composition.

Zhao J.Li et al . in (2016)[24]. Researching the solvent halogenation process used to process organic solar cells, a hydrocarbon-based processing system was introduced that is not only more environmentally friendly, but produces cells with energy conversion efficiencies of up to 11.7%. The synergistic effects of hydrocarbon solvent, other substances, a particular side chain of the polymer, and temperature are addressed.certified assembly of the donor polymer. It provided scientific insights that would facilitate further improvement in the performance of organic solar cells.

Wenchao Zhao et al. in (2017)[25]. They studied the donor (PBDB-T-SF) and acceptor (IT-4F) were constructed in non-fullerene organic photovoltaics (OSCs) applications. The effect of fluorescence on absorption bands and other electronic properties of the PBDB-T-donor and acceptor was studied.SF:IT-4F based OSC showed a good cell efficiency of about 13.1%, and more than 12% efficiency can be obtained with a thickness of 100-200 nm.

Hyojung Cha et al. in (2018) [26]. A comparison of the efficiency, stability, and photophysics of organic solar cells that use some material blended with either an acceptor or a fullerene derivative,phenyl C71 acid methyl ester (PC71BM) as an electron acceptor. The mixture of solar cells fabricated without any additive processing achieved power conversion efficiencies (PCEs) of $9.5 \pm 0.2\%$. The

devices display a high open circuit voltage of 1.08 ± 0.01 V, attributed to the lowest unoccupied molecular orbital (LUMO) level of the EH-IDTBR. Photocurrent quenching and transient absorption data are used to elucidate ultrafast kinetics and charge separation efficiencies in both mixtures, with PffBT4T-2OD exciton diffusion kinetics within polymer domains, PC71BM solar cells exhibit significant efficiency loss under simulated solar irradiation.

AL-saadiy Enam A. S. in (2018) [2]. studied some suggested compounds based on anthracene molecule for photovoltaic applications as dyes sensitized solar cells. The studied compounds showed delocalization of LUMO and localization of HOMO, they both changed significantly to suggest different structures play important roles in electronic properties. On the other hand, the LUMO energy levels of the compounds as dyes are higher than that of TiO_2 and PCBM conduction, both HOMO and LUMO levels of the studied compounds agree well with the requirement for an efficient photosensitizer, the electron injection from the compounds to the conduction band of TiO_2 and PCBM, and the subsequent regeneration are possible in organic sensitized solar cell.

Tomas Delgado et alin (2020) [27]. Eight novel metal-free organic sensitizers are proposed for dye-sensitized solar cells (DSSCs), theoretically calculated and studied via density functional theory with D- π -A structure. These proposals were formed to study the effect of novel π -bridges, using carbazole as the donor group and cyanoacrylic acid as the anchorage group. Free energy of electron injection (ΔG_{inj}) and light-harvesting efficiency (LHE) also were calculated and discussed. On the other hand, absorption wavelengths, oscillator strengths, and electron transitions were calculated through time-dependent density functional theory with the M06-2X/6-31G(d) level of theory.

Aryaman Bhatnagar et al in (2021) [28]. The study mainly focuses on the thermal properties of various phase change materials, air-water complex and their composition. The photovoltaic module is often used in a variety of ways to achieve better efficiency.

The use of the latest technologies such as nanofluids as well as the performance of phase change materials has been optimized in the system.

The conclusion of the study deals with a concentration of 0.3vol.% of nanofluid, increasing the thermal efficiency of PV/T hybrid solar collectors, flat plate, and evacuated tubes by up to 96.3%, 95.13%, and 93.42%, respectively which depend on the mass flow rate and temperature change. Practically can achieve thermal efficiency (th) = 56.19% and electrical efficiency (ele) = 13.75% after hybridization.

Tingxuan Wang et al in (2021) [29]. Three novel carbazole sensitizing dyes are synthesized with fluorenone as the auxiliary acceptor, benzene, furan and thiophene as π bridge and cyanoacrylic acid as the anchoring acceptor. Compared with the similar D- π -A carbazole dye, the incorporation of fluorenone improved markedly the molar extinction coefficients of carbazole dyes, which increased the short-circuit current density and accordingly the photoelectric conversion efficiency. The presence of thiophene or furan bridge favors the short-circuit current density while the introduction of benzene bridge benefits the open-circuit voltage. Among three carbazole dyes, dye with benzene bridge exhibited the optimal efficiency 4.88% due to its highest open-circuit voltage and factor fill (VOC = 690 mV, JSC = 8.30 mA/cm², and FF = 0.86).

Noor Abdul Ameer H.in (2022) [30]. In this study, the possibility of using azo dye nanostructures dotted with (S, Ti, Si, Ni, Cu, Al, Zn) atoms as a sensor for dye solar cells was investigated. The possibility of sensitizing the nanostructures of dye-sensitized solar cells (DSSCs) was studied by using the occupied upper molecular orbital (HOMO) and the virtual molecular orbital (LUMO) of the nanostructures relative to the energy of a special electrolyte solution and the lower energy band of the (TiO₂) electrodes, respectively, as well as the local distribution of charges in addition to the energy gap.

Rui Sun et al. in (2023)[31]. As it is known that polymer blend systems are not comparable to their counterparts based on small molecule acceptors in conversion efficiencies (PCEs), but the triple combination method gives an easy way to provide a

good mixture. Conversion to 18.2%, and this is the best conversion rate that has been reached at the present time. This work has a good future in raising the efficiency of polymeric systems by the new design by mixing three polymeric compounds together.

1.8 Aims of the Study

The aims of this study are as follows:

- 1- Building new organic nanostructures for solar cell applications and studying their photovoltaic properties and electronic transitions.
- 2- The study aims to choose low-cost and high-quality materials in the production of electrical energy from sunlight.

Chapter Two

Theoretical

Part

Theoretical Part

2.1 Introduction

Quantum theory is the theoretical basis of modern physics that explains the nature and behavior of matter and energy on the atomic and subatomic level. The nature and behavior of matter and energy at that level is sometimes referred to as quantum physics and quantum mechanics.

Organizations in several countries have devoted significant resources to the development of quantum computing, which uses quantum theory to drastically improve computing capabilities beyond what is possible using today's classical computers which are called molecular modeling methods[34], so molecular modeling methods in physics and theoretical chemistry are widespread for examining many computational properties such as energies of molecules, molecular geometry, electronic structure, electron and charge distribution, infrared (IR), ultraviolet (UV), and nuclear magnetic resonance (NMR) spectra, physical properties, catalytic drugs, and other molecular systems. Theoretical physicists and chemists use four main methods in their calculations: molecular mechanics methods, semi-empirical (SE) methods, ab-initio methods and density functional theory methods[33].

Perhaps the best of these methods is the density functional theory test (DFT) [30], because of the success of DFT test in atomic and molecular physics issues and solid state calculations, this method has proven successful even in nuclear calculations, so it is a method approved by many physicists [32].

2.2 Schrodinger Equation

Schrodinger's immediate focus when developing his equation to treat the hydrogen atom, and the solution reached in 1926 convinced him. The creation of a wave equation that may describe stealthy, wave-like behavior of the first step is to create a quantum particle. In developing a theoretically consistent theory of nonrelativistic quantum mechanics. Schrodinger equation is the name for this equation. In quantum physics, Schrodinger equation has a similar role to in classical

mechanics Schrodinger equation is a partial differential equation that describes how a quantum particle's wave function ebbs and flows. Newton's second law is a differential equation that outlines how a classical particle moves. In addition, both Newton laws and Schrödinger equation were suggested and then evaluated for time-independent systems, where total energy(E) is equal to the sum of total kinetic and potential energy[35].

$$E = KE + PE \quad \dots\dots\dots(2.1)$$

where (KE) is kinetic energy, and PE is potential energy.

kinetic energy of the electron can be calculated through the following equation [36] .

$$KE = \frac{\hat{p}^2}{2m} = -\frac{\hbar^2}{2m} \nabla^2 \dots\dots\dots(2.2)$$

where m is the mass of the particle, and p denotes the momentum of the particle. An electron moving in a field of charge Ze has a potential energy of [39].

$$PE = -\frac{Ze^2}{r} \dots\dots\dots(2.3)$$

where r is the distance between the electron and the nucleus and e is the unit of electronic charge. As a result, the total energy of an electron is :

$$E = -\frac{\hbar^2}{2m} \nabla^2 - \frac{Ze^2}{r} \dots\dots\dots(2.4)$$

a kinetic energy contribution and a potential energy function added together [37] .

$$\left\{ -\frac{\hbar^2}{2m} \nabla^2 - \frac{Ze^2}{r} \right\} \psi(r) = E \psi(r) \quad \dots\dots\dots(2.5)$$

Where:

\hbar : Reduce Plank constant (h) divided by 2π . and Ψ : wave function of an electron.

∇^2 :The Laplacian operator is a kind of operator (kinetic energy operator).

Eq.(2.6)denotes the Hamiltonian operator, denoted by the symbol \hat{H} . Where Schrodinger equation was written in terms of the Hamiltonian operator as[39].

$$\hat{H}\Psi(r)=E\Psi(r)\dots\dots\dots(2.6)$$

The Hamiltonian operator with a large number of electron can be expressed in a similar way. It is the sum of the kinetic energy operators of the nucleus and electrons, as well as the potential energy operator denoted by the many Coulomb interactions by the following equation[39].

$$H^T = -\frac{1}{2} \sum_A^N \frac{1}{M_A} \nabla_A^2 - \frac{1}{2} \sum_p^{2n} \nabla_p^2 + \sum_{p<d}^{2n} r_{pd}^{-1} - \sum_A^N \sum_p^{2n} Z_A r_{Ap}^{-1} + \sum_{A<B}^N Z_A Z_B R_{AB}^{-1} \dots\dots\dots(2.7)$$

Where M_A is the mass of nucleus A , m electron mass, Z_A, Z_B are the charges on nuclei A and B, respectively, r_{pd} is the distance between p and d electrons, and R_{AB} is the distance between nuclei A and B. The general form of Schrödinger equation will be[40].

$$H^T(1,2,\dots,N,1,2,\dots,n) \Psi(1,2,\dots,N,1,2,\dots,n)=E\Psi(1,2,\dots,N,1,2,\dots,n) \dots\dots\dots(2.8)$$

Where $\Psi(1,2,\dots,N,1,2,\dots,n)$ is the entire wave function for all particles in the molecule and is the overall energy of the system.

2.3 Wave Function

The wave function Ψ cannot be seen physically, but it can be explained physically, as the square of the wave function $[\Psi]^2$ represents the probability density of the particle being studied within the coordinates of the site. Acceptable wave functions for a system must be

1. Orthogonal one to another.
2. Normalized.
3. Form a complete set.

Orthonormality refers to the characteristic that wave functions have:

$$\int \Psi_i^* \Psi_j dx_N = \langle \Psi_i | \Psi_j \rangle = \delta_{ij} \equiv \begin{cases} 1, & \text{if } i = j \\ 0, & \text{if } i \neq j \end{cases} \dots\dots\dots(2.9)$$

Completeness refers to the ability to create the "delta function," which is the sharpest possible function of the unit area, from the whole set of eigen functions. The energy of a wave function can be calculated using the Hamiltonian operator's predicted value [41,42].

$$E = \langle \hat{H} \rangle = \frac{\int \Psi^* \hat{H} \Psi \, d\mathbf{v}}{\int \Psi^* \Psi \, d\mathbf{v}} \dots\dots\dots(2.10)$$

The wave function Ψ describes the many-particle systems.

2.4 Hartree - Fock (HF) Approximation

When applying the Pauli exclusion principle in solving the Schrödinger equation for many-electron atoms, molecules, or solids, the wave function becomes asymmetric. The physicist Hartree was the first to derive the many-electron Schrödinger equations, and the entire wave function, according to Hartree, can be approximated as a series of one-electron wave functions[43].

$$\Psi_{tot} = \prod_{i=1}^n \Psi_i(x) \dots\dots\dots(2.11)$$

When Hartree solved the non-time dependent Schrödinger equation, he did not take into account the Pauli exclusion principle so Fock and Slater updated this method to include the effect of electron exchange and the exclusion principle; So he used Slater's determinant, and the wave function resulted, including systems consisting of n electrons, as shown below [44].

$$\Psi(1,2, \dots, n) = \frac{1}{\sqrt{n!}} \begin{vmatrix} \Psi_1(x_1) & \Psi_2(x_1) & \dots & \Psi_n(x_1) \\ \Psi_1(x_2) & \Psi_2(x_2) & \dots & \Psi_n(x_2) \\ \vdots & \vdots & \ddots & \vdots \\ \Psi_1(x_n) & \Psi_2(x_n) & \dots & \Psi_n(x_n) \end{vmatrix} \dots\dots\dots(2.12)$$

Hartree-Fock equations, are a type of self-consistent field equation. These equations are formatted as follows:

$$[H^{core} + \sum_j (2J_j - K_j)]\Psi_i = \sum_j \varepsilon_{ij} \Psi_j \quad i = 1, \dots, n \dots\dots\dots(2.13)$$

$$F\Psi = \sum_j \varepsilon_{ij} \Psi_j \quad i = 1, \dots, n \dots\dots\dots(2.14)$$

Empirical wave functions are used to interchange potential integrals and differential equations and to solve the N Hartree-Fock equations. Solving the n equations results in a new set of wave functions. Then, the new wave functions are used to calculate a new set of possible integrals. The cyclic approach is repeated for the estimated wave functions or potential integrals to remain unchanged, because the final wave functions produce potential integrals, which in turn produce identical wave functions within a given admission, this approach is known as the self-consistent field method [45,46].

2.5 Density Functional Theory(DFT)

The quantum mechanical method of density functional theory (DFT) is frequently used to study the electronic structure of many-electron systems in physics and chemistry. It is presently one of the most important techniques for determining the ground state properties of metals, semiconductors, and insulators [47].

Thomas Fermi's model provided the basis for density theory. In 1927, Thomas and Fermi described the energy of an atom as a function of electron density, integrating that with standard equations, nuclear, electron, and electron–electron interactions can be expressed in terms of electron density [48]. The system is only affected by three coordinates, regardless of the number of electrons in it [47].

$$N = \int \rho(\vec{r})d\vec{r}.....(2.15)$$

where ρ is numerical density

The ground state energy can be calculated by DFT, the ground state properties depend on the electron density. The electronic density corresponds to the fine ground conditions of the system when the total energy is low [49, 50].

2.6 Time-Dependent Density Functional Theory (TD-DFT)

The time-dependent density functional theory (TD-DFT) spreads the important idea of the ground-state DFT which can be used to examine the excited-state properties of a system in the presence of time-dependent potentials, such as electric or magnetic fields. The influence of fields on molecules can be studied with TD-DFT as an application for representative excitation energies, oscillator strength,

wavelength, molecular orbital character and electronic transitions of the molecules[51-52].

The theoretical of TD-DFT based on the Runge-Gross theorem (R-G theorem) in 1984. The R-G theorem explained the association between the time-dependent external potential $\widehat{V}_{\text{ext.}}(\vec{r}, t)$ and $\rho(\vec{r}, t)$ of the system. R-G theorem designated that when two external potentials $\widehat{V}_{\text{ext.}}(\vec{r}, t)$ and $\widehat{V}'_{\text{ext.}}(\vec{r}, t)$ have an alteration of more than a time-dependent function, their own electron densities $\rho(\vec{r}, t)$ and $\rho'(\vec{r}, t)$ are also dissimilar[53-54].

Runge and Gross discussed how excited states are obtained using TD-DFT. The starting point of studying time-dependent systems is the time-dependent Schrodinger equation. The TD-DFT is straight related to the Schrodinger equation $[i\hbar \frac{\partial}{\partial t} \Psi(\vec{r}, t) = \widehat{H}\Psi(\vec{r}, t)]$ where the Hamiltonian is known to be[56-58]:

$$\widehat{H} = \widehat{T} + \widehat{V}_{\text{elec. elec.}} + \widehat{V}_{\text{ext.}}(\vec{r}, t) \dots \dots \dots (2.16)$$

where, \widehat{H} consists of the kinetic energy operator \widehat{T} , electron-electron repulsion $\widehat{V}_{\text{elec. elec.}}$ (Coulomb operator) and the external potential $\widehat{V}_{\text{ext.}}(\vec{r})$. Where $\widehat{V}_{\text{ext.}}(\vec{r})$ is given in the following operators:

$$\widehat{V}_{\text{ext.}}(\vec{r}) = \sum_{i=1}^N V_{\text{ext.}}(\vec{r}_i, t) \dots \dots \dots (2.17)$$

The densities of the system rise from a fixed first state $\Psi(t_0) = \Psi(0)$. The first state, $\Psi(0)$, is arbitrary, it must not be the ground-state or some other eigen state of the first potential $\widehat{V}_{\text{ext.}}(\vec{r}, t_0) = \widehat{V}_0(\vec{r})$. R-G theorem indicates that there exists an one-to-one correspondence between the time-dependent external potential $\widehat{V}_{\text{ext.}}(\vec{r}, t)$, and the time-dependent electron density $\rho(\vec{r}, t)$, for systems developing from a fixed first many-body state. Translation to it, the density determines the external potential, and next helps in obtaining the time-dependent many-body wave functions[54,55].

As this wave-function controls all observables of the system an important, the saying point is that all observables are functional of $\rho(\vec{r}, t)$. the statement of the theorem is the densities $\rho(\vec{r}, t)$ and $\rho'(\vec{r}, t)$ evolving from the same initial state $\Psi(0)$ under the effect of two potentials $\widehat{V}_{\text{ext.}}(\vec{r}, t)$ and $\widehat{V}'_{\text{ext.}}(\vec{r}, t)$ are always different provided that the potentials differ by additional than a chastely time-dependent function[55,56,58]:

$$\widehat{V}_{\text{ext.}}(\vec{r}, t) = \widehat{V}'_{\text{ext.}}(\vec{r}, t) + C(t) \dots \dots \dots (2.18)$$

Where the $C(t)$ allows increase to wave functions that are different only by a phase factor $\exp(-iC(t))$, therefore, the same electronic density is stable. R-G theorem states that the density is a functional of the external potential and of the first wave function on the space of potentials differing by more than the addition of $C(t)$.

2.7 Exchange-Correlation Functional

In modern exchange–correlation functional, the electronic energy per unit volume may depend on several properties or functional of the electron density, both local (for example, spin densities, their gradients, and local spin kinetic energy densities) and nonlocal (such as Hartree–Fock exchange).

2.7.1 The Local Spin Density Approximation (LSDA)

The local spin density approximation (LSDA) is a class of the methods to approximate the $E_{\text{XC}}[\rho(\vec{r})]$ in DFT found by Kohn and Sham in 1962[44]. This functional assumes that the system is a homogenous electron gas and $E_{\text{XC}}[\rho(\vec{r})]$ relied only on the local value of electron density $\rho(\vec{r})$. In general, according to LDA approximation the $E_{\text{XC}}[\rho(\vec{r})]$ is presented as in the following equation[45,46]:

$$E_{\text{XC}}^{\text{LDA}}[\rho] = \int \rho(\vec{r}) \varepsilon_{\text{XC}}(\rho(\vec{r})) d\vec{r} \dots \dots \dots (2.19)$$

Where $\varepsilon_{\text{XC}}(\rho(\vec{r}))$ denotes the exchange-correlation energy per particle of an electron gas, it agrees to the electron gas, which is considered to be locally uniform in the

LDA. Also $\epsilon_{XC}(\rho(\vec{r}))$ is diverged into exchange and correlation parts, [$\epsilon_{XC}(\rho(\vec{r})) = \epsilon_X(\rho(\vec{r})) + \epsilon_C(\rho(\vec{r}))$].

The LSDA refers to the exchange correlation energy in terms of the density of α and β spins and was developed for computing the properties of open-shell systems. LSDA is a straightforward generalization of the LDA to include electron spin as in the following equation[47]:

$$E_{XC}^{LSDA} [\rho_\alpha, \rho_\beta] = \int \rho(\vec{r}) \epsilon_{XC}(\rho(\vec{r})_\alpha, \rho(\vec{r})_\beta) d\vec{r} \dots \dots \dots (2.20)$$

Where $\epsilon_{XC}(\rho(\vec{r})_\alpha, \rho(\vec{r})_\beta)$ represented the exchange-correlation energy per particle of an electron gas with uniform spin densities ($\rho(\vec{r})_\alpha, \rho(\vec{r})_\beta$). The LSDA cannot determine the highly precise energy data as required by many computational chemists, but it provides better results than HF method for certain properties such as equilibrium structures, energy, vibrational frequencies and dipole moments. In general, the LSDA provides reliable information for the systems that closely resemble a uniform electron gas, in which the density varies slowly with position. However, atomic and molecular systems do not possess uniform electron densities and thus more sophisticated models are required [48].

2.7.2 The Generalized Gradient Approximation (GGA)

For suggesting a more precise approximation of the exchange-correlation energy, functional which include not only the electron density, but also the gradient of the electron density, because the electron density in a real molecule changes greatly from place to place. These growths are mentioned to as generalized gradient approximations (GGA). Where in GGA the exchange-correlation energy E_{XC}^{GGA} is an integral over functional depending on both density and its derivatives[48]:

$$E_{XC}^{GGA} [\rho_\alpha(\vec{r}), \rho_\beta(\vec{r})] = \int f(\rho_\alpha(\vec{r}), \rho_\beta(\vec{r}), \nabla\rho_\alpha(\vec{r}), \nabla\rho_\beta(\vec{r})) d\vec{r} \dots (2.21)$$

Generally, GGA is an improvement over the LSDA since it accounts for the variation of density with position. To simplify the problem, E_{XC} is separated into the exchange E_X and correlation E_C parts as in the form [48]:

$$E_{XC}[\rho_\alpha(\vec{r}), \rho_\beta(\vec{r})] = E_X[\rho_\alpha(\vec{r}), \rho_\beta(\vec{r})] + E_C[\rho_\alpha(\vec{r}), \rho_\beta(\vec{r})] \dots \quad (2.22)$$

The exchange-energy functional can then be obtained from the HF exchange term with the KS orbitals in place of the HF orbitals and approximate solutions for E_C are sought. Various exchange and correlation functionals have been developed independently and can be combined in different ways. For instance, one popular GGA functional is BLYP, where Becke's 1988 exchange functional is paired with the Lee-Yang-Parr correlation functional [44].

2.8 Kohn-Sham Equations

Theorems of Hohenberg and Kohn-Sham (HK) allow FHK to be written in a variety of ways [45]:

$$F[n] = T_S[n] + J[n] + E_{xc}[n] \dots \dots \dots \quad (2.23)$$

Where $F[n]$ is a universal functional of the density. $T_S[n]$ is the kinetic energy of a non-interacting electronic system. The (non-classical) exchange binding energy $E_{xc}[n]$ of the interacting electron system can be defined in the model [48]:

$$E_{xc}[n] = T[n] - T_S[n] + E_{xc}[n] \dots \dots \dots \quad (2.24)$$

Where $E_{xc}[n]$: the DFT exchange-correlation energy. By applying the variation principle, $\partial E / \partial n(r) = 0$, to the Kohn-Sham functional [49]:

$$E[n] = \int n V_\omega dr + T_S[n] + J[n] + E_{xc}[n] \dots \dots \dots \quad (2.25)$$

The density $n(r)$ is given by [49]:

$$n(r) = \sum_{i=1}^n |\Psi_i(r)|^2 \dots \dots \dots \quad (2.26)$$

This leads to the Hartree-type of one–electron equations [50]:

$$\left[-\frac{1}{2}\nabla^2 + V(r) + \int \frac{n(\mathbf{r}')}{|\mathbf{r}-\mathbf{r}'|}d\mathbf{r}' + V_{xc}(\mathbf{r})\right]\Psi_i(\mathbf{r}) = \varepsilon_i \Psi_i(\mathbf{r}) \dots\dots\dots (2.27)$$

Where ε_i Kohn–Sham orbital energies, $\Psi_i(\mathbf{r})$ is Kohn–Sham orbitals, and $V_{xc}(\mathbf{r})$ is the exchange-correlation potential [50]:

$$V_{xc}(\mathbf{r}) = \frac{\delta E_{xc}[n]}{\delta n} \dots\dots\dots (2.28)$$

Eqs. (2.20)–(2.22) are Kohn-Sham equations, are technically precise and only have one unknown term, $E_{xc}[n]$ [50].

The basic goal of DFT is to discover the exchange-correlation energy E_{xc} , which has only been utilized as a mathematical word thus far. If the precise exchange-correlation function is known, the system can be solved appropriately. As previously stated, this function is generated from the difference in Hamiltonians between interacting many-electron systems and non-interacting single electron systems. As a result, this phrase encompasses all consequences of exchange and correlation interactions, such as Pauli exclusion between electrons with the same spin orientation and the instantaneous response of electrons with opposite spins,

Kohn –Sham equations are said to have a circular aspect to them. To solve Kohn–Sham equations, Hartree potential must be determined, and the electron density must be known to define Hartree potential. However, single-electron wave functions must be differentiated in order to calculate the electronic density, and the Kohn–Sham equations must be solved to determine these wave functions[51].

2.9 Hybrid Functional

The hybrid exchange-correlation functional occupy a priv atesite in the molecular applications of the DFT and nowadays it is very popular used in computational physics and chemistry[58,59]. These functionals combine the

exchange-correlation GGA functional and an exact exchange functional. The most widely hybrid functional, B3LYP uses Becke's 1988 exchange functional (E_X^{B88}) and Lee-Yang-Parr correlation functional (E_C^{LYP}) as gradient corrections to the LSDA exchange and correlation functionals. The exchange-correlation term of B3LYP is shown as in the following form[59-60]:

$$E_{XC}^{B3LYP} = (1 - a)E_X^{LSDA} + aE_{XC}^{HF} + bE_X^{B88} + cE_C^{LYP} + (1 - c)E_C^{LSDA} \dots \dots (2.29)$$

Where the three parameters ($a=0.20$, $b=0.72$ and $c=0.81$), these values were found by fitting the experimental data. The first parameter (a) specified the amount of exact exchange, while (b) and (c) control the contribution of exchange and correlation.

2.10 Basis Sets

A basis set is a set of functions that are used to represent the electron wave function in the Hartree-Fock method or density functional theory in order to transform the partial differential equations of the model into algebraic equations suitable for efficient implementation on a computer, a basis set consists of a collection of functions used to explain the orbital structure of an atom. Linear combinations of base functions and angular functions are used to build molecule orbitals and full wave functions.

A collection of bases must be described after initio or density functional theory computations. Although a set of basis can be developed from scratch, the vast majority of calculations are performed with pre-existing basis sets. The type of computation used and the basis selected are the two most important aspects in determining the correctness of the results[63]. Slater type orbitals(STO) are exponential that mimic the exact eigen functions of the hydrogen atom. A typical STO is expressed as[62,63]:

$$\chi^{STO} = N r^{n-1} e^{-\xi r} Y_{lm}(\theta, \varphi) \dots \dots \dots (2.30)$$

Where N is a constant of normalization, n represents a principal quantum number, ξ is a constant related to the effective charge of the nucleus, \vec{r} denotes the distance of the electron from the nucleus, $Y_{lm}(\theta, \varphi)$ denotes a spherical harmonic and l, m are the orbital and magnetic quantum numbers, respectively.

2.13 Gaussian-type Orbitals (GTO)

The use of GTOs in electronic structure was first proposed by Boys in 1950. The GTOs can be written in terms of Cartesian coordinates as in the following form[2,67,61,64]:

$$\chi^{\text{GTO}} = N x^{l_x} y^{l_y} z^{l_z} e^{-\xi r^2} \dots \dots \dots (2.33)$$

Here; ξ denotes the orbital exponent that explained how compact (**large ξ**) or diffuse (**small ξ**) is the resulting function. The r^2 dependence in the exponential is a deficiency of the **GTOs** with respect to the **STOs**. The sum of angular momentum l_x, l_y and l_z determines the type of orbitals.

Additionally, some primitive Gaussian functions are diverse to give a contracted Gaussian function (**CGF**) as in the following form[60,67]:

$$\chi_j^{\text{CGF}} = \sum_i^M C_{ij} \chi_a^{\text{GTO}} \dots \dots \dots (2.34)$$

Where M is the number of Gaussian primitives used in a linear combination and C_{ij} are the orbital expansion coefficients.

2.14 Polarization and Diffuse Functions

Polarization functions are functions of higher angular momentum such as d- and f-type functions for heavy atoms and p- and d-type functions for hydrogen and helium atom[65]. Polarization functions are used because they often result in more precise calculated geometries and frequencies. This increases the flexibility of the basis set by allowing the shape of the orbital to become polarized in one direction.

The inclusion of polarization functions can be significant for systems in which hydrogen is complicated such as hydrogen-bonding and proton transfers since these will allow the s orbital to become distorted from its regular spherical shape[64,72].

The addition of polarization functions is indicated in brackets after the reduction arrangement while wordy functions denoted by '+'. For instance, the **6-31++G(d, p)** basis set includes a set of d-type functions on all heavy atoms and p-type functions on hydrogen and helium. The first '+' indicates that diffuse s- and p-type functions are included on heavy atoms, while the second '+' indicates that diffuse s-type functions have been included on hydrogen. Another group of basis sets that are industrialized exactly for use in calculations that include electron correlation. These basis sets are the correlation-consistent polarized valence (double/triple) zeta basis sets, **cc-pVXZ**, where X denotes the degree of splitting[65,72,74]. For heavy metals, the relativistic Effective-Core Potentials (**ECPs**) such as Stuttgart Dresden triple zeta **ECPs (SDD)** basis set is used. The types of Los Alamos Nationwide Laboratory 2-double-zeta (**LANL2DZ**) and SDD basis sets are powerfully recommended for heavy metals. Scalar relativistic corrections are more rigorous than ECPs and spin-free computes are not much more expensive[71,74].

2.15 Computations Properties

The computation of molecular electronic properties in this study are carried out by Koopmans theorem (**KT**). The description of the calculated properties are shown as below.

2.15.1 Energy of HOMO, LUMO and Band Gap

HOMO and LUMO are two most significant of molecular orbitals, where the HOMO denotes highest occupied molecular orbital and the LUMO refers the lowest unoccupied molecular orbital. These orbitals are called the frontier orbitals as they lie at the outmost boundaries of the electrons of the molecules. The HOMO, which is the highest energy orbital containing electrons, is the orbital acting as an electron donor.

Inversely, the LUMO, is the lowest energy orbital having space to accept electrons. The energy gap E_{gap} regards the difference of the energies between the HOMO and LUMO levels as[75,76]:

$$E_{\text{gap}} = E_{\text{LUMO}} - E_{\text{HOMO}} \dots \dots \dots (2.35)$$

HOMO and LUMO and their resultant energy gap did not only determine the path the molecules interacts with other species, but their energy gap helps label the chemical reactivity and kinetic constancy of the molecule. A molecule with a small frontier orbital gap is more polarizable and is generally related with a high chemical reactivity, low kinetic stability and it is also termed as a soft molecule[65,76].

2.15.2 Total Energy, Ionization Potential and Electron Affinity

The total energy E_{T} signifies the sum of total kinetic and potential energy of the system, at the relax structure where the total energy of the molecule must be at the lowest value because the molecule is at the equilibrium position, which means the resulting of the real forces is zero[75,77].

The ionization potential (**Ionization Energy I_{E}**) for a molecule is the quantity of energy needed to remove an electron from an atom or molecule and expressed as the energy difference between the positive charged energy E_{+} and the neutral E_{n} ($I_{\text{E}} = E_{+} - E_{\text{n}}$). The HOMO and LUMO energy were also used to compute I_{E} in the framework of Koopmans theorem as in the following association[79,80]:

$$I_{\text{E}} = -E_{\text{HOMO}} \dots \dots \dots (2.36)$$

The electron affinity (**E_{A}**) of an atom or molecule is the energy change when an electron added to the neutral atom to form a negative ion and expressed as the energy difference between the E_{n} and the negative charged energy E_{-} according to the following relative ($E_{\text{A}} = E_{\text{n}} - E_{-}$)[93,94]. According to Koopmans theorem, the HOMO and LUMO energies were also used to calculate the E_{A} as[78,79]:

$$E_{\text{A}} = -E_{\text{LUMO}} \dots \dots \dots (2.37)$$

2.15.3 Chemical Potential, Chemical Hardness and Softness

Within the plan of the DFT, one of the global amounts is chemical potential (χ), it measures the escape tendency of an electronic cloud. It is a constant, through all space, for the ground state of an atom, molecule or solid, and equals the slope of the energy versus N curve at constant potential $V(\vec{r})$:

$$\chi = \left[\frac{\partial E}{\partial N} \right]_{V(\vec{r})} \dots \dots \dots (2.38)$$

Also, χ is related experimentally to two known quantities, I_E and E_A , as in the following relationship [72,79,81]:

$$\chi \approx \frac{1}{2}(E_{\text{HOMO}} + E_{\text{LUMO}}) \approx -\frac{1}{2}(I_E + E_A) \dots \dots \dots (2.39)$$

Hardness (H) is a measure of a molecule's resistance to change in its electronic charge and is specified in the model [81]:

$$H = \frac{1}{2} \left(\frac{\partial \chi}{\partial N} \right)_{V(\vec{r})} \dots \dots \dots (2.40)$$

In terms of I_E and E_A , the hardness is half of the energy gap between two frontier orbitals [79,81]:

$$H = \frac{I_E - E_A}{2} \dots \dots \dots (2.41)$$

The hard molecule has a large energy gap. The theoretical meaning of chemical hardness has been providing by the DFT as the second derivative of electronic energy with respect to the number of electrons N , for a constant potential $V(\vec{r})$ [80,81]:

$$H = \frac{1}{2} \left[\frac{\partial^2 E}{\partial N^2} \right]_{V(\vec{r})} = \frac{1}{2} \left[\frac{\partial \chi}{\partial N} \right]_{V(\vec{r})} \dots \dots \dots (2.42)$$

The soft molecules have a small energy gap and this means small excitation energies to the various of excited states, their electron density changes more simply than hard molecules, and due to that, soft molecules will be more reactive than hard

molecules. The electronic softness S is a property of molecules that measures the degree of chemical reactivity. It is the inverse of H [80,83]:

$$S = \frac{1}{2H} = \left(\frac{\partial^2 N}{\partial E^2} \right)_{V(\vec{r})} = \left(\frac{\partial N}{\partial K} \right)_{V(\vec{r})} \dots \dots \dots (2.43)$$

2.15.4 Electrophilic Index and Electronegativity

The Electrophilic index is a measure of energy lowering due to maximal electron flow between donor and acceptor. In which the Electrophilic index (ω) given in the following form[83]:

$$\omega = \frac{x^2}{2H} \dots \dots \dots (2.44)$$

The Electrophilicity is built up from the electronic structure of molecules independent of the nucleophilic. The electrophiles are species that stabilize upon receiving on additional amount of electronic charge from the environment[83,84].

The Electronegativity (E_N) is a measure of the tendency to attract electrons by an atom in a chemical bond and defined as the negative of the chemical potential ($E_N = -x$) in DFT and given as[78,86]:

$$E_N = \frac{1}{2}(I_E + E_A) \dots \dots \dots (2.45)$$

To evaluation the Electronegativity according to Koopmans theorem, it can be defined as the negative value for average of the energy levels of the HOMO and LUMO [78]

$$E_N = -\frac{1}{2}(E_{\text{HOMO}} - E_{\text{LUMO}}) \dots \dots \dots (2.46)$$

2.15.5 Molecular Polarizability and Total Dipole Moment

The electric dipole polarizing ability is an indicator of the linear reaction of the electron density to a magnetic field F , and it represents an additional variation in energy[85,86]:

$$\alpha_{a,b} = \left(\frac{\partial^2 E}{\partial F_a \partial F_b} \right) (a, b = x, y, z) \dots \dots \dots (2.47)$$

The polarizability $\langle\alpha\rangle$ is calculated as the mean value and given as in the following equation [87]:

$$\langle\alpha\rangle = \frac{1}{3} (\alpha_{XX} + \alpha_{YY} + \alpha_{ZZ}) \dots \dots \dots (2.48)$$

Here α_{XX} , α_{YY} and α_{ZZ} denoted the eigen values of the polarizability tensor.

The dipole moment (P) signifies the first derivative of the energy with respect to an applied electric field. It is a measure of the asymmetry in molecular charge distribution. The unit measurement of dipole moment is Debye (1 Debye = 3.336×10^{-30} Coulomb.meter). In quantum mechanical account of dipole moment, the charge is a continuous distribution that is a function of (\vec{r}) . The total dipole moment is given by the following equation [86,87]:

$$P_T = P_X + P_Y + P_Z \dots \dots \dots (2.49)$$

Where (P_T) is the total dipole moment, and (P_X) is the dipole moment on the (X) axis, (P_Y) is the dipole moment on the (Y) axis, and (P_Z) is the dipole moment on the (Z) axis.

2.16 Fermi Energy

Fermi energy, the fundamental variation principle in DFT, is used to measure the escaping trend of a cloud of electrons. It is a constant through all space and can be calculated according to the following equation [89]

$$E_F = \left[\frac{\partial E}{\partial N} \right] v(r) \dots \dots \dots (2.50).$$

Where E is the energy and N is the number of electrons.

Experimentally, Fermi energy E_F is correlated with E_{HOMO} and E_{LUMO} , as in the following equation [89].

$$E_F \approx \frac{1}{2} (E_{HOMO} + E_{LUMO}) \dots \dots \dots (2.51)$$

2.17 Geometrical Structures Optimization

All molecules have their own geometry and shape that distinguishes them from others, and this is affected by the following factors:

1. The number and kinds of atoms.
2. Bonds' number and types.
3. Bond lengths that are relevant $r : 0 < r < \infty$.
4. Bond aspect that is relevant $\theta : -180^\circ < \theta < 180^\circ$ (units of degrees).

Geometry optimization is a physical chemistry computation that determines the lowest energy or most relaxed conformation of a molecule. The approach is an iterative process in which the molecular shape is changed slightly at each stage and the energy of the molecule is compared to the preceding cycle. The computer gently pushes the molecule in order to achieve the most relaxed condition possible. Calculates the energy, then pushes it a bit further till the lowest energy is determined. At the ideal geometry, the molecule's energy minimum is discovered[89].

2.18 Open-Circuit Voltages(VOC)

Is considered to be an important property that pointed gain voltaic for proposed nano-system. The VOC can be calculated as shown in equation(2.52):

$$\text{VOC} = | \text{HOMO (Doner)} | - | \text{LUMO (Acceptor)} | - \Delta \dots \dots \dots (2.52).$$

where Δ is an empirical value ranging from 0.3 to 0.5 eV

$| \text{HOMO(D)} | - | \text{LUMO (A)} |$ represents the donor/acceptor effective energy gap. It should be noted that the value Δ depends on the choice of donor/acceptor system. Atypical value of $\Delta = 0.3$ eV and its value may be greater or smaller in different OSCs [90].

The open circuit voltage is the maximum voltage that the solar panel can produce with no load on it (i.e. measured with a multimeter across the open ends of the wires attached to the panel). If two or more panels are wired in series it will be Voc of panel 1 + Voc of panel 2, etc. The voltage is generally highest mid-morning as the sun rises rapidly and the panel temperature is still quite low. The Voc + approx 3.5 per cent must be less than the maximum solar voltage permitted by the solar-charge controller. Some controllers shut down if it's exceeded, while some may continue to operate but the lifespan of the controller could be compromised or it may result in immediate destruction of the device[91].

2.19 Electron Injection Process

The valence band is an energy band that lies below the conduction band. When the valence band is filled to the brim with electrons and the conduction band is devoid of any electron, the material loses its electrical conductivity. Therefore, there must be some voids within the valence band to conduct electricity, or the presence of some electrons in the conduction band. One of these spaces is called an electron hole. In order for an electron to move from the valence band to the conduction band it needs energy at least equal to the bandgap. In order to fall from the conduction band to the valence band, it must lose energy at least equal to the bandgap in the form of light (photon) or heat (phonon). This process is called **electron injection**. If the bandgap is direct, the electron releases its energy in the form of a photon. If the bandgap is indirect, release its energy in the form of a phonon. The transfer of electrons between the conduction and valence bands is used in several applications, the most important of which are the solar cell, lasers, masers, and the luminous diode [92].

and this process can be calculated through the following equation. [90]:

$$\Delta G^{\text{injuct}} = E^* - E_{\text{CB}} (\text{TiO}_2) \dots \dots \dots (2.53)$$

where E^* represents the energy of the excited state

$$E^* = E^{\text{dye}} - \Delta E = -\text{HOMO} \text{ and } \Delta E = 1240 / \lambda_{\text{max}} \dots \dots \dots (2.54)$$

$$E_{CB}(\text{TiO}_2) = 3.9$$

$$\text{then } \Delta G^{\text{injected}} = -\text{HOMO} - (1240 / \lambda_{\text{max}}) - 3.9 \dots\dots\dots(2.55) \text{ [110].}$$

Where the constant (1240) is the product of the net Planck constant ($6.62607015 \times 10^{-34}$ m² kg/s) and the speed of light (3×10^8 m/s) divided by the wavelength in units of nanometers, After reducing the units and converting the unit of the resulting quantity to electron volts get this formula.

2.20 Light Harvesting Efficiency (LHF)

One of the important parameter for design efficient photonic device is light harvesting efficiency (LHF), it proportional directly with oscillation strength value, this can have been computed by equation[90] :

$$LHE = 1 - 10^{-f} \dots\dots\dots(2.56)$$

Where (f) represent oscillation strength associated with maximum wave length of absorption [93].

2.21 Electronic Transitions

The absorption of UV or visible radiation agrees to the excitation of outer electrons. There are three types of electronic transition which can be considered as the first are the transitions involving p, s, and n electrons, the second are the transitions involving charge-transfer electrons and the third are the transitions involving d and f electrons.

When an atom or molecule absorbs energy, electrons are promoted from their ground state to an excited state. In a molecule, the atoms can rotate and vibrate with respect to each other. These vibrations and rotations also have separate energy levels, which can be considered as existence packed on top of each electronic level.

Absorption of ultraviolet and visible radiation in organic molecules is limited to certain functional groups (chromophores) that contain valence electrons of low excitation energy. The spectrum of a molecule containing these chromospheres is

complex[94]. The possible electronic transitions of p, s, and n electrons are shown as in Figure (2.1).

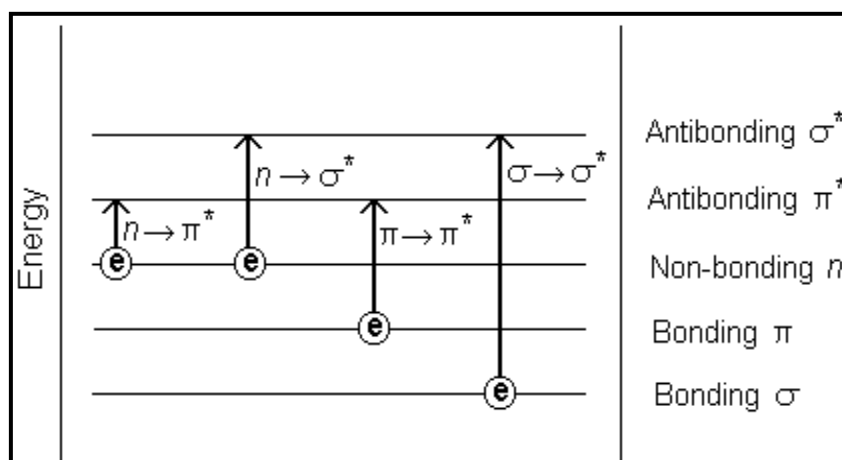


Figure 2.1:The Electronic Transitions of P, S, and N electrons [94].

2.21. 1 Infrared IR-Spectrum

infrared IR spectrum is an electromagnetic radiation. The N-atoms system absorbs amount of energy will oscillate with three degrees of freedom for both translation and rotation, and $(3N-6)$ degrees of freedom for vibration for ring molecules. The vibration of a molecule is modeled by normal modes of simple harmonic oscillator to absorb and emit the energy. The normal oscillations that are associated with changes in dipole moments are active and they appear in the range of infrared radiation.

The oscillations of a system have two types of bands, fundamental and unfundamental oscillation bands. The fundamental bands are accompanied with more changes in dipole moments and they are classified according to high intensity as stretching, distortion, wagging, twisting, rocking and bending oscillations. While unfundamental bands, overtone and hot bands which have low intensity[73]. The vibration analysis is valid only when the first derivative of the energy with respect to displacement of the atoms is zero[95].

2.21.2 UV- Visible radiation

The excitation of electrons in both atoms and molecules from lower to higher energy levels is connected to the absorption of visible (Vis) and ultraviolet (UV) light. Because matter's energy levels are quantized, only light with precisely the right amount of energy can drive transitions from one level to the next. Ultraviolet radiation is a type of radiation that exists just below the visible spectrum of light. It has a range of wavelengths from 100 to 400 nanometers, while the visible spectrum extends between 390 to 710 nm [94]. Different molecules are able to absorb different wavelengths of light. The absorption spectrum shows the nature of the molecular structure of the compound in terms of the type of bonds present, their dimensions, etc [96].

2.22 The Software

All calculations in this study have been performed by using the Gaussian 09 package of programs, **Gauss View 5.0.8**, **Gauss Sum 3.0** and other assistant programs. These programs are described as below:

2.22.1 Gaussian 09 (G09) Program

The Gaussian program is a computational software package initially published by John Pople in 1970. Gaussian program is a very high-end quantum mechanical software package. The “09” mentions to the year 2009 in which the software was published [97].

Gaussian is capable of running all of the major methods in molecular modeling, including molecular mechanics, ab-initio, semi-empirical, HF and DFT. Moreover, excited state computes can be done by different methods in this program [98].

The name originates Gaussian comes from the use of the Gaussian type orbitals that Gaussian's originator, John Pople, used to try to overcome the computational difficulties that get up from the use of Slater type orbitals. A number of researchers, such as S.F. Boys and Isaiah Shavitt, Pople, quite brilliantly, recognized that the

(relatively) simple, substitution of a series of Gaussian functions for the Slater function, would greatly simplify the rest of the calculation of the Schrödinger equation. Pople (1998) was awarded the Nobel Prize in chemistry (along with Walter Kohn) for this work[97,98].

2.22.2 Gauss View Program

Gauss View was designed to import the input files for the Gaussian program and also used to prove the output files for Gaussian program in the dimensional photo, Gaussian view which not used as calculation program, but it is simplicity the work on Gaussian program and supply the users three major advantages. First: enable the user to draw the molecules including the big one, also enable the rotation, transferring and changing it size easily. Second: Gaussian view permits to achieve many of the Gaussian calculation, making the complex input preparation for the routine work and the advanced method. Third: Gaussian view permits the inspection of Gaussian calculations results using variety of geometrical techniques and this involved the balanced molecular patterns electronic density surfaces[97,98].

2.22.3 Gauss Sum 3.0

The Gauss Sum 3.0 is a software application recorded by Noel O'Boyle. Gauss Sum 3.0 uses the plotting program (Gnuplot17) for picture graphs. The Gauss Sum is that can examines the output of widely computational physics and chemistry program (such as Gaussian 09 Program)[97,99].

Gauss Sum can get ready more information such as a geometry optimization, plot the density of states (**DOS**) spectrum, source information on the UV-Vis. Transition states, scheme the UV-Vis spectrum and the circular dichroism spectrum, abstract data on IR and Raman vibrations and plotting the IR and Raman spectra, which may be scaled using general or individual scaling factors[100, 101].

2.22.4 Avogadro Software

It is a cutting-edge molecular editor and illustrator designed for cross-platform use in computational chemistry, molecular modeling, bioinformatics, materials science, and related fields. It provides flexible, high-quality display and powerful add-on architecture. Typical uses include constructing molecular structures, formatting input files, and analyzing the output of a wide range of computational chemistry packages[102].

Chapter Three

Results and

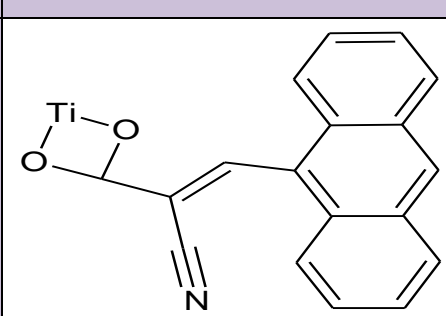
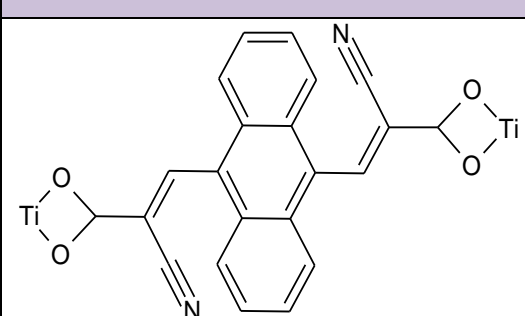
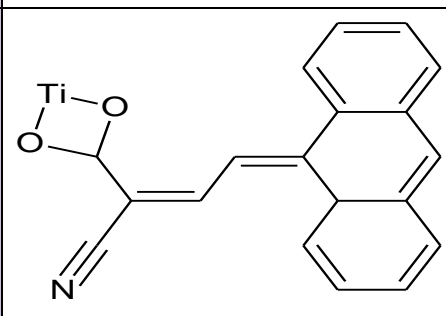
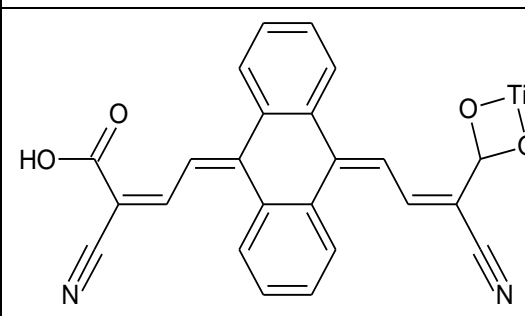
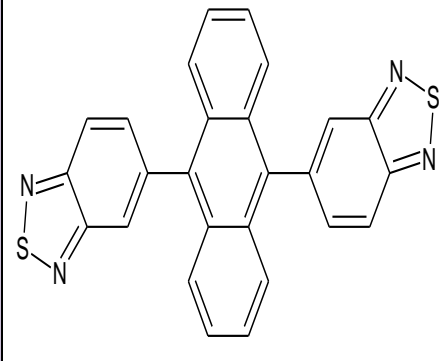
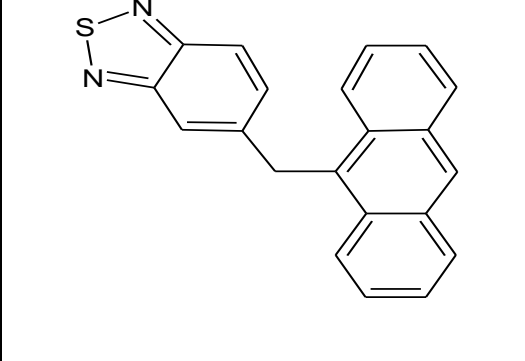
Discussion

Results and Discussion

3.1 Introduction

This chapter deals with the calculations and study of the electronic and optical properties of the proposed 24 compounds, 11 of which depend on the anthracene molecule, and the other 13 compounds are based on the benzobisthiadiazole (BBT) molecule.

Before starting the calculations to know some of the electronic and spectroscopic properties of the proposed compounds, a schematic drawing of the proposed compounds was designed as in Figure (3.1).

Comps	Chemistry drawing	Comps	Chemistry drawing
Comp.1		Comp.2	
Comp.3		Comp.4	
Comp.5		Comp.6	

Comps	Chemistry drawing	Comps	Chemistry drawing
Comp.7		Comp.8	
Comp.9		Comp.10	
Comp.11		Comp.12	
Comp.13		Comp.14	
Comp.15		Comp.16	

Comps	Chemistry drawing	Comps	Chemistry drawing
Comp.17		Comp.18	
Comp.19		Comp.20	
Comp.21		Comp.22	
Comp.23		Comp.24	

Figure (3.1): Scheme of the chemical designs of the proposed compounds

Initially, the proposed compounds were modeled in **Gauss View 5.0.8** software and then mitigated by applying the(**three-parameter Lee-Yang-Parr**)(**B3LYP**) hybrid density functional theory by **DFT** method along with **6-31G** basis sets in **Gaussian 09** package of soft ware,to study its ground state and spectral characteristics. The excited-

state and transition-state properties of the relaxation structures were studied using time-dependent density functional theory (TD-DFT).

We have designed the chart below Figure (3.2) to summarize our work.

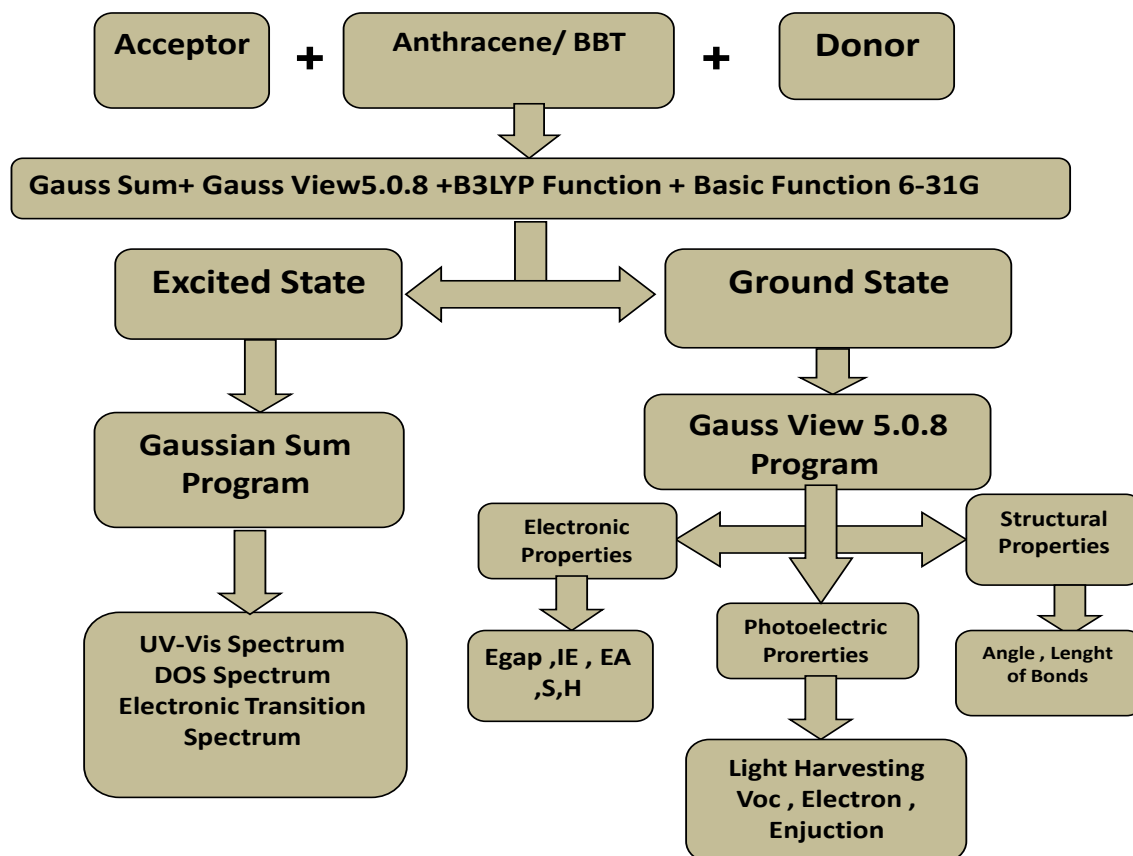


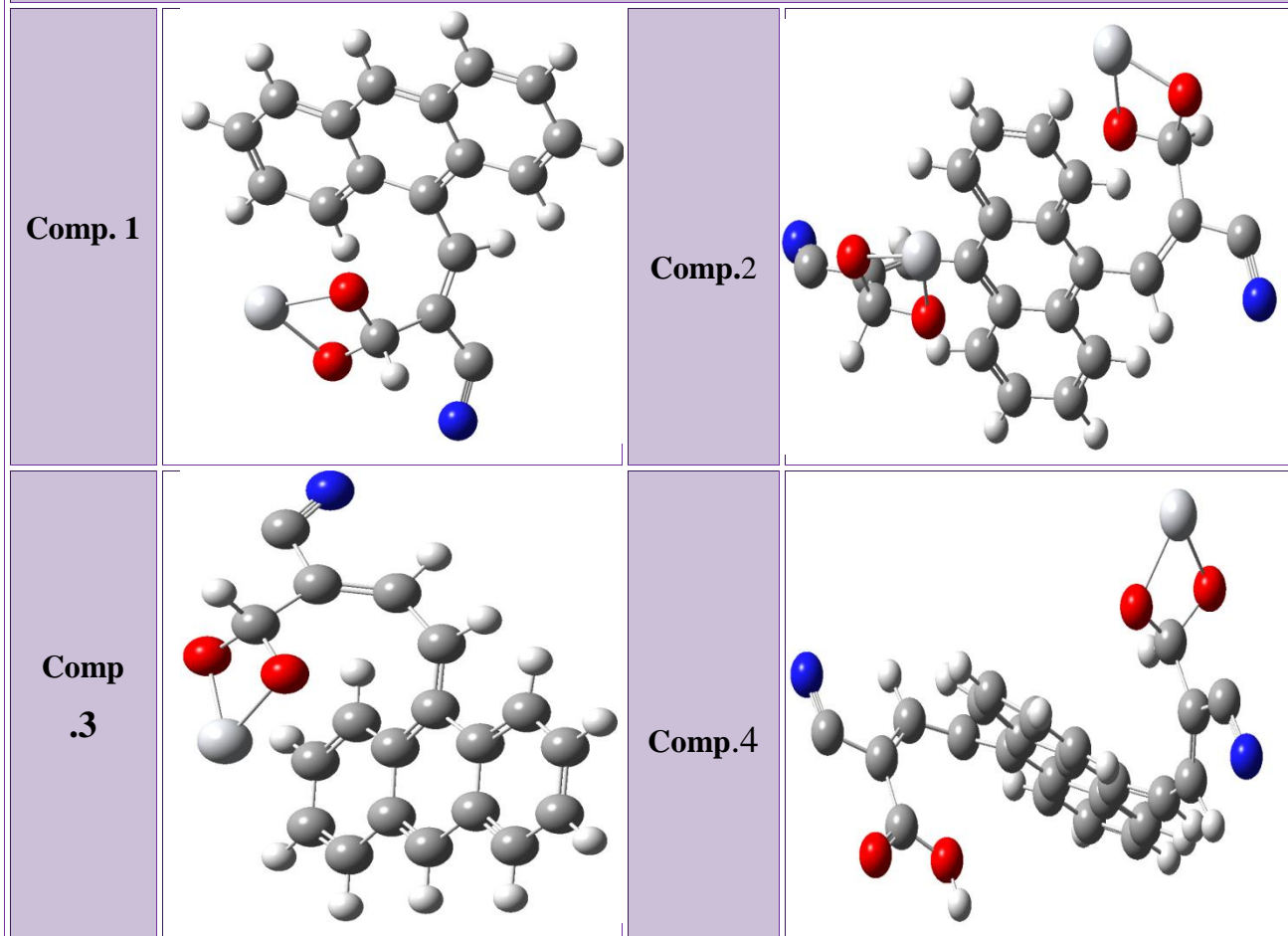
Figure (3.2): Work steps chart

The Figure (3.3) shows the molecular structure of the proposed compounds, which are 24 compounds, of which 11 are based on anthracene and 13 are based on (BBT) compound.

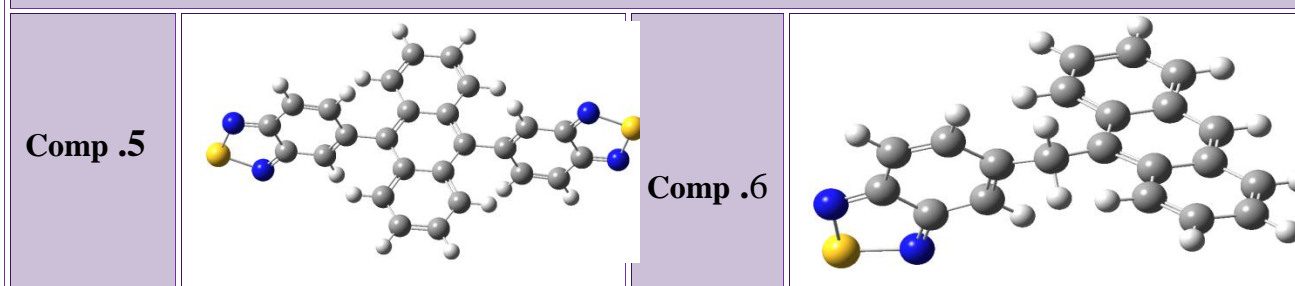
3.2 Molecular Structure of the Proposed Compounds

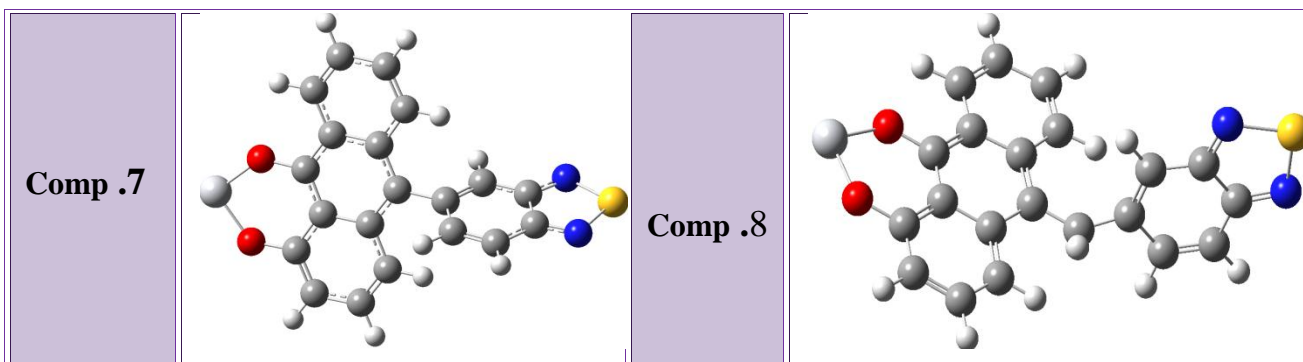
In order to study the spectral and electronic properties of the compounds included in this study, the compounds were built and implemented using the programs described in paragraph (2.22). Figure (3.3) shows the spatial distribution of the compound.

**The First Section :Compounds Based on Anthracene with the Sub-Group
(Cyanoacrylic Acid) (CYN) / TiO₂**

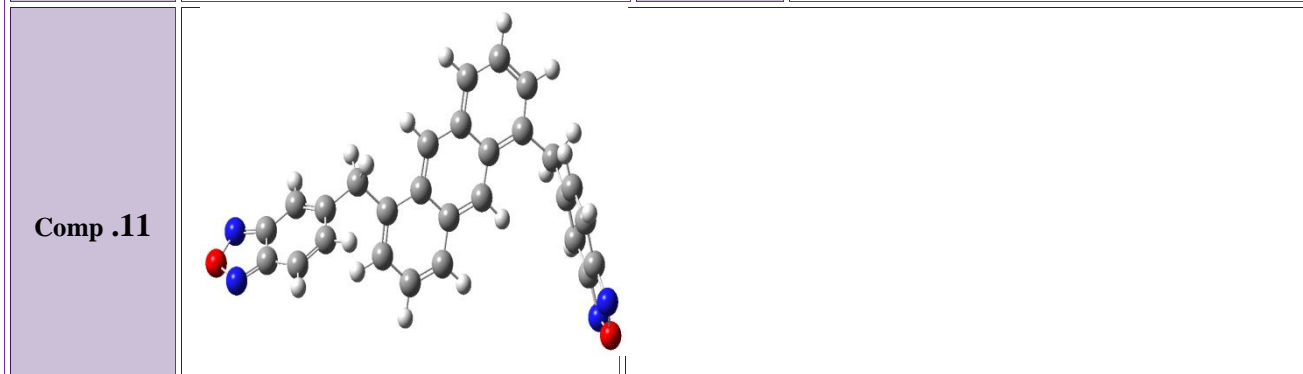
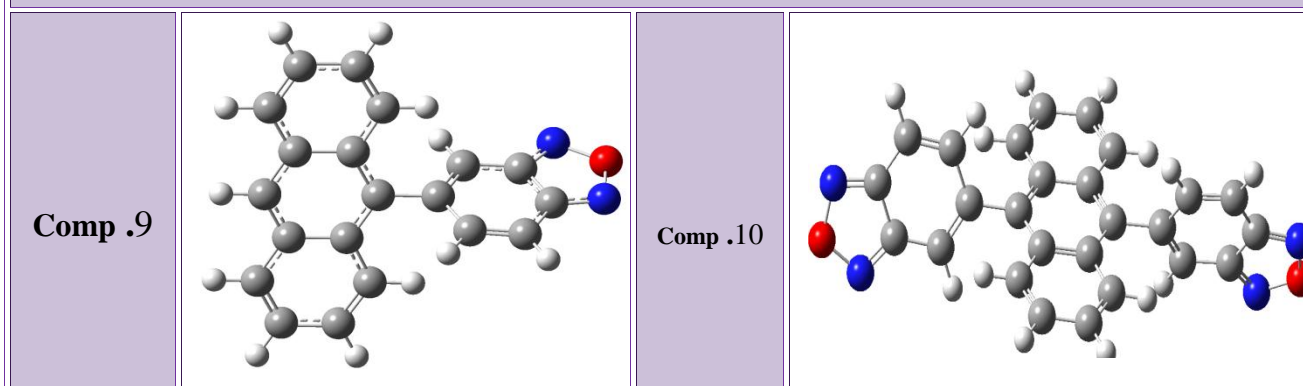


**The Second section :Compounds Based on Anthracene with the Sub-
Group(Benzothiadiazole)**

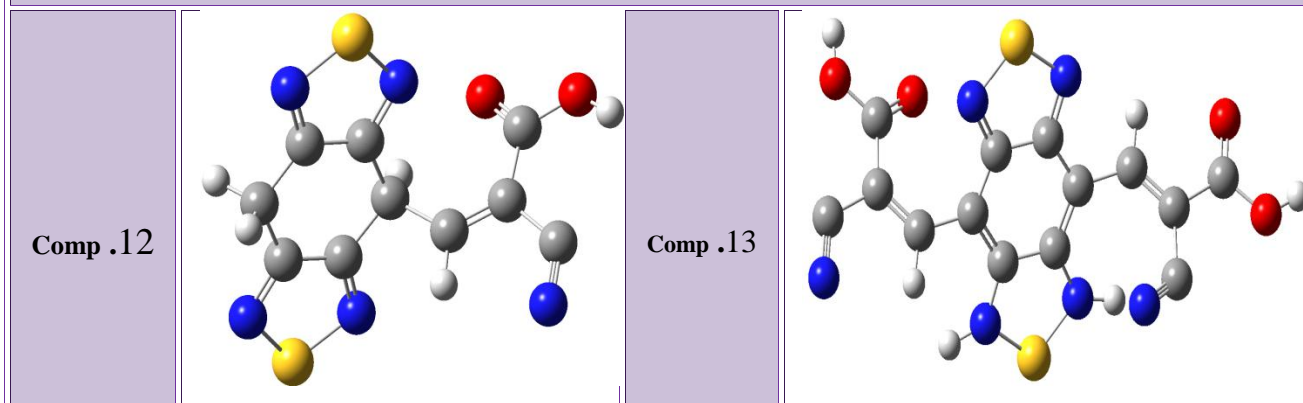


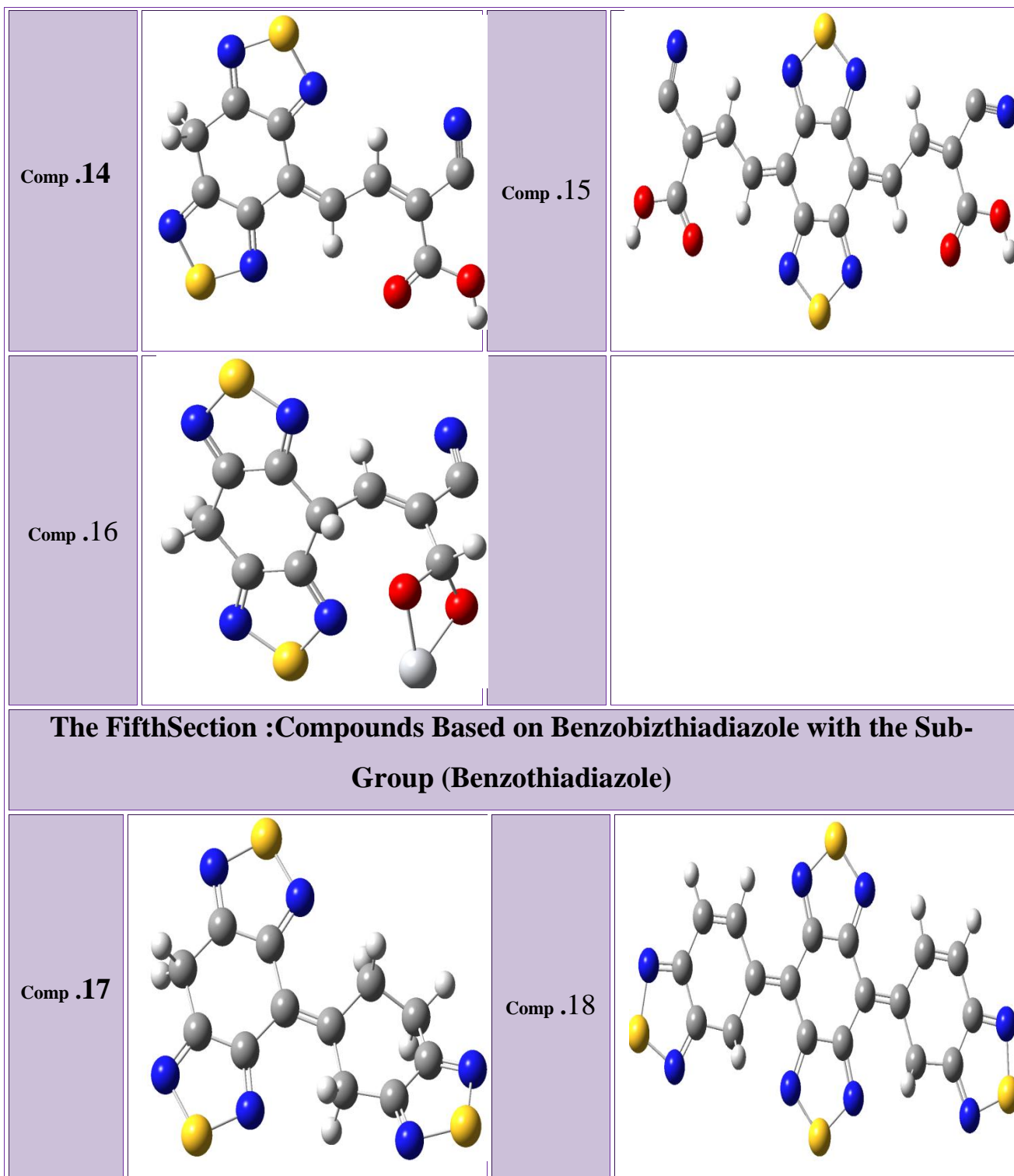


The Third Section :Compounds Based on Anthracene with the Sub-Group(Benzoxadiazole)



The FourthSection :Compounds Based on Benzobizthiadiazole(BBT) with the Sub-Group (Cyanoacrylic Acid) (CYN)





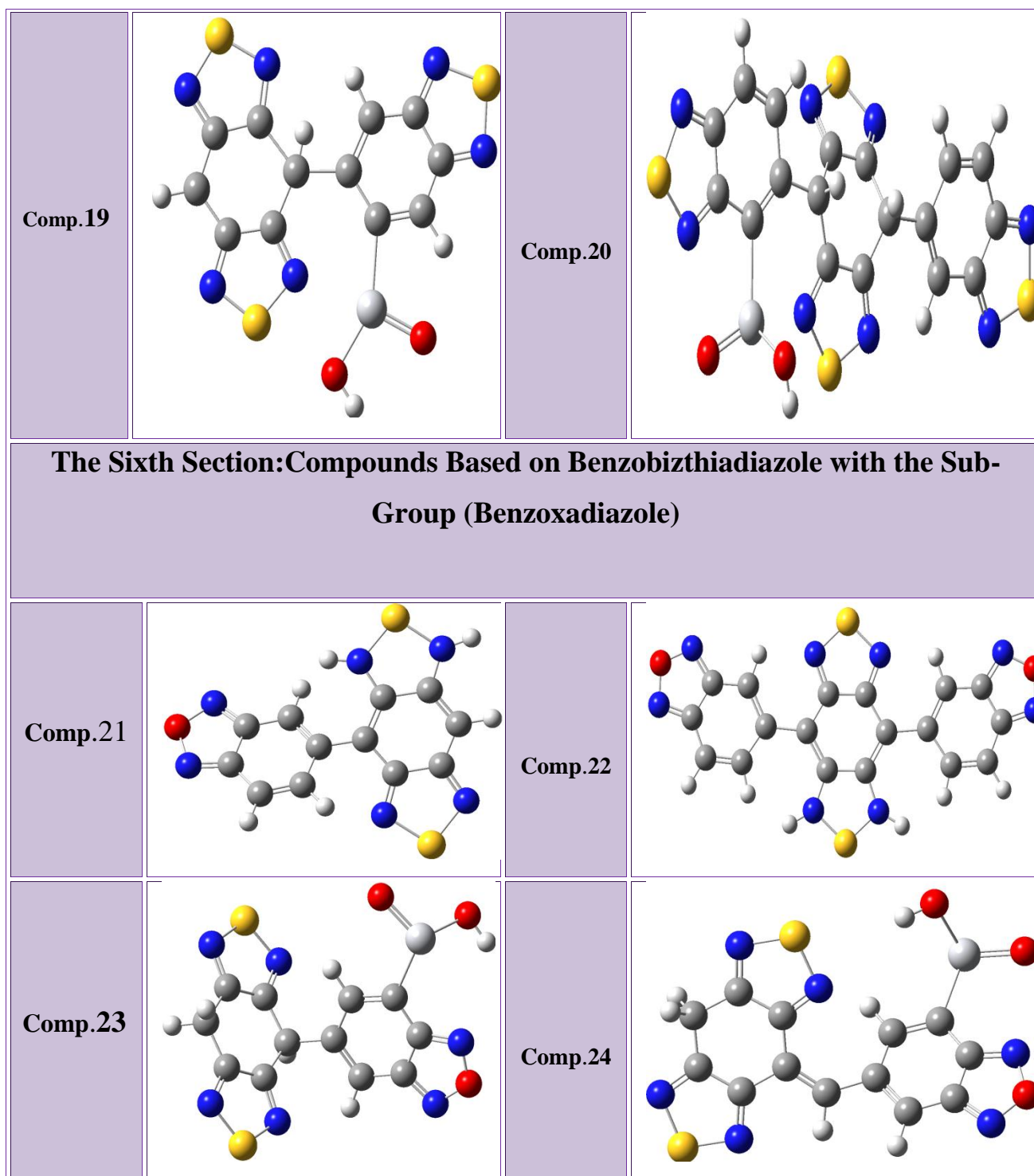


Figure (3.3): The nanostructure of suggested compounds.

Where the atoms shown in the Figure (3.3) are as follows: the small and white atoms are represent Hydrogen atom, the large and white atoms are represent Titanium atom, the medium and grey atoms are represent Carbon atom, the blue atoms are represent

Nitrogen atom, the red atoms are represent Oxygen atom. the yellow atoms are represent Sulfur atom.

The structural construction of the above compounds shows that the bonds are of the covalent type, and it is known that this type of bond is non-centralized, that is, the electronic density between the bonded atoms is not affiliated with a particular atom, and this is the reason for calling it non-localized bonds[102] .

The effect of adding sub-groups of **Cyanoacrylicacid**($C_4H_3NO_2$) (CYN) , **Benzothiadiazole**($C_6H_4N_2S$)and **Benzoxadiazole**($C_6H_4N_2O$) rings to the anthracene molecule and the benzobesthiadiazole molecule (BBT) was studied in order to be able to investigate the effect of inconsistency. The effect of electron acceptance and donation was also studied, including the ability to inject electrons and light harvesting.

It was found that the geometry parameters (the lengths of the bonds and the angles between the bonds) from the DFT calculations are in good agreement with the results obtained from scanning X-ray data obtained by other researchers [103]. the Figure(3.3).Table (3.1) Shows the lengths of the bonds and the angles between those bonds in each compound:

Table (3.1) : The Geometrical parameters for each compound.

Compound	Bond				Compound	Bond			
	Angle	Value (degree)	Length	(Value Å)		Angle	Value (degree)	Length	Value (Å)
Compound 1	C≡C=C	121.150	C=C	1.375	Compound 2	C≡C=C	121.150	C=C	1.374
	C≡C-C	118.854	O=C	1.324		C≡C≡C	118.403	C≡C	1.447
	C≡C-H	118.165	O-Ti	1.861		C≡C-H	118.451	C-C	1.487
	O=C-H	115.168	O-N	1.431		C-O-Ti	90.029	O-Ti	1.842
	C-N≡C	130.257	C-C	1.449		C-N-C	129.105	C-N	1.425
	O-Ti-O	110.001	C-H	1.085		O-C-H	108.965	C-H	1.083
Compounds	Bond				Compounds	Bond			
	Angle	Value (degree)	Length	(Value Å)		Angle	Value (degree)	Length	Value (Å)
Compound 3	C≡C=C	120.928	C=C	1.367	Compound 4	C≡C=C	120.116	C=C	1.374
	C≡C-C	122.712	C=N	1.291		C≡C-C	123.088	C≡C	1.433
	C≡C-H	119.081	C=C	1.422		C≡C-H	119.814	C=N	1.288
	O-C-H	109.385	O-C	1.490		O=C-C	126.692	C-C	1.449
	C=N-C	122.153	Ti-O	1.782		C-N≡C	118.111	Ti-O	1.844
	Ti-O-C	88.598	C-H	1.085		O-C-O	120.894	C-H	1.079
Compounds	Bond				Compounds	Bond			
	Angle	Value (degree)	Length	(Value Å)		Angle	Value (degree)	Length	Value (Å)

Compound 5	C≡C=C	120.250	C=C	1.373	Compound 6	C≡C=C	119.780	C=C	119.984
	C≡C-C	119.981	C≡C	1.435		C≡C-C	119.415	C≡C	1.417
	C≡C-H	118.641	S-N	1.789		C≡C-H	119.739	S-N	1.791
	S-N≡C	106.196	N≡C	1.335		S-N≡C	106.253	N≡C	1.337
	N≡C-C	116.273	C-H	1.083		N≡C-C	124.652	C-C	1.459
	C=C≡C	119.578	C-C	1.449		C=C≡C	119.756	C-H	1.0
Compounds	Bond				Compounds	Bond			
	Angle	Value (degree)	Length	(Value Å)		Angle	Value (degree)	Length	Value (Å)
Compound 7	C≡C=C	120.739	C=C	1.373	Compound 8	C≡C=C	120.209	C=C	1.373
	C≡C-C	119.984	C≡C	1.411		C≡C-C	119.795	C≡C	1.424
	C≡C-H	118.778	Ti-O	1.797		C≡C-H	118.647	Ti-O	1.794
	S-N≡C	106.193	S-N	1.790		S-N≡C	106.206	N≡C	1.334
	N≡C-C	116.139	C-C	1.453		N≡C-C	116.297	S-N	1.792
	Ti-O-C	132.832	C-H	1.083		O-Ti-C	122.009	C-H	1.084
Compounds	Bond				Compounds	Bond			
	Angle	Value (degree)	Length	(Value Å)		Angle	Value (degree)	Length	Value (Å)
Compound 9	C≡C=C	120.777	C=C	1.374	Compound 10	C≡C=C	120.301	C=C	1.373
	C≡C-C	117.670	C≡C	1.426		C≡C-C	118.191	C≡C	1.435
	C≡C-H	118.968	C-C	1.497		C≡C-H	119.646	C-C	1.449

	O—N≡C	103.977	N≡C	1.334		O—N≡C	103.943	N≡C	1.334
	N—O—N	111.668	O—N	1.430		N≡C≡C	110.259	O—N	1.275
	C=C—H	119.872	C—H	1.082		C=C—H	122.244	C—H	1.084
Compounds	Bond				Compounds	Bond			
	Angle	Value (degree)	Length	(Value Å)		Angle	Value (degree)	Length	Value (Å)
Compound 11	C≡C=C	120.213	C=C	1.371	Compound 12	C≡C≡C	117.313	C≡C	1.401
	C≡C—C	119.220	C≡C	1.431		C≡C—C	122.199	C—C	1.475
	C≡C—H	120.094	C—C	1.448		C≡C—H	121.501	S—O	1.761
	O—N≡C	103.961	N≡C	1.334		S—N≡C	106.529	O=C	1.235
	N—O—N	111.631	O—N	1.432		O=C—O	121.518	C—O	1.382
	C=C—H	119.550	C—H	1.082		C=C—H	120.679	C—H	1.080
Compound	Bond				Compound	Bond			
	Angle	Value (degree)	Length	(Value Å)		Angle	Value (degree)	Length	Value (Å)
Compound 13	C≡C≡N	121.834	C≡C	1.412	Compound 14	C≡C=C	121.451	C=C	1.343
	C≡C—C	122.686	C—C	1.478		C≡C—C	122.346	C≡C	1.411
	C=C—H	120.597	C=C	1.355		C≡C—H	121.479	C—C	1.479
	S—N≡C	30.948	S—N	1.767		C=C—H	121.732	N≡C	1.354
	O=C—O	121.663	O=C	1.235		N—S—N	96.068	S—N	1.761
	C=C—H	120.597	C—O	1.380		S—N≡C	107.37910	C—O	1.445
C	Bond				C	Bond			

	Angle	Value (degree)	Length	(Value Å)		Angle	Value (degree)	Length	(Value Å)
Compound 15	C≡C=C	122.600	C=C	1.344	Compound 16	C≡C≡C	115.848	C≡C	1.401
	C≡C-C	122.644	C≡C	1.411		C≡C-C	122.637	C=C	1.358
	C-O-H	110.207	C-C	1.479		C≡C-H	121.615	C-C	1.473
	C=C-H	121.748	N≡C	1.354		Ti-C-H	128.161	N≡C	1.339
	O-C-O	111.243	S-N	1.756		O=C-O	117.320	C-Ti	2.143
	S-N≡C	108.113	C-H	1.083		S-N≡C	107.097	O-Ti	1.636
Compounds	Bond				Compounds	Bond			
	Angle	Value (degree)	Length	(Value Å)		Angle	Value (degree)	Length	Value Å
Compound 17	C≡C=C	119.777	C=C	1.364	Compound 18	C≡C=C	119.359	C=C	1.385
	C≡C-C	118.022	C≡C	1.423		C≡C-C	122.860	C≡C	1.425
	C-O-H	117.962	C-C	1.487		C≡N-S	107.389	C-C	1.471
	C=C-H	118.726	C≡N	1.35		C≡C-H	118.944	C≡N	1.338
	O-C-O	124.177	S-N	1.759		N-S-N	95.227	S-N	1.786
	N-S-N	95.234	C-H	1.078		C-C-C	119.974	C-H	1.082
Compounds	Bond				Compounds	Bond			
	Angle	Value (degree)	Length	Value Å		Angle	Value (degree)	Length	Value Å
Compound	C≡C≡N	125.309	C≡C	1.396	Compound	C≡C=C	30.548	C=C	1.364
	C≡C-C	118.022	C-C	1.486		C≡C-C	120.814	C≡C	1.425

	N—S—N	95.983	C≡N	1.350		C—C—C	119.974	C≡N	1.350
	C≡C—H	118.967	S—N	1.755		C=C—H	119.310	S—N	1.758
	C=C—H	118.726	C—Ti	2.112		N—S—N	95.227	C—Ti	2.154
	C—C—C	121.024	O—Ti	1.631		S—N≡C	106.188	O—Ti	1.634
Compounds	Bond				Compounds	Bond			
	Angle	Value (degree)	Length	Value Å		Angle	Value (degree)	Length	Value Å
Compound 21	C≡C≡N	123.484	C=C	1.367	Compound 22	C≡C≡N	122.605	C=C	1.367
	C≡C—C	122.117	C≡C	1.419		C≡C—C	119.582	C≡C	1.422
	N—S—N	96.441	C—C	1.474		N—S—N	95.919	N≡C	1.351
	C≡C—H	121.495	N≡C	1.352		N—O—N	111.704	S—N	1.756
	N—O—N	111.689	S—N	1.761		C=C—H	121.773	O—N	1.424
	S—N≡C	107.172	C—H	1.080		S—N≡C	107.434	C—H	1.082
Compounds	Bond				Compounds	Bond			
	Angle	Value (degree)	Length	Value Å		Angle	Value (degree)	Length	Value Å
Compound 23	C≡C≡N	122.624	C=C	1.367	Compound 24	C≡C≡N	122.940	C=C	1.381
	C≡C—C	119.907	C≡C	1.425		C≡C—C	121.892	C≡C	1.410
	N—S—N	96.527	C—C	1.473		N—S—N	41.622	C—C	1.480
	C≡C—H	120.246	N—S	1.766		C≡C—H	121.435	Ti—C	2.157
	N—O—N	111.682	Ti—C	2.159		O—Ti—O	113.933	N—S	1.762
	O—Ti—C	119.856	O—Ti	1.632		Ti—C=C	160.897	C—H	1.082

The Table (3.1) shows that the angles between the bonded atoms are confined between (180 , -180) degrees, and this range gives a clear explanation for the final form of the compounds studied, and this depends on the theory of repulsion of the pair of electrons of the valence shell (**Valence Shell Electron Pair Repulsion Theory**) (**VSEPR**). This theory can be summarized as that the pairs of electrons surrounding the central atom repel each other because of their negative charge, and then they try to move away from each other as much as possible until they reach the most stable geometry (with less energy and less repulsion), The spatial distribution of electrons determines the geometric shape of the molecule. When it is required to describe the geometric shape of a molecule, all bonds must be calculated. This theory made it possible to describe the geometric shape of molecules [104], all of the measurements in Table (3.1) are identical or close to some previous studies[2].

3.3 Electronic properties

The electronic properties are a set of parameters and representations that fully describe the state and behavior of electrons in the material.

3.3.1 Energy Gap

To know the practical feasibility of applying the studied compounds in solar cell applications, it is necessary to know their behavior in absorbing some wavelengths. For this, the electronic structures of the studied compounds must be studied and the energy gap between the highest occupied energy level (HOMO) and the lowest unoccupied energy level (LUMO) and the levels generated by adding subgroups to the basic compounds (Anthracene and Benzobisthiadiazole (BBT)) and knowing the electronic and optical properties of each compound and in each case of addition (adding any compound from the subgroups). Table (3.2) and Figure (3.4) shows the change in the energy gap level of the different compounds under study due to the change of energy level position (LUMO) in each compound. The sub-molecules added to (BBT)

molecules reduce the energy gap, as it create energy levels located between the HOMO-LUMO levels ,its facilitates the electronic transition between the valence and conduction bands. Also, the presence of $C=C$ double bonds leads to a lower LUMO and a lower energy gap due to the delocalization of both HOMO and LUMO energies, and this result agrees with the experimental data [103].

Table (3.2): The HOMO, LUMO, E_{gap} for the compounds.

Compounds	LUMO (eV)	HOMO (eV)	E_g (eV)
Comp.1	-2.358	-3.482	1.123
Comp.2	-2.143	-4.249	2.105
Comp.3	-2.334	-4.194	1.859
Comp.4	-3.049	-4.479	1.430
Comp.5	-2.92	-5.619	2.696
Comp.6	-3.396	-4.751	1.354
Comp.7	-2.818	-4.505	1.687
Comp.8	-2.847	-5.419	2.571
Comp.9	-2.820	-5.573	2.753
Comp.10	-3.024	-5.847	2.822
Comp.11	-2.827	-5.741	2.914
Comp.12	-4.542	-5.389	0.847
Comp.13	-4.690	-5.474	0.783
Com.14	-4.546	-6.386	1.839
Comp.15	-4.699	-6.408	1.708
Comp.16	-3.771	-5.278	1.506
Comp.17	-4.514	-6.065	1.551
Comp.18	-4.581	-6.007	1.426
Comp.19	-4.441	-6.016	1.575

Comp.20	-4.653	-6.113	1.459
Comp.21	-4.604	-6.298	1.694
Comp.22	-4.839	-6.339	1.500
Comp.23	-4.901	-6.378	1.477
Comp.24	-4.524	-6.4041	1.879

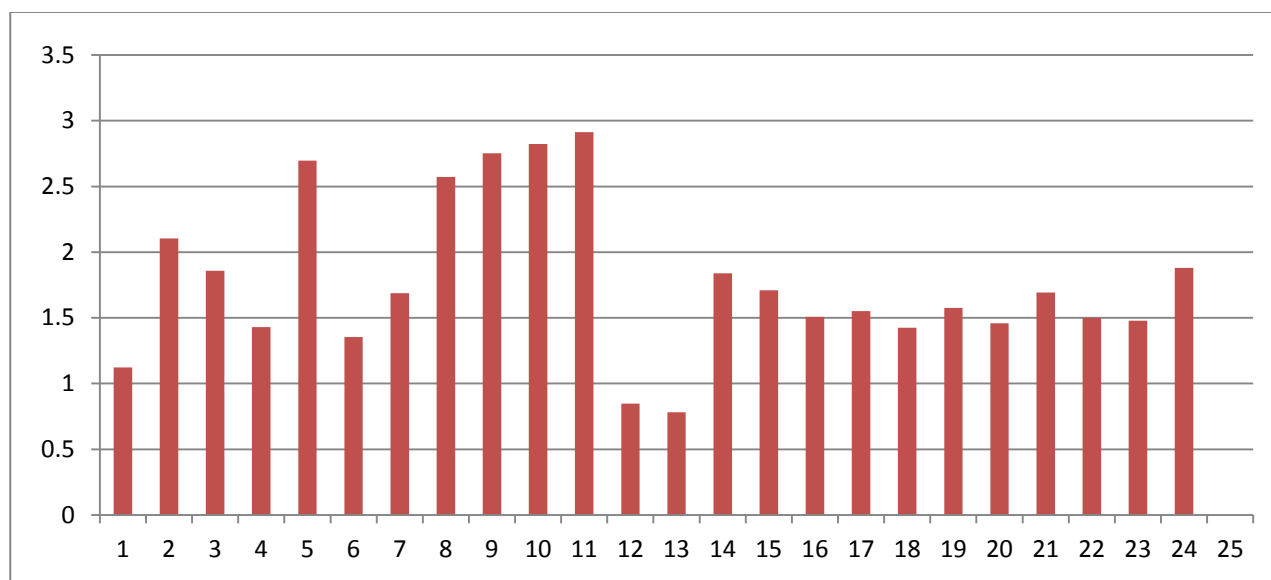


Figure (3.4): E_{gap} for the compounds.

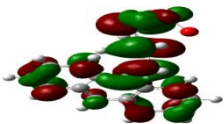
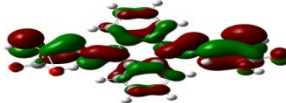
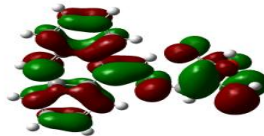
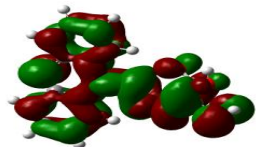
The results shown in the Table (3.2) showed many differences in the (HOMO) and (LUMO) energy level in the compounds under study, and therefore the energy gap in some compounds is large and some are small.

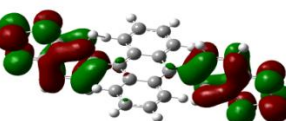
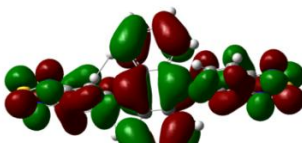
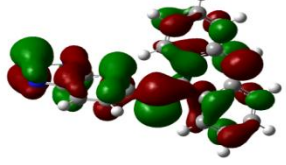
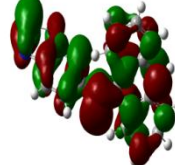
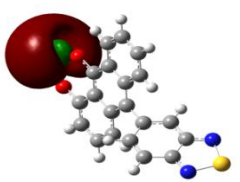
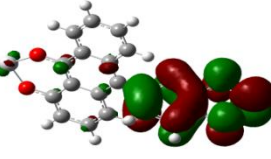
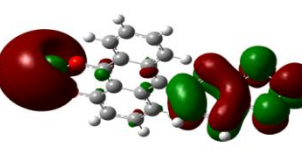
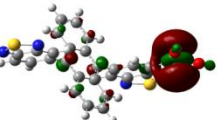
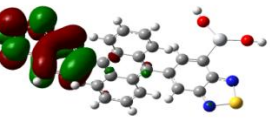
The studied structures are characterized by the presence of an energy gap between the HOMO-LUMO states, which occurs as a result of a large amount of charge transfer between the molecules from the donor electron sites overlapping with the active electron sites (the acceptor). Each compound shows a different amount of electronic

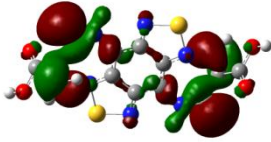
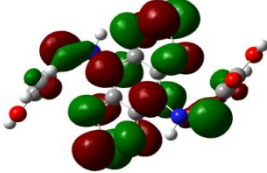
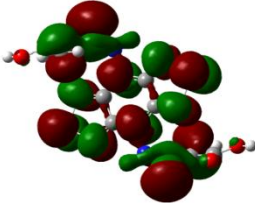
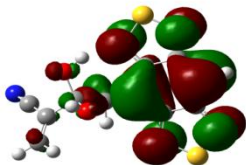
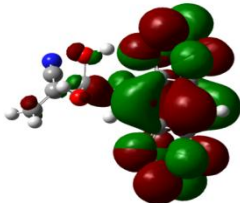
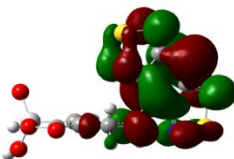
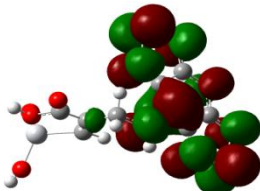
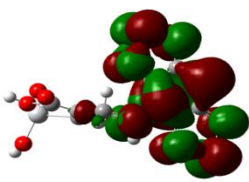
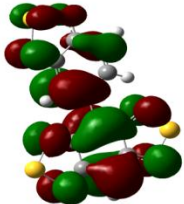
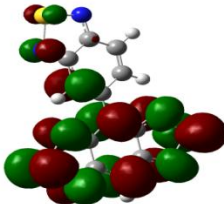
transitions that differs from the other compound, and this is the reason each compound was distinguished from other compounds by its .

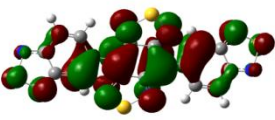
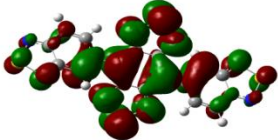
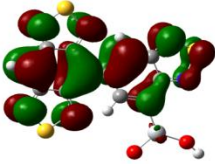
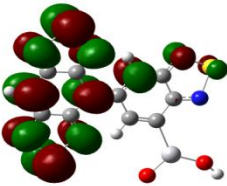
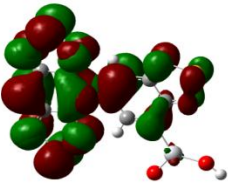
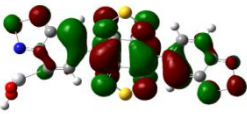
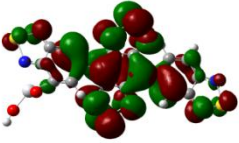
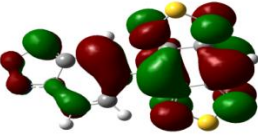
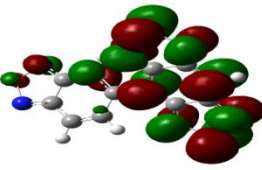
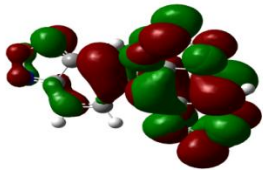
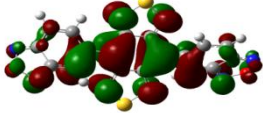
The results indicate that the presence of subgroups around anthracene and benzobisthiadiazole (BBT) molecules in the studied compounds leads to a decrease in LUMO because their presence attracts electrons, as these compounds act as acceptors and donors. From Figure(3.4) and Table (3.2), it became clear that the energy gap in the case of using anthracene is greater than when using Benzobisthiadiazole (BBT), and therefore the use of the latter is more useful in solar cell applications because of the ease of electron transition from the valence band to the conduction band in the case of using this compound and these results that we obtained are better than some previous studies [2]. the following Figure (3.5) represent HOMO and LUMO levels of suggested compounds .

3.3.2 The HOMO and LUMO levels according LCAO

compounds	HOMO	LUMO	HOMO+LUMO
Comp.1			
Comp.2			
Comp.3			

compounds	HOMO	LUMO	HOMO+LUMO
Comp. 4			
Comp.5			
Comp.6			
Comp.7			
Comp.8			

compounds	HOMO	LUMO	HOMO+LUMO
Comp.13			
Comp.14			
Comp.15			
Comp.16			
Comp.17			

compounds	HOMO	LUMO	HOMO+LUMO
Comp.18			
Comp.19			
Comp.20			
Comp.21			
Comp.22			

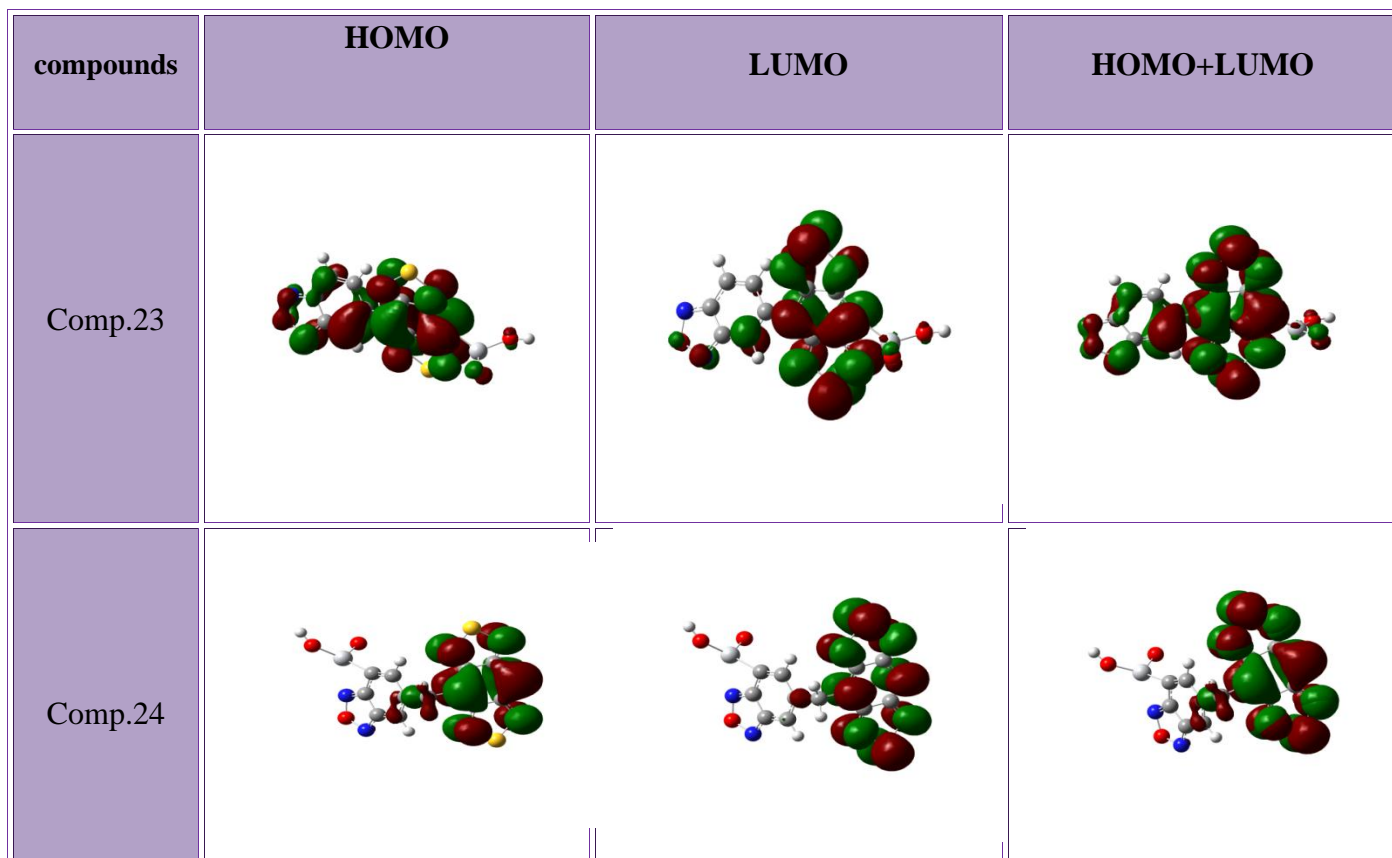


Figure (3.5) : The HOMO and LUMO levels of suggested compounds.

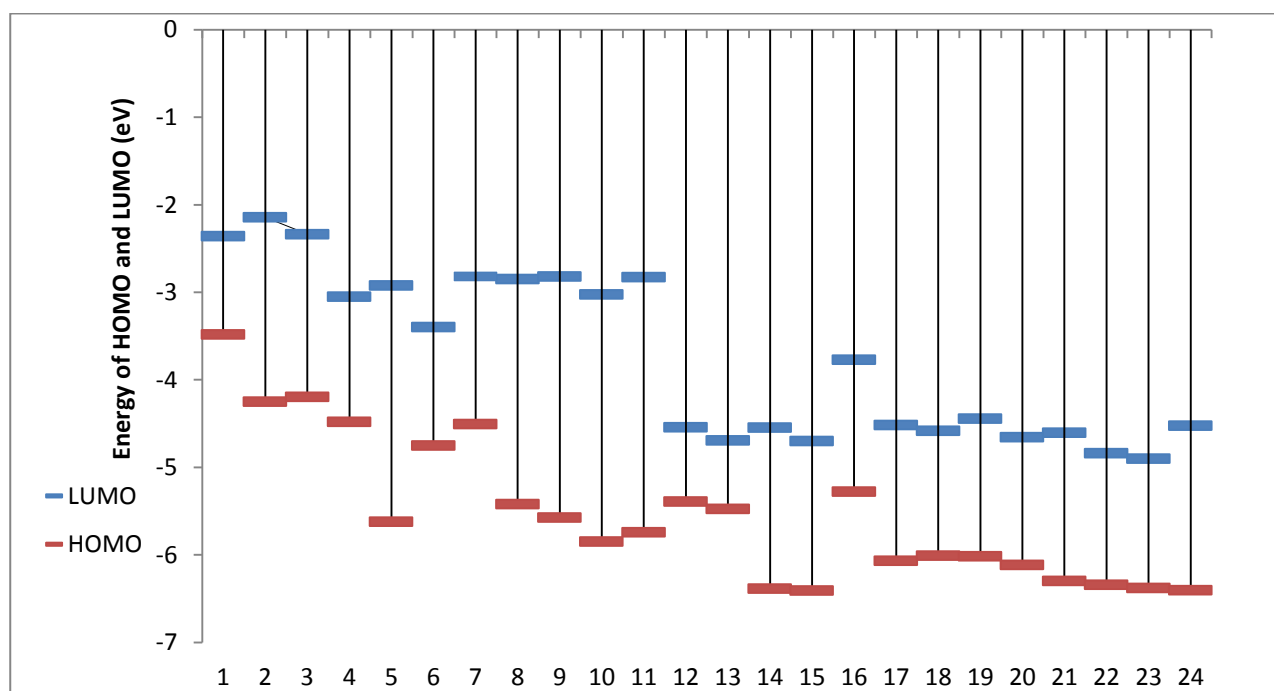


Figure (3.6):The HOMO and LUMO for the compounds.

From the Figure(3.6), it is clear that the HOMO_LUMO levels when using the compound benzobisthiadiazole (BBT) is lower than when using anthracene as a basic compound, and this indicates the importance of this compound in solar cells applications more than the importance of anthracene .

3.4 Some Electronic Variables

In this section, some electronic variables for the compounds under study are determined depending on the values of frontier molecular orbitals (HOMO and LUMO). These variables represent the electronic properties of the compounds. They are ionization energy, electron affinity, electronegativity, quantitative chemical parameters (chemical hardness and softness), electrophilic index and net electronegativity.

3.4.1 Ionization Energy and Electron Affinity

Ionization Energy (IE) and Electron Affinity (EA) were calculated for the studied compounds and the results are as shown in Table (3.3).

Table(3.3): The ionization energy and electron affinity for the compounds.

Compounds	Ionization Energy(IE) (eV)	Electron Affinity(EA) (eV)
Comp.1	3.482	2.358
Comp.2	4.249	2.143
Comp.3	4.194	2.334
Comp.4	4.479	3.049
Comp.5	5.619	2.922
Comp.6	4.751	3.396
Comp.7	4.505	2.818
Comp.8	5.419	2.847
Comp.9	5.573	2.820

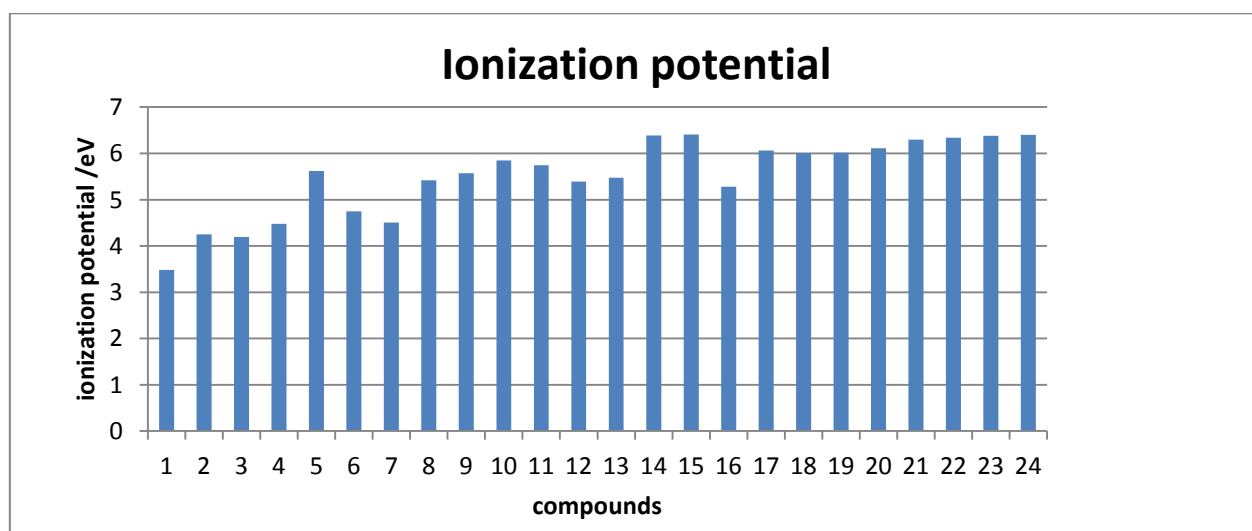
Compounds	Ionization Energy(IE) (eV)	Electron Affinity(EA) (eV)
Comp.10	5.847	3.024
Comp.11	5.741	2.827
Comp.12	5.389	4.542
Comp.13	5.474	4.690
Comp.14	6.386	4.546
Comp.15	6.408	4.699
Comp.16	5.278	3.771
Comp.17	6.065	4.514
Comp.18	6.007	4.581
Comp.19	6.016	4.441
Comp.20	6.113	4.653
Comp.21	6.298	4.604
Comp.22	6.339	4.839
Comp.23	6.378	4.901
Comp.24	6.404	4.524

The results show that compound No. (1) has the lowest ionization potential among the rest of the studied compounds. Compound No. (1) is the most studied compounds able to donate an electron to be an active compound compared to other compounds, and from this we can conclude an important fact, which is that the gap between the valence and conductivity edges of compound No. (1) is low.

In the same context, compound No. (15) will have the largest ionization potential among the rest of the studied compounds because the energy gap between valence and conduction is large and it needs high energy to be able to donate an electron compared to the rest of the studied compounds. In general, the ionization potentials are lower for

elements with a larger atomic number, and the relationship between it and the atomic number is opposite due to the decrease in the force of attraction of the nucleus to the outer electrons, which makes it possible to extract them with the least force, because the benzobisthiadiazole compound contains sulfur and nitrogen, which have an atomic number greater than the atomic number of carbon which consists only of the anthracene molecule. The ionization potential of the resulting compound (benzobaisthiadiazole with its sub-groups) is less than the ionization potential of anthracene with its sub-groups, as shown in Figure (3.7).

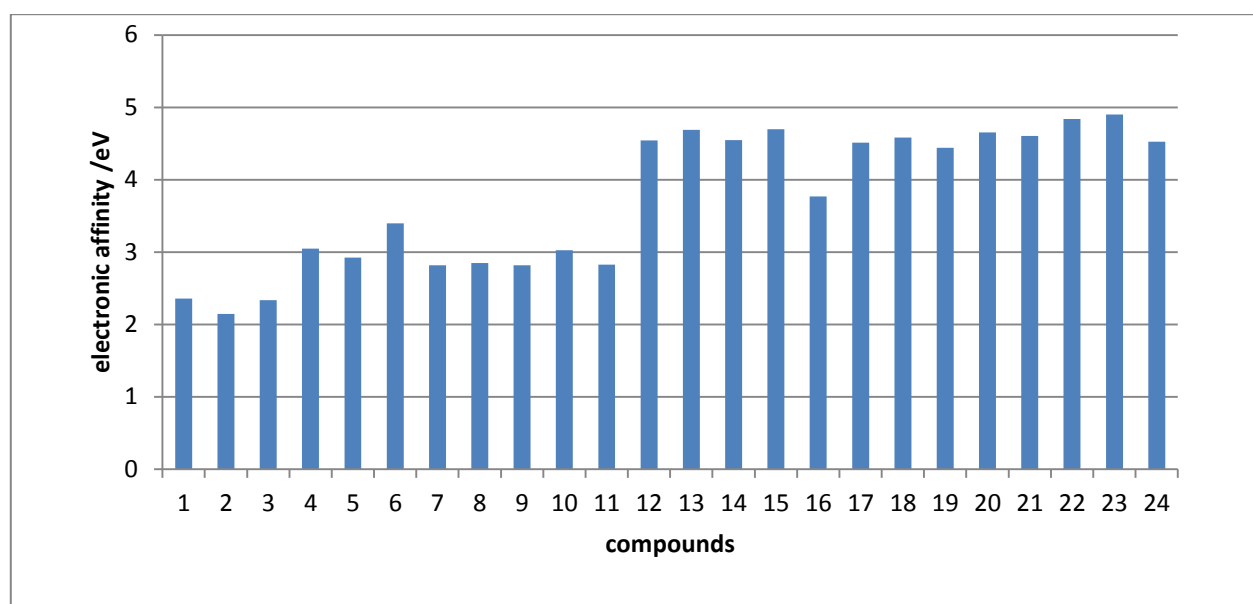
Figure (3.7) shows the gradation of elements according to their ionization capacity:



Figure(3.7):The Ionization potential of the compounds.

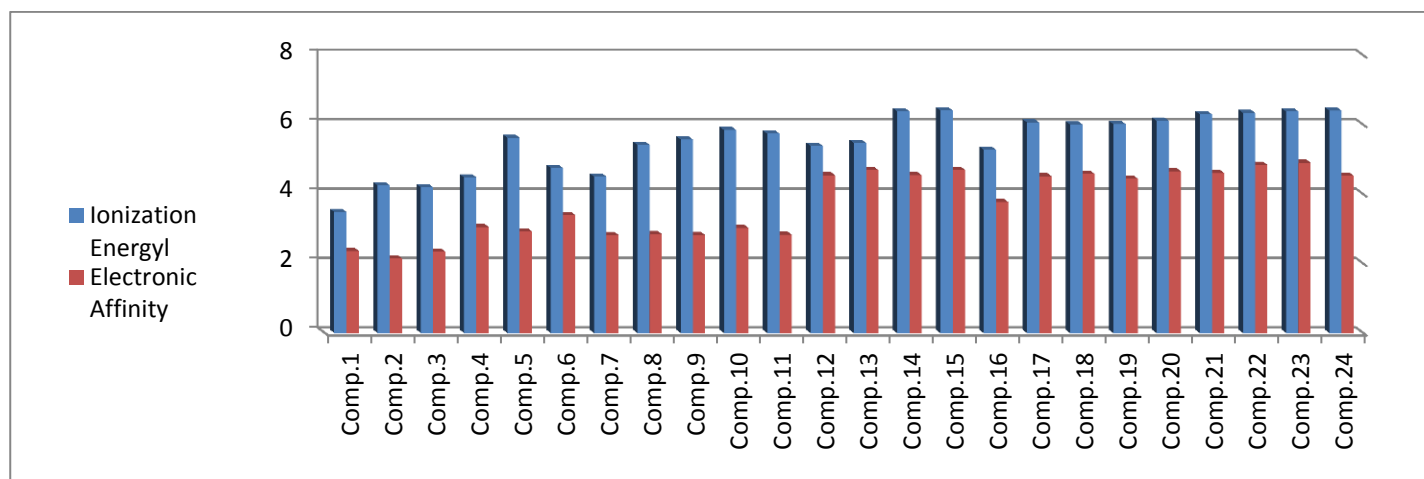
As for the electron affinity(EA), from the observation of the Table (3.3), we note that compound No. (2) is the least electronic affinity among the rest of the studied compounds. By observing Table (3.3), we found that benzobaisthiadiazole (BBT)-based compounds have greater electronic affinity than the anthracene-based compounds.

From the same point of view, compound No. (23) will have the largest electronic affinity among the rest of the studied compounds. The Figure (3.8) show that the change of electronic affinity between the studied compounds



Figure(3.8): The electronic affinity (EA) of the compounds.

As it was passed through the previous electronic properties, and as shown in Figure (3.8), the benzopisthiadiazole compound with its sub-groups has a greater electronic affinity than the anthracene compound with the same sub-groups because of what the BBT compound possesses of elements in its atomic structure of sulfur and nitrogen, which have electronic affinity high. If want to combine the two parameters together, will get the following figure :



Figure(3.9): The IE and EA of compounds.

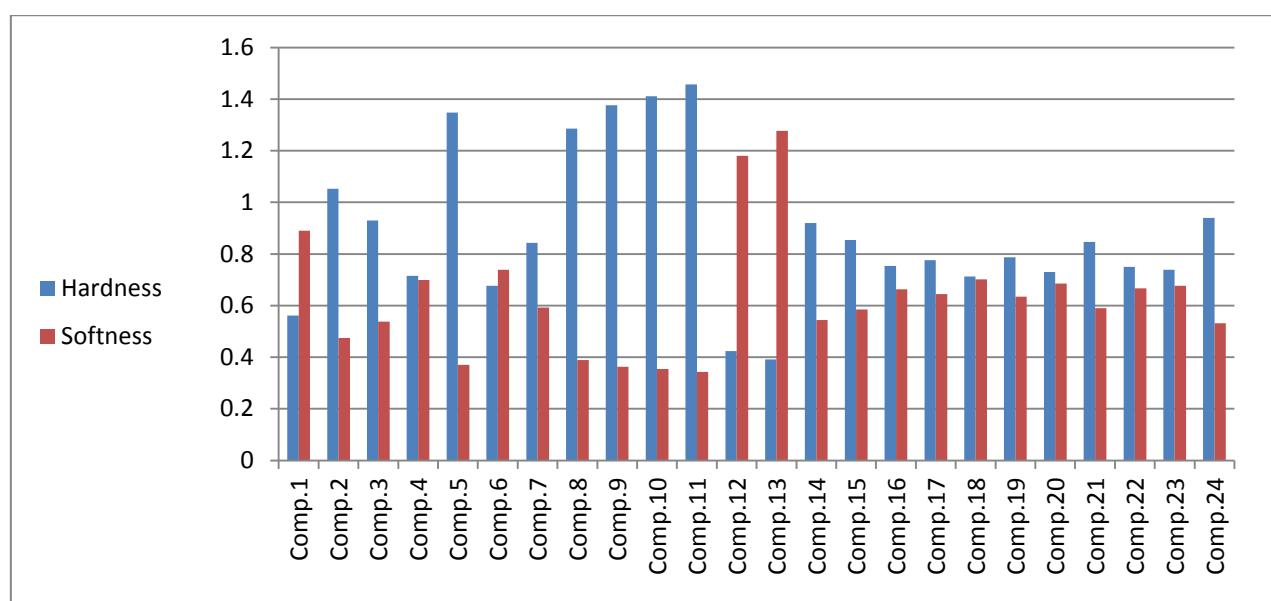
By comparing the present results with previous research and studies, have obtained better results than many previous studies [2].

3.4.2 The Hardness and Softness

Table (3.4): The values of chemical hardness and softness for the studied compounds

Compounds	Hardness(eV)	Softness(eV) ⁻¹
Comp.1	0.561	0.889
Comp.2	1.052	0.474
Comp.3	0.929	0.537
Comp.4	0.715	0.699
Comp.5	1.348	0.370
Comp.6	0.677	0.738
Comp.7	0.843	0.592
Comp.8	1.285	0.388
Comp.9	1.376	0.363
Comp.10	1.411	0.354
Comp.11	1.457	0.343
Comp.12	0.423	1.180
Comp.13	0.391	1.276
Comp.14	0.919	0.543
Comp.15	0.854	0.585
Comp.16	0.753	0.663
Comp.17	0.775	0.644
Comp.18	0.7130	0.701
Comp.19	0.7876	0.634
Comp.20	0.729	0.685
Comp.21	0.847	0.590
Comp.22	0.750	0.666
Comp.23	0.738	0.676
Comp.24	0.939	0.531

Where chemical hardness is defined as **(a measure of the resistance of chemical species to changes in their electronic composition)**. With regard to our study, the electronic change intended here is electronic transitions and how these transitions occur? and within what extent will the absorption spectrum of these transitions be? and it should be noted the fact that the interaction between species the chemically harsh ones are mostly electrostatic, while the soft ones are mostly in between through mixing orbitals[105]. Figure (3.10) shows the chemical hardness and softness of the proposed compounds.



Figure(3.10): The chemical hardness and softness for the studied compounds.

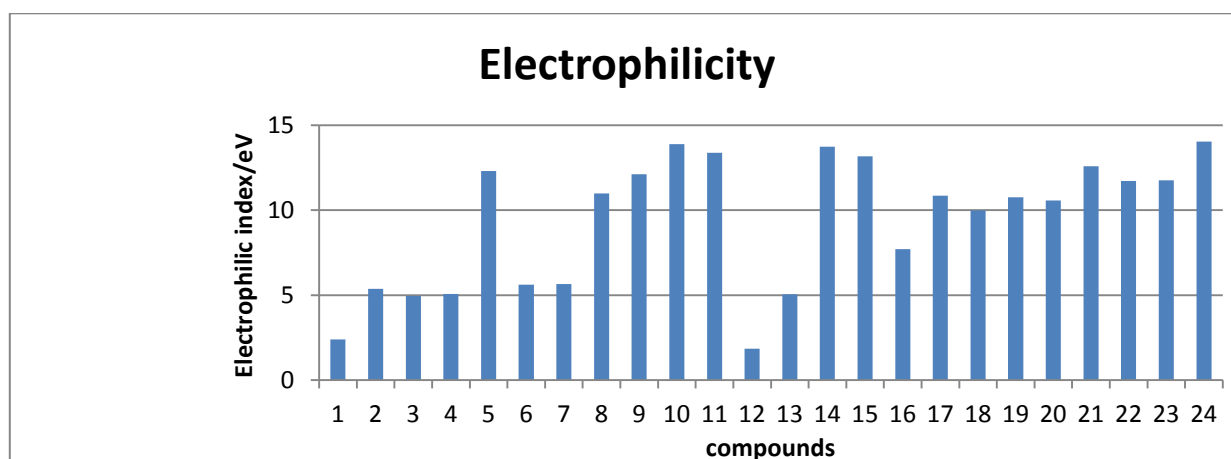
By observing the previous Figure (3.10) and Table(3.4) , it is clear that the compound (BBT) and its sub-groups are more suitable than anthracene and its dependencies in solar cell applications, due to the ease of electronic transitions from the HOMO level to the LUMO level directly or through indirect transitions from the energy levels arising from the addition of the sub-groups that increase the amount of electronic transitions. From Table(3.4), it becomes clear that compound No. (1) is the least hardness compound, meaning that it is the most amenable to changing its electronic structure, while compound No. (11) shows more reluctance to change its electronic structure, meaning that it does not change easily.

Contrary to what was mentioned above, compound No. (11) is the least soft, while compound No. (13) is the softest, meaning that compound (13) is the most studied compounds subject accepting to change of its electronic structure.

As noted, compounds 12 and 13 have the highest value of electronic softness compared to the others, which indicates that these compounds need a small excitation energy for electron transfer. Because a soft compound means it has a small energy gap. on the other hand and in general, approximately the majority of compounds in this study have high index of electrophilicity but the compounds 10 and 24 have the highest, this result refers to that these two compounds have high ability to interact with other surrounding species (molecules or subgroups). Table (3.4) and Figure (3.14) illustrate the electrophilic index of the compounds.

Table (3.4): Electrophilicity of the compounds.

Compounds	Electrophilicity (eV) Of Comp Based on Anthracen	Compounds	Electrophilicity(eV) Of Comp Based on (BBT)
Comp.1	2.395	Comp.13	5.057
Comp.2	5.380	Comp.14	13.742
Comp.3	4.954	Comp.15	13.177
Comp.4	5.066	Comp.16	7.7136
Comp.5	12.298	Comp.17	10.850
Comp.6	5.619	Comp.18	9.993
Comp.7	5.656	Comp.19	10.768
Comp.8	10.984	Comp.20	10.576
Comp.9	12.124	Comp.21	12.585
Comp.10	13.885	Comp.22	11.718
Comp.11	13.375	Comp.23	11.750
Comp.12	1.8436	Comp.24	14.031



Figure(3.11) : The electrophilic index of the studied compounds.

The almost majority of compounds in this study have a high electrophilic index but compounds 10 and 24 have the highest, this result indicates that these two compounds have a high ability to interact with other surrounding species (molecules or subgroups). Table (3.4) and Figure (3.10) show the electrophilic index of the compounds. As we mentioned in the study of the previous characteristics, the benzopisthiadiazole compound has a better electrophilicity index than the anthracene compound due to the fact that the compound (BBT) contains the elements sulfur and nitrogen, which interact with the medium a greater intensity than carbon. It consists only of the compound anthracene.

3.4.3 The Light Harvesting Efficiency (LHE)

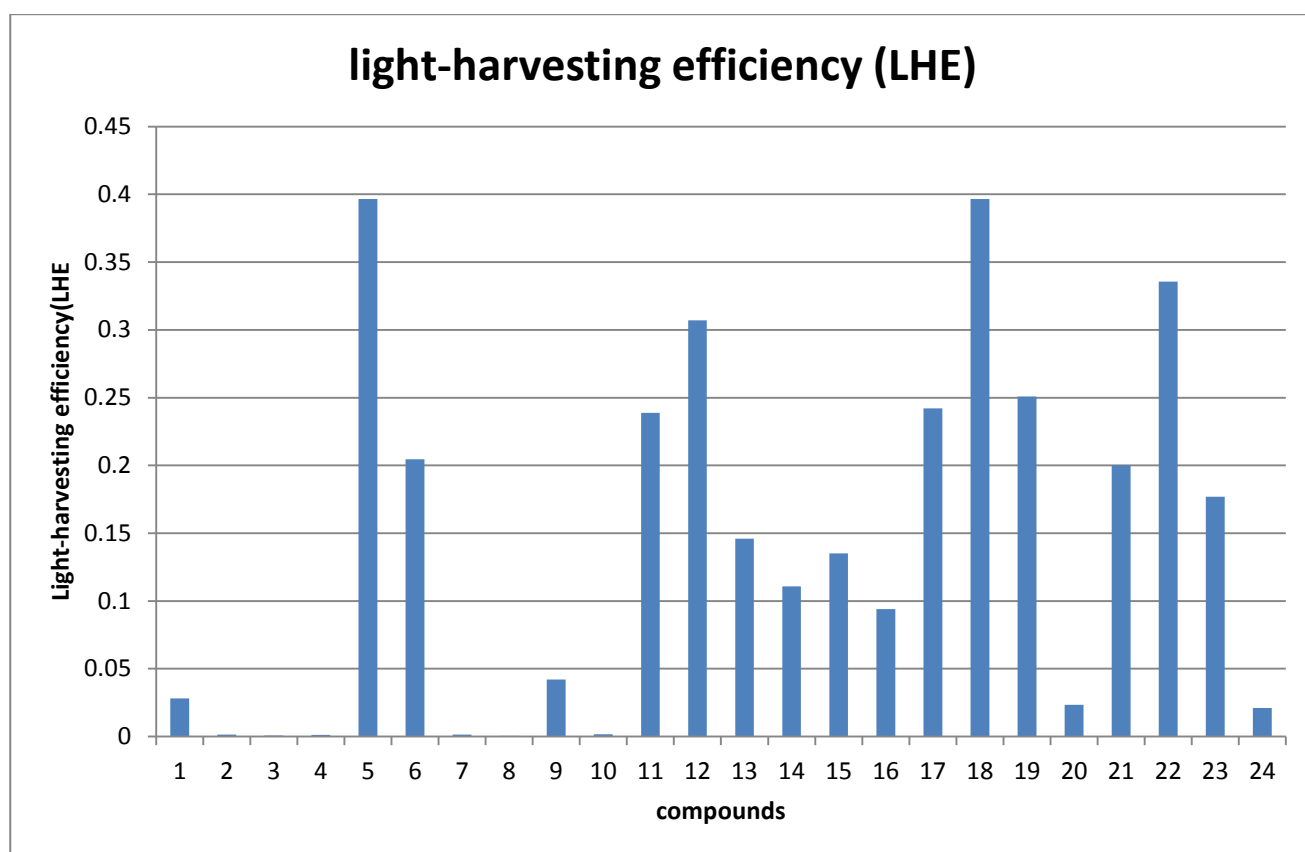
The light harvesting efficiency (LHE) calculation concluded that (BBT) and its subgroups are better than the light harvest obtained when using the anthracene molecule and its subgroups.

Where the nanostructure of the compound (BBT) has the ability to generate an electron-hole pair more than the anthracene compound and because it has high oscillation strength values. Table (3.5) and Figure (3.11) show the light harvesting of the studied compounds. From the results of the LHE values of the compounds, they

recorded different values, and this means that the compounds ,It will give a contrasting light stream .

Table (3.5): Values of light-harvesting efficiency (LHE) for the studied compounds.

Compounds	Oscillation Strength(<i>f</i>) of Comp. Based on Anthracen	Light-Harvesting Efficiency (LHE) of Comp. Based on Anthracen	Compounds	Oscillation Strength(<i>f</i>) of Comp. Based on BBT	Light-Harvesting Efficiency (LHE) of Comp. Based on BBT
Comp.1	0.0124	0.0281	Comp.13	0.0158	0.1459
Comp.2	0.0006	0.0013	Comp.14	0.051	0.1107
Comp.3	0.0003	0.0006	Comp.15	0.0631	0.1352
Comp.4	0.0005	0.0011	Comp.16	0.0429	0.0940
Comp.5	0.0361	0.3966	Comp.17	0.1204	0.2421
Comp.6	0.0415	0.2045	Comp.18	0.0361	0.3966
Comp.7	0.0006	0.0013	Comp.19	0.1254	0.2507
Comp.8	0.0002	0.0004	Comp.20	0.2233	0.0234
Comp.9	0.0187	0.0421	Comp.21	0.0969	0.1999
Comp.10	0.1776	0.0016	Comp.22	0.1776	0.335
Comp.11	0.0565	0.2387	Comp.23	0.0115	0.1769
Comp.12	0.1069	0.3070	Comp.24	0.0565	0.0209



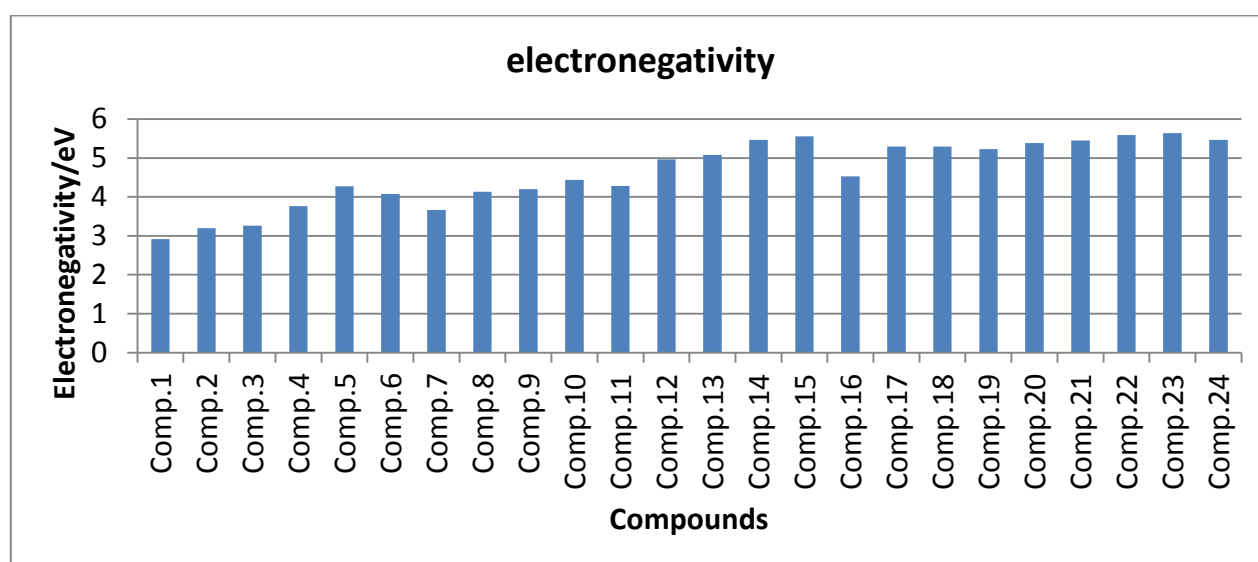
Figure(3.12) : Light-harvesting efficiency (LHE) of the studied compounds.

3.4.4 Electronegativity (En)

As for the electronegativity (En), where Table (3.6) and Figure (3.12) show the electronegativity values of the proposed compounds, where electronegativity is defined as a measure of the tendency to attract electrons by an atom in a chemical bond. The results showed a tendency for benzobethiadiazole (BBT) to possess more electrons than anthracene, due to the difference in the nanostructure of this compound, as it contains in its structure the elements nitrogen and sulfur, which have higher electronegativities than the carbon atom, therefore the whole compound will have the ability to withdraw electrons more than anthracene whose structural structure is limited to carbon only [113], and therefore the compound (BBT) would be more efficient than anthracene in photovoltaic applications in general and solar cells in particular, and the studied compounds.

Table (3.6) : Values of electronegativity for the studied compounds.

Compounds	Electronegativity of Comps. Based on Anthracen	Compounds	Electronegativity of Comps. Based on BBT
Comp.1	2.920	Comp.13	5.082
Comp.2	3.1968	Comp.14	5.466
Comp.3	3.264	Comp.15	5.553
Comp.4	3.764	Comp.16	4.524
Comp.5	4.270	Comp.17	5.289
Comp.6	4.073	Comp.18	5.294
Comp.7	3.661	Comp.19	5.229
Comp.8	4.133	Comp.20	5.383
Comp.9	4.197	Comp.21	5.451
Comp.10	4.435	Comp.22	5.589
Comp.11	4.284	Comp.23	5.640
Comp.12	4.965	Comp.24	5.464

**Figure(3.13) :** Electronegativity of the studied compounds.

3.4.5 Open Circuit Voltage (Voc)

Available data was collected and carefully examined to accurately predict the open circuit voltage (Voc) for each proposed compound to find out the practical benefit of using these compounds in solar cells, the Table (3.7) shows the change in the Voc values of the studied compounds. By applying the special equation and considering that the acceptor compound is TiO₂ and where the LUMO energy level of this compound is 3.9eV[106,107]. The results listed in Table (3.7).

Table (3.7): Shows the open circuit voltage values for the proposed compounds

Compounds	E _{HOMO} (eV) Comp. Based on Anthracen	Voc (eV) Comp. Based on Anthracen	Compounds	E _{HOMO} (eV) Comp. Based on BBT	Voc(eV) Comp. Based on BBT
Comp. 1	-3.482	-0.717	Comp.13	-5.474	1.274
Comp. 2	-4.249	0.049	Comp.14	-6.386	2.186
Comp.3	-4.194	-0.005	Comp.15	-6.408	2.208
Comp.4	-4.479	0.279	Comp.16	-5.278	1.078
Comp.5	-5.619	1.419	Comp.17	-6.065	1.865
Comp.6	-4.751	0.551	Comp.18	-6.007	1.807
Comp.7	-4.505	0.305	Comp.19	-6.016	1.816
Comp.8	-5.419	1.219	Comp.20	-6.113	1.913
Comp.9	-5.573	1.373	Comp.21	-6.298	2.098
Comp.10	-5.847	1.647	Comp.22	-6.339	2.139
Comp.11	-5.741	1.541	Comp.23	-6.378	2.178
Comp.12	-5.389	1.1894	Comp.24	-6.404	2.204

By observing the resulting values in Table(3.7), show that the Voc values depend on the strength of the HOMO of the donor and the LUMO of the acceptor, which indicates that an electron can be injected from the LUMO level into the conduction band of TiO₂, noting some negative values of Voc, which indicate that the electron cannot be injected

when using these indicator compounds, there are negative values for (V_{oc}), since the HOMO TiO_2 energy level for these compounds is higher than the LUMO level of the intended composite. It is noteworthy that the V_{oc} values of the anthracene-based compounds are relatively low compared to (V_{oc}) of the (BBT)-based compounds.

3.4.6 Electronic Injection Process

Electron injection into OSCs is an important parameter to characterize the rate and efficiency of the photoelectron chemical reaction. Figure (3.13) and Table (3.8) show the change in injection energy that occurs as a result of the electron transfer from the valence band to the conduction band as a result of the generation of electron-hole pairs after adding sub-groups to the basic compounds (anthracene and (BBT)), which are considered important factors. Which is useful in predicting the short circuit current density (J_{sc}) [114- 115].

Table (3.8): The Electron Injection Process of Compounds.

Compounds	λ max (nm)	$\Delta E = 1240 / \lambda$ max(eV)	E^*	ΔG
Comp.1	3508.324	0.353	3.128	-0.771 -
Comp.2	807.446	1.535	2.714	-1.185
Comp.3	6827.323	0.181	4.012	0.112
Comp.4	817.778	1.5163	2.963	-0.936
Comp.5	564.539	2.196	3.422	-0.477
Comp.6	1698.169	0.3256	4.020	0.120
Comp.7	3807.868	0.552	4.179	0.279
Comp.8	2243.651	2.236	4.866	0.966

Compounds	λ max (nm)	$\Delta E = 1240 / \lambda$ max(eV)	E*	ΔG
Comp.9	555.367	2.307	3.337	-0.562
Comp.10	537.263	2.455	3.539	-0.360
Comp.11	504.986	1.602	3.286	-0.613
Comp.12	773.831	0.372	3.786	-0.113
Comp.13	3330.222	1.636	5.101	1.201
Comp.14	757.612	1.455	4.749	0.849
Comp.15	851.650	1.245	4.952	1.052
Comp.16	995.210	1.409	4.032	0.132
Comp.17	879.882	2.196	4.656	0.756
Comp.18	564.539	1.422	3.810	-0.089
Comp.19	871.961	1.283	4.594	0.694
Comp.20	965.909	1.520	4.829	0.929
Comp.21	815.470	1.328	4.777	0.877
Comp.22	933.124	0.376	5.010	1.110
Comp.23	757.612	0.376	6.001	2.101
Comp.24	735.942	1.684	4.719	0.819

The results established in the Table (3.8) for the values of (ΔG) if it has a negative value, means that the reaction is giving off energy and is spontaneous. However, when its value is positive, the reaction requires energy to proceed and is non-spontaneous. when the free energy is zero, the reaction is to be equilibrium. [106,108,116].

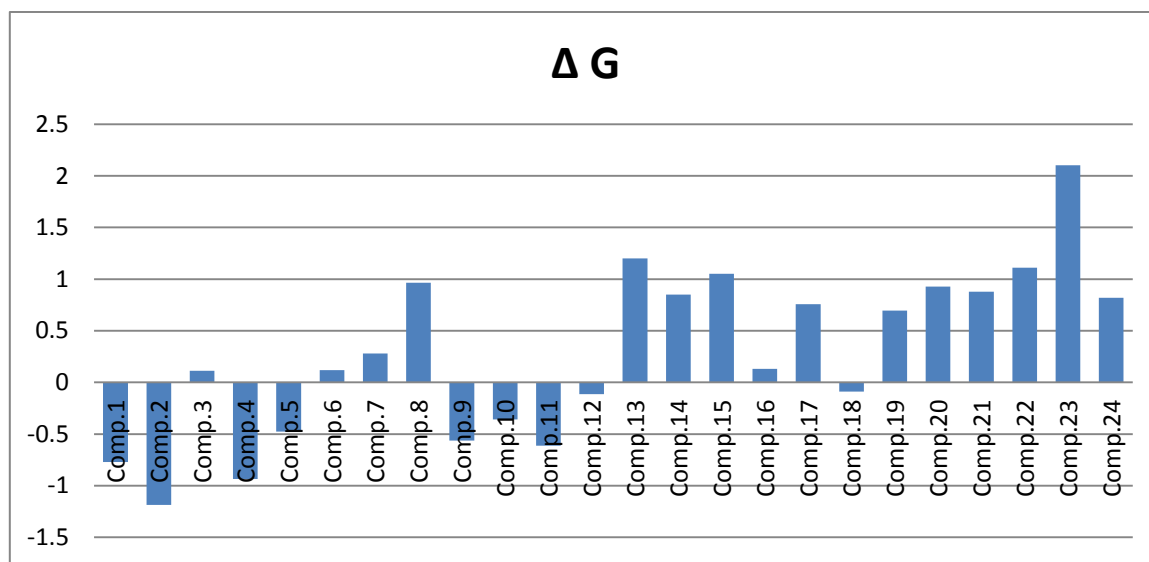
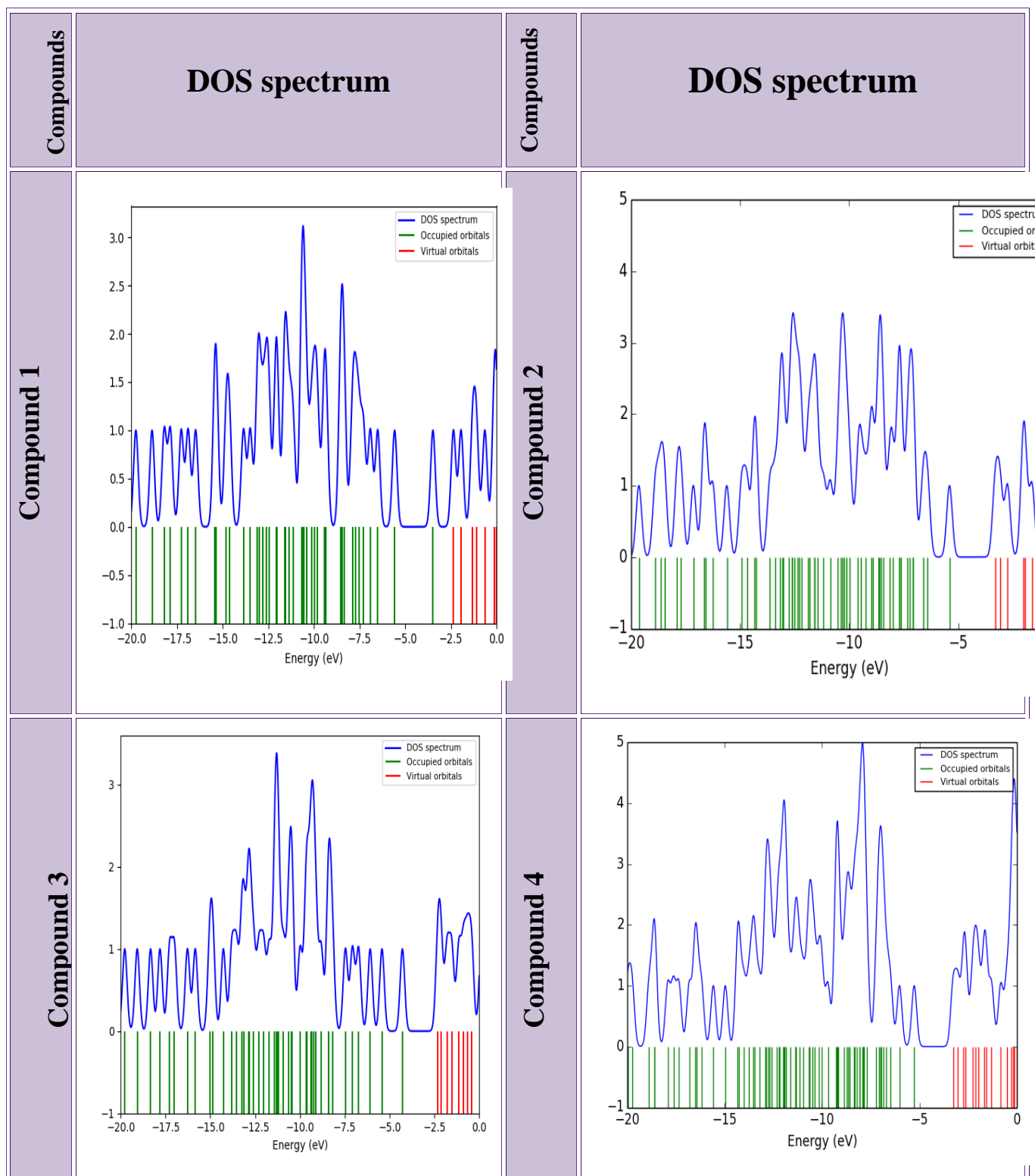


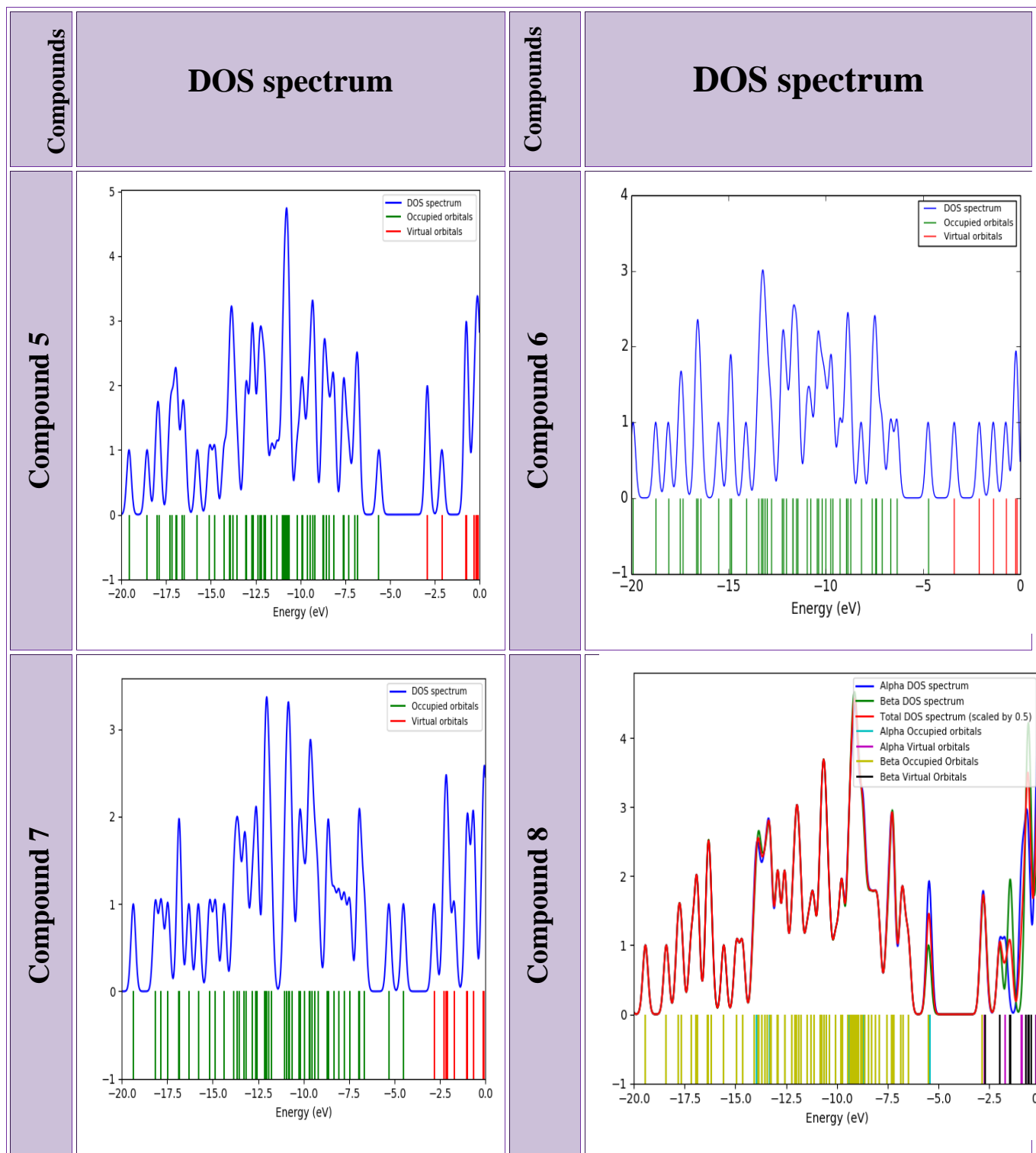
Figure (3.14): Electron Injection of the Compounds.

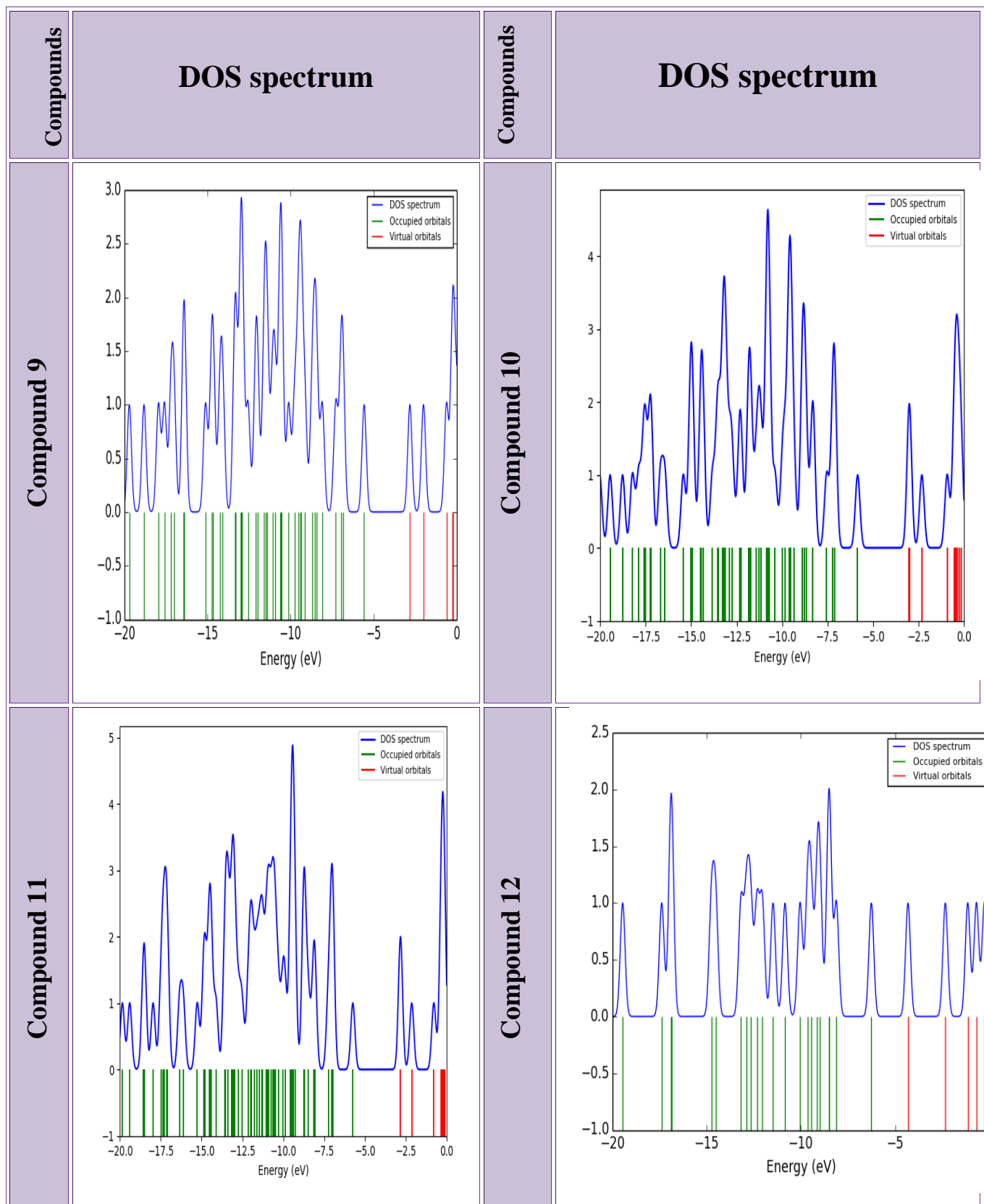
3.4.7 Density of State

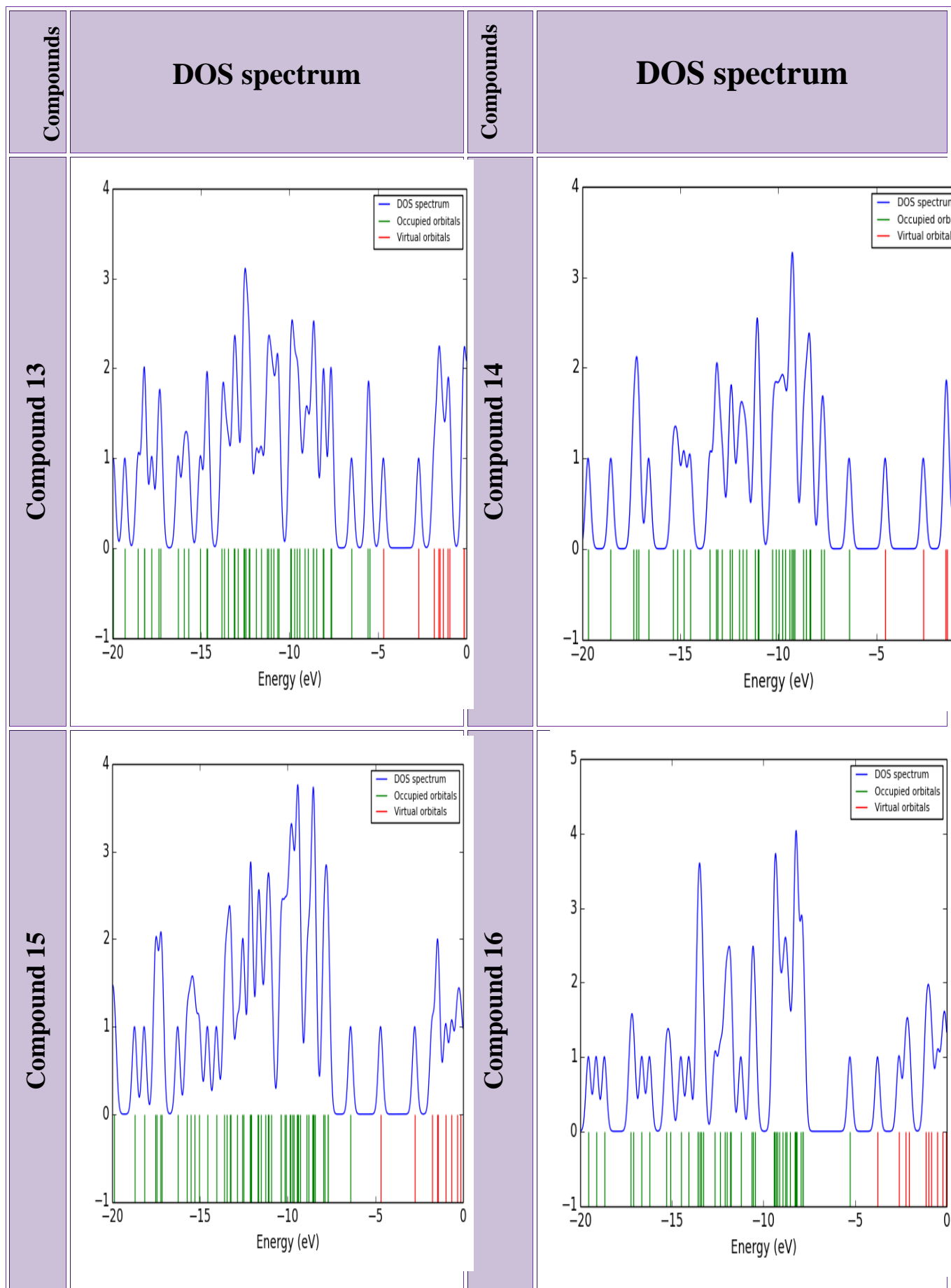
Density of state, DOS governs many physical properties and therefore plays an important role in the electronic properties of compounds. It is important to predict the change of DOS depending on the change of different geometries of the electronic nanostructure. DOS system describes the number of states in each given range of energy at each level available for electronic transitions. The distribution of energy between identical particles depends in part on how these particles are located within a specific energy range. The DOS spectrum of anthracene and (BBT) and its subgroups as a function of Fermi energy was calculated using the TD-DFT function as shown in Figure (3.13). From the DOS spectrum, we can estimate the energy gap for each compound, and according to the linearity, which is the combination of atomic orbitals to form

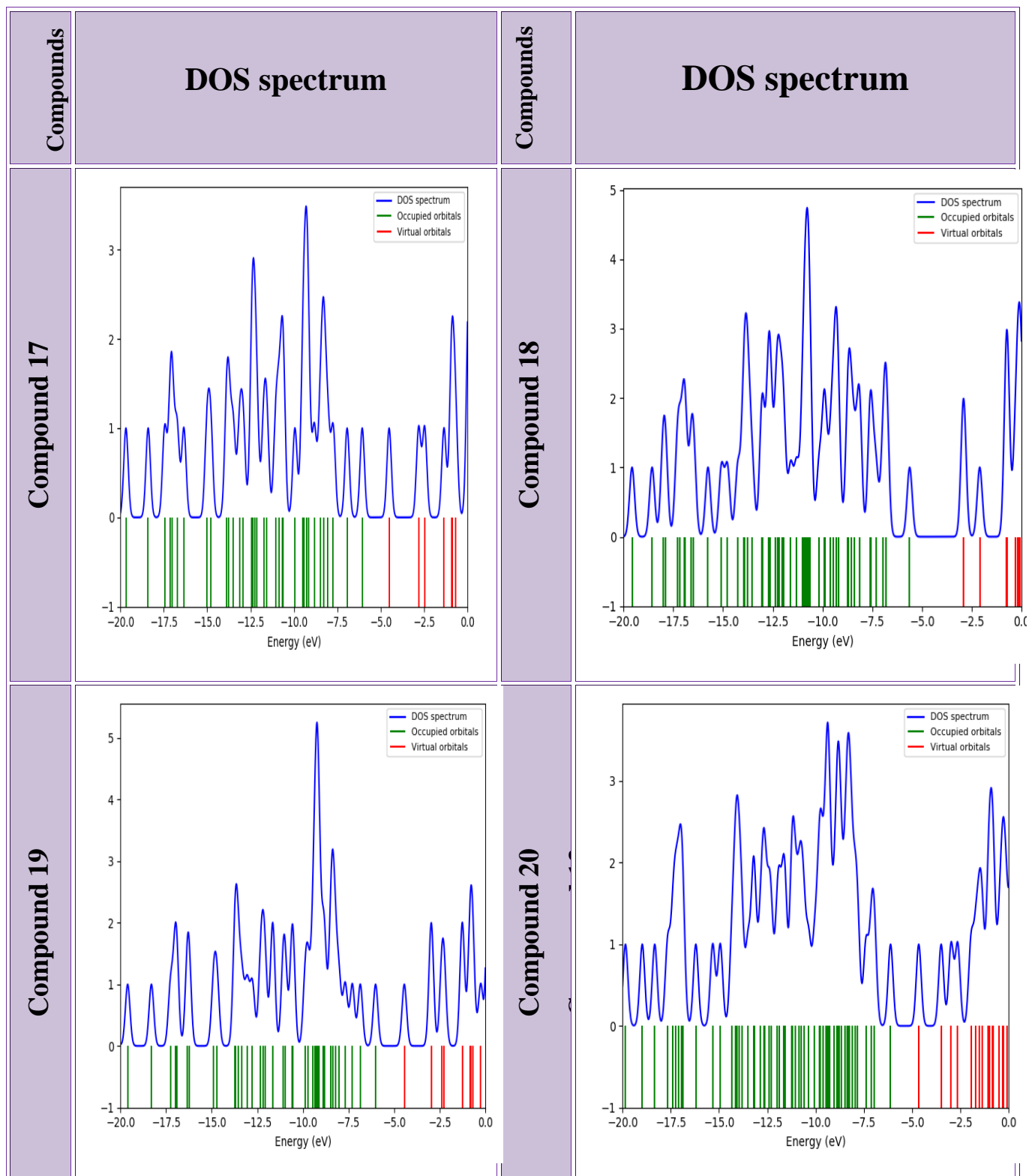
molecular orbitals due to the presence of (O_2 , N, S, TiO_2) atoms, while the pure anthracene orbitals are the result of carbon atoms only [108-110].











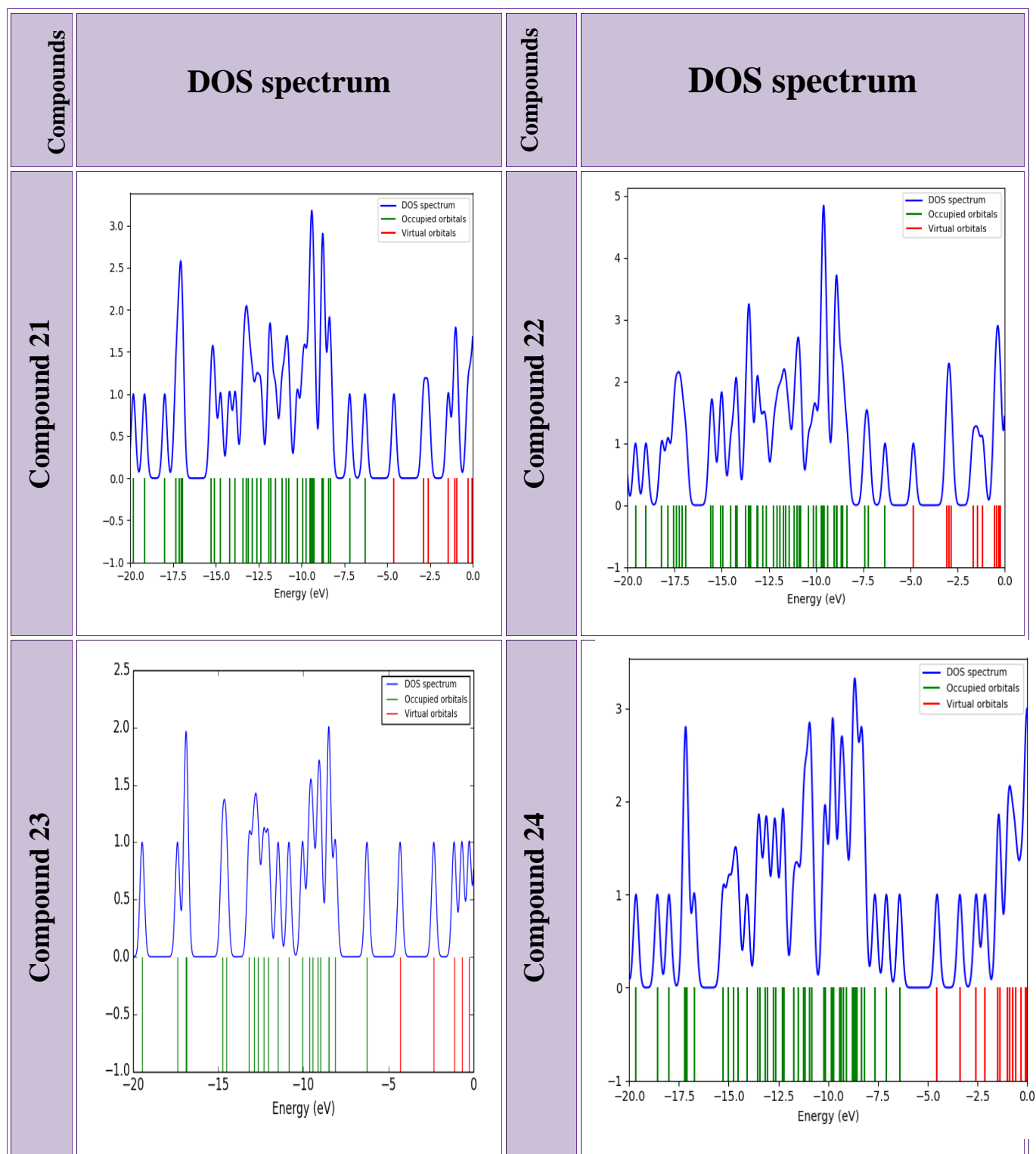


Figure (3.15):Density of state spectrum of the suggested compounds.

As shown, in all compounds shown in the Figure (3.15), the decays of occupied molecular orbitals are larger than the hypothetical molecular orbitals, which indicates HOMO localization and LUMO delocalization and indicates that DOS is distributed in

the conduction band larger than in the valence band. The electron in compounds (4,5,11,18,19,22) can easily shift from valence to conduction band compared to other compounds, for the reason that DOS in conduction band is larger than DOS in valence band. This property enables these compounds to behave in suitable electronic applications when they interact with other molecules or species, and as we mentioned in the previous characteristics, the levels reached by DOS spectrum when using benzobethiadiazole (BBT) were higher than its levels when using anthracene.

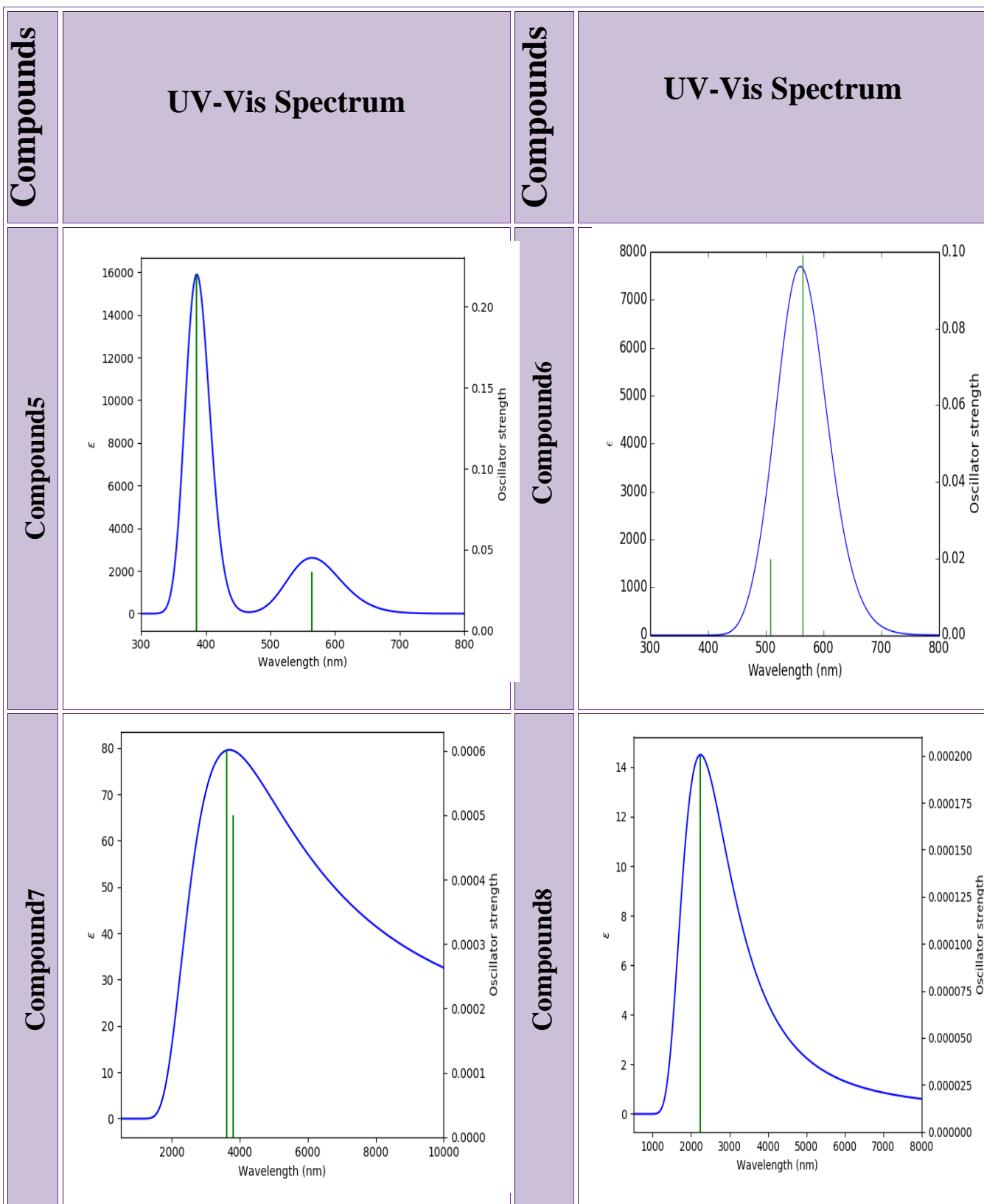
3.4.8 Ultraviolet and Visible Spectrum (UV-Vis)

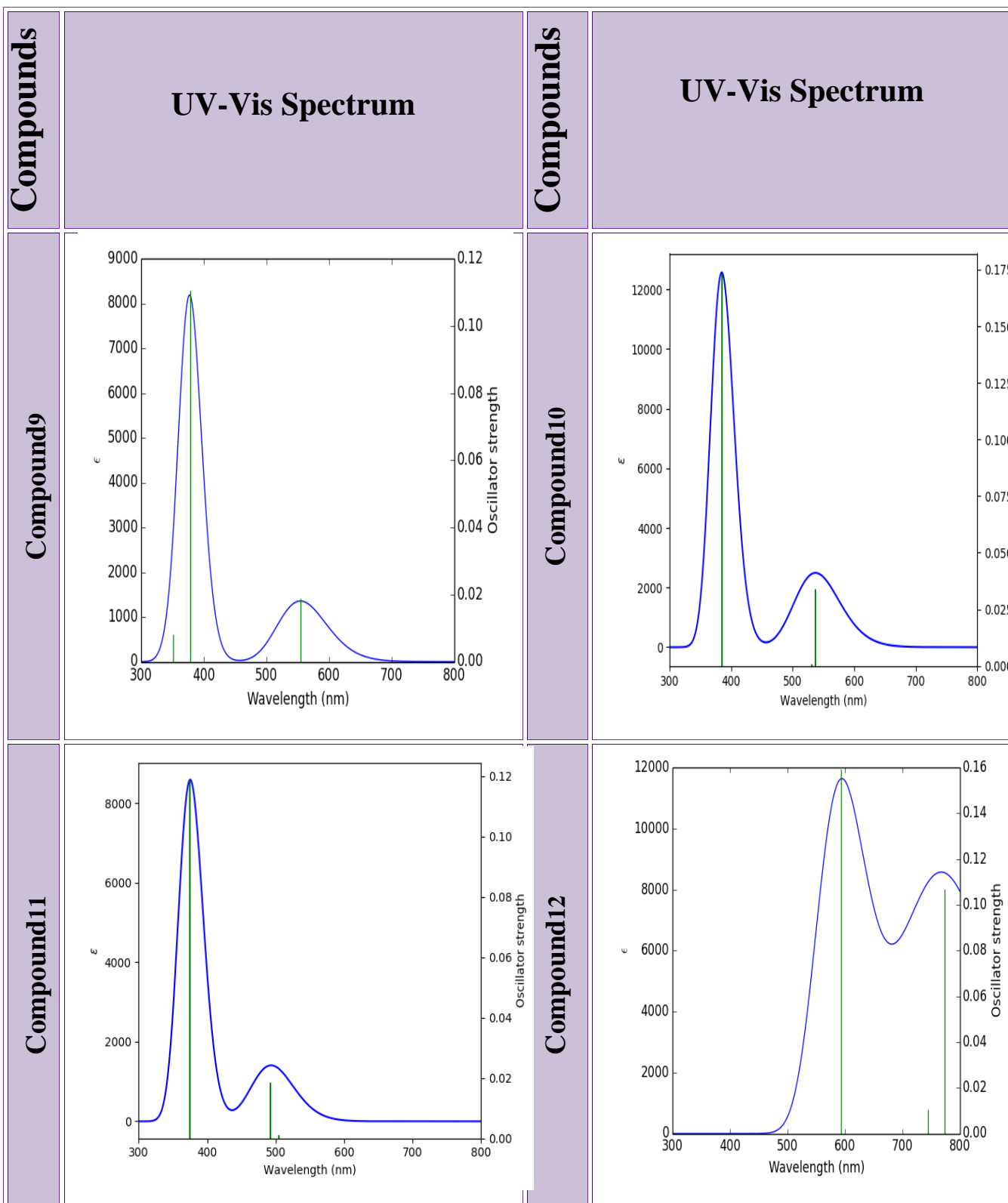
The study of the absorption spectra in general and of the proposed compounds in particular is one of the most important ways through which we learn about the feasibility of using these compounds in photovoltaic applications in general and solar cells in particular, and which compounds have a spectrum within the visible or ultraviolet limits.

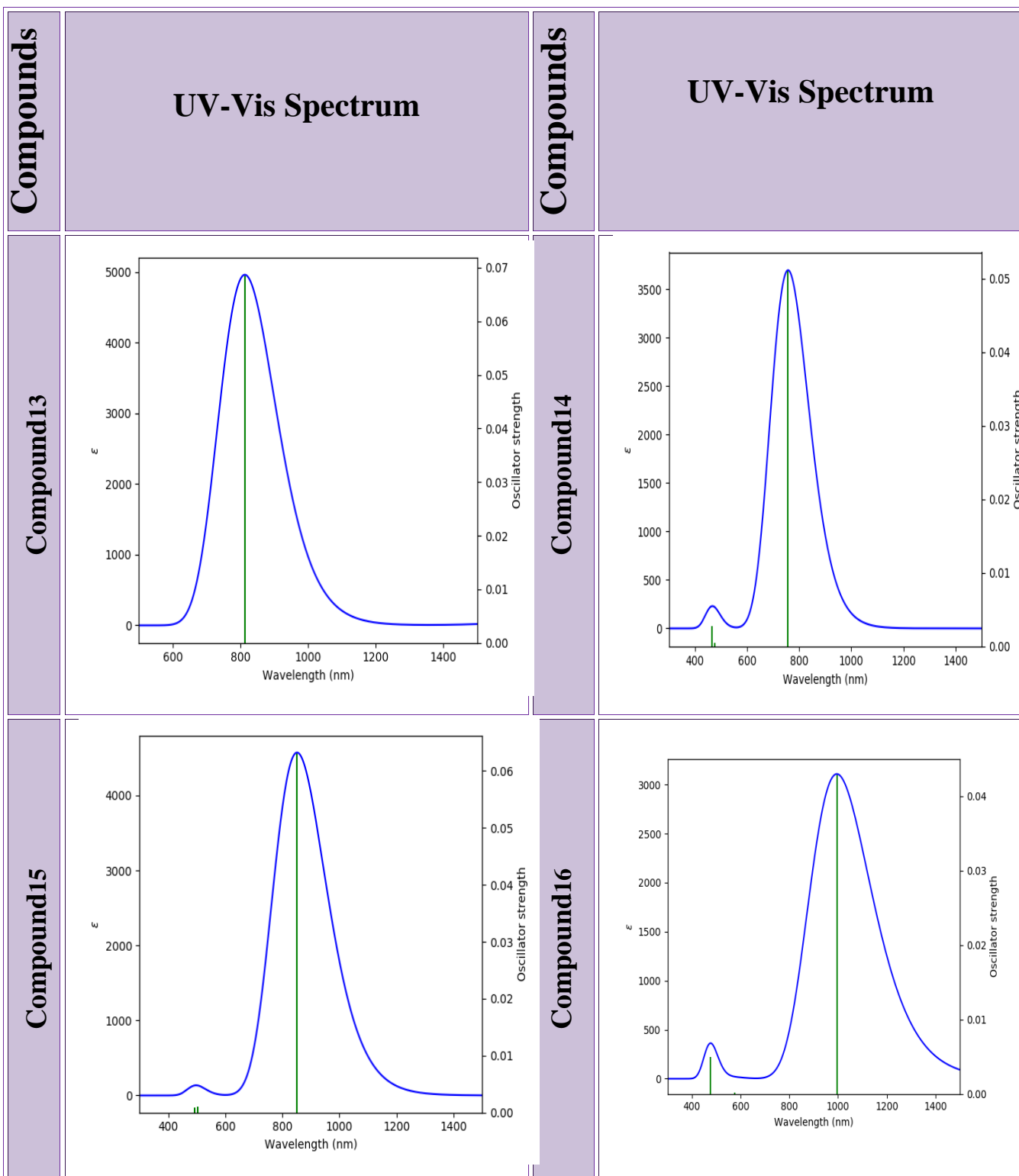
The absorption spectra of these compounds were studied as shown in Figure (3.14) in their excited state, using the density function theory, and choosing the 6-31G basis set, and the hybrid function B3LYP.

We can identify the absorption spectrum of these compounds by knowing the electronic transitions from the valence band to the conduction band. Some compounds have direct transitions, while others have direct and indirect transitions by the action of the associated sub-groups on both sides of the anthracene compound and the compound Benzobisthiadiazole (BBT), where these groups work a sub-levels increase the amount of electronic transitions by creating additional energy levels between the two main levels (HOMO-LUMO), which facilitates the transition process[111]. The Figure (3.16) shows the direct and indirect transfers of the proposed compounds.

Compounds	UV-Vis Spectrum		Compounds
Compound1			Compound2
Compound3			Compound4







Compounds	UV-Vis Spectrum	Compounds	UV-Vis Spectrum
Compound17		Compound18	
Compound19		Compound20	

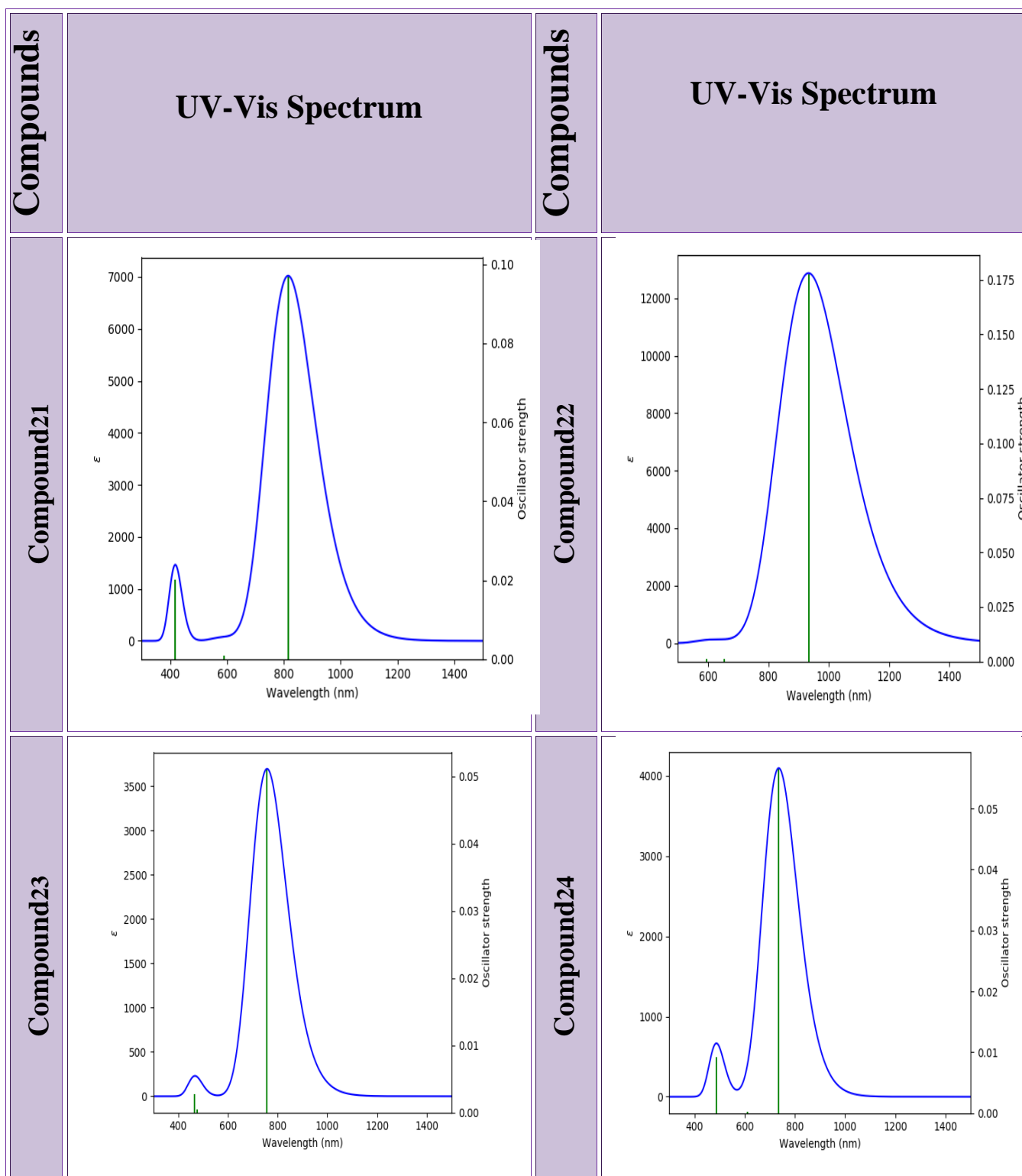


Figure (3.16): UV-Visspectrum of the proposed compounds.

By observing Table (3.9), it is clear that most of the compounds have an absorption spectrum that falls within the visible and ultraviolet (UV-Vis) region, and this spectrum is generated either by direct or indirect electronic transitions, or both,

except for some compounds whose absorption spectrum is located outside this region. It has been observed that compounds No. (1, 7,13) have their absorption spectrum located at wavelengths outside the UV-Vis limits for both direct and indirect transmissions.

Table (3.9) shows the calculated values of E_{abs} absorption energy (eV) It can be obtained through the following equation : $E = hc/\lambda_{\text{max}}$ Where it can be written as follows : $E = 1240/\lambda_{\text{max}}$ [112].

Where the constant (1240) is the net product of the Planck constant ($6.62607015 \times 10^{-34}$ m² kg / s) and the speed of light (299,792458 m / s) divided by the wavelength in units of nanometers and after abbreviating the units and converting the unit of the resulting quantity to electron volts we get this formula .absorption wavelength λ_{max} (nm), oscillator strength Osc, molecular orbital character (MOC) and transition states.

Table (3.9): Wavelength and Osc. and λ_{max} and major and contribs of compounds.

Compounds	Wavelength (nm) λ_{max}	Osc.	$\Delta E, (E_{\text{abs}})$ =1240/ λ_{max}	Major contribs
Comp.1	3508.324	0.0124	0.353	HOMO → LUMO (69%) HOMO->LUMO (17%) HOMO->LUMO (27%)
Comp.2	807.446	0.0006	526.647	HOMO->LUMO (99%) HOMO->L+1 (83%) HOMO->L+1 (17%)
Comp.3	6827.323	0.0003	0.181	HOMO->LUMO (33%) HOMO->L+2 (99%) HOMO->L+4 (98%)
Comp.4	817.778	0.0005	1.516	HOMO->LUMO (99%) HOMO->L+1 (62%) HOMO->L+2 (25%)
Comp.5	564.539	0.0361	2.196	HOMO->LUMO (99%) HOMO->L+1 (100%) HOMO->L+2 (97%)
Comp.6	1698.169	0.0415	0.730	HOMO->LUMO (104%) H-1->LUMO (11%) H-1->LUMO (56%)
Comp.7	3807.868	0.0005	0.325	HOMO->L+1 (105%) HOMO->L+2 (33%) HOMO->L+2 (39%)
Comp.8	2243.651	0.0002 -2.003-A	0.552	HOMO(A)->L+1(A) HOMO(A)->L+4(A) H-1(A)->L+2(A)
Comp.9	555.367	0.0187	2.236	HOMO->LUMO (99%) HOMO->L+1 (98%) H-1->LUMO (96%)

Compounds	Wavelength (nm) λ_{\max}	Osc.	$\Delta E, (E_{\text{abs}})$ $=1240/\lambda_{\max}$	Major contribs
Comp.10	537.2630	0.0337	2.307	HOMO->LUMO (99%) HOMO->L+1 (100%) HOMO->L+2 (98%)
Comp.11	504.986	0.0011	2.455	HOMO->LUMO (64%) HOMO->LUMO (35%) HOMO->L+2 (98%)
Comp.12	773.831	0.1069	1.602	H-1->LUMO (71%) H-1->LUMO (14%) H-2->LUMO (74%)
Comp.13	3330.222	0.0158	0.372	HOMO->LUMO (100%) H-1->LUMO (118%) H-2->LUMO (100%)
Comp.14	757.612	0.051	1.636	HOMO->LUMO (100%) H-2->LUMO (72%) H-2->LUMO (27%)
Comp.15	851.650	0.0631	1.455	HOMO->LUMO (100%) H-4->LUMO (16%) H-3->LUMO (54%)
Comp.16	995.210	0.0429	1.245	HOMO->LUMO (100%) HOMO->L+1 (100%) HOMO->L+3 (91%)
Comp.17	879.882	0.1204	1.409	HOMO->LUMO (100%) H-1->LUMO (98%) H-2->LUMO (62%)
Comp.18	564.539	0.0361	2.196	HOMO->LUMO (99%) HOMO->L+1 (100%) HOMO->L+2 (97%)
Comp.19	871.961	0.1254	1.422	HOMO->LUMO (98%) H-1->LUMO (98%) H-2->LUMO (98%)
Comp.20	965.909	0.2233	1.283	HOMO->LUMO (99%) H-1->LUMO (96%) H-2->LUMO (97%)
Comp.21	815.470	0.0969	1.520	HOMO->LUMO (97%) H-1->LUMO (98%) H-2->LUMO (33%)
Comp.22	933.124	0.1776	1.328	HOMO->LUMO (98%) H-1->LUMO (98%) H-2->LUMO (99%)
Comp.23	757.612	0.051	0.376	HOMO->LUMO (99%) H-2->LUMO (72%) H-2->LUMO (27%)
Comp.24	735.942	0.0565	1.684	HOMO->LUMO (103%) H-1->LUMO (100%) HOMO->L+1 (100%)

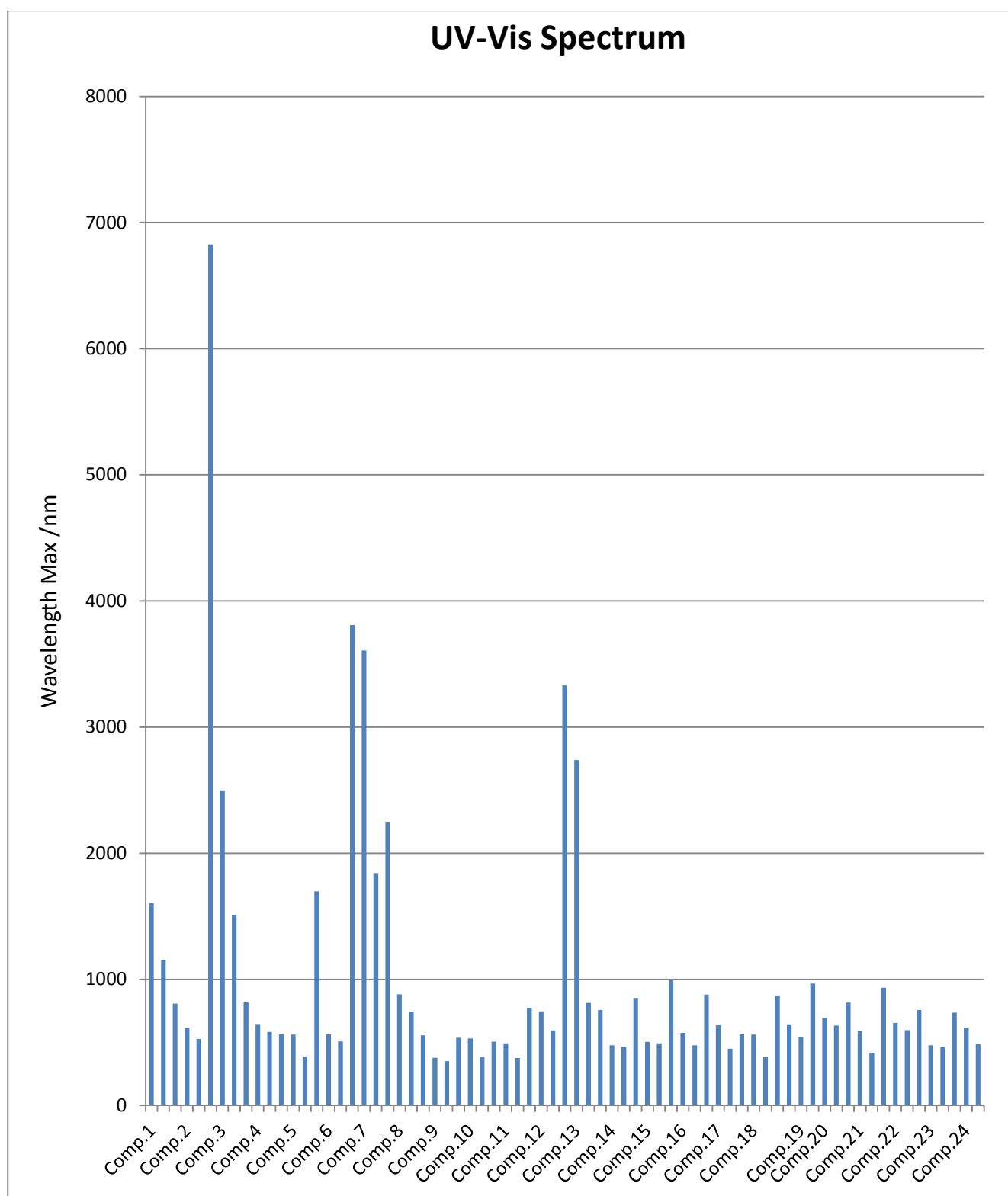


Figure (3.17): The electronic transitions-wavelength max.

Figure (3,14) shows the wavelengths at which most electronic transitions occur between the main HOMO - LUMO levels of the main compounds (anthracene and benzobisthiadiazole) and the implicit levels generated by the addition of subgroups,

which include (sub-energy levels below the HOMO level and levels of energy higher than the LUMO level), through the Figure. (3.17) we notice that most of the electronic transitions occur within the (UV-Vis. Spectrum), by checking the Figure (3.17), notice that most of the transitions that fall within the UV-Vis spectrum. It occurs when using the compound (BBT), but when using the anthracene compound, we notice a large number of transitions that occur outside the UV-Vis region towards the infrared region (IR).

3.4.9 General Comparison :

In this part of the work, a comparison between the electronic and optical properties of the basic compounds that were used with the fixation of the subgroups.

Table (3.10) : General comparison between properties of compounds .

Properties	Anthracene	Benzopisthiadiazole	Results
The geometrical parameters	The majority of angles between atoms are in the range of (115-120) degrees, except for some angles	The majority of angles between atoms are in the range of (115-120) degrees, except for some angles	The geometry of the two compounds is somewhat similar
E. gap	Depending on the difference between the energy of (HOMO and LUMO), the energy gap for anthracene compounds ranges between (0.8 - 2.9) eV.	Depending on the difference between the energy of (HOMO and LUMO), the energy gap for anthracene compounds ranges between (0.7-1.8) eV	(BBT) compounds are better because they require less catalytic energy than the energy needed to catalyze anthracene compounds
Ionization Energy (IE)	IE for anthracene compounds ranges from (3-5) eV	IE for BBT compounds ranging from (5-6)eV	The ionization energy of BBT compounds is greater than that of anthracene compounds
Electron Affinity (EA)	EA for anthracene compounds ranges Between (2-4) eV	EA for BBT ranges Between (3-4)eV	BBT compounds are more inclined to gain electrons than

Properties	Anthracene	Benzopisthiadiazole	Results
			anthracene compounds, so they are more suitable than anthracene compounds in solar cell applications.
Chemical hardness	The hardness of six of the anthracene compounds ranged between (1-1.4) and the remaining six hardnesses ranged between (0.4-0.9)	Hardness of (BBT) compounds ranged between (0.3-0.9)eV	Anthracene compounds do not interact easily with intermediate compounds, as their resistance to change in their structural structure is high
Chemical softness	The reaction rate of anthracene compounds with the medium is relatively low.	The reaction rate of (BBT) compounds is relatively high	(BBT) compounds are softer in their interactions with the medium
Electrophilicity index	Electrophilicity index of anthracene compounds for five compounds out of 12 compounds ranging from (10-13) eV and seven compounds ranging from (1-5) eV	Benzopisthiadiazoles contain nine compounds out of 12 compounds that are between (10-14) eV and three compounds are 5 eV, 7 eV and 9 eV	Benzopisthiadiazoles have an electrophilicity index higher than that of anthracene
light-harvesting efficiency (LHE)	Eight anthracene compounds out of 12 light-harvesting compounds ranged between (0.0006-0.04) and four compounds ranged between (0.2-0.3)	Nine benzopisthiadiazoles ranged between (0.1-0.3) and three compounds ranged between (0.02-0.09).	Light harvest in benzopisthiadiazole compounds is higher than in anthracene compounds
Electronegativity	Anthracene compounds have an electronegativity ranging from (2.9-4.9)	Benzobaisthiadiazoles have an electronegativity in the range (4.5-5.6).	Anthracene compounds have a lower electronegativity than benzobisthiadiazole compounds
	Density of state	Density of state spectrum	Density of State

Properties	Anthracene	Benzopisthiadiazole	Results
Density of State	spectrum in anthracene compounds ranges from (2-5)	in benzopisthiadiazole compounds ranges from (2-5)	spectrum almost identical in the two compounds
UV-Vis Spectrum	The UV-Vis Spectrum of anthracene compounds ranges between the UV-IR regions. There are three compounds that do not have a spectrum within the UV-Vis region, and the other compounds have direct and indirect transmissions, some of which are within the UV-Vis region and others outside this region.	The UV-Vis Spectrum of benzopisthiadiazole compounds extends from the UV region to the IR region, only one compound does not have a spectrum within the UV-Vis region, and the other compounds have direct and indirect electronic transitions, some within UV-Vis and others outside this region	The electronic transitions in the benzobisthiadiazole compound record an absorption spectrum within the UV-Vis region more than the transitions of the anthracene compound.
Open circuit voltage (Voc)	The Voc values of the anthracene-based compounds are relatively low compared to the presence of two compounds (1, 3) where the Voc values were negative.	Voc values for BBT based compounds are relatively high as Voc values were positive for all compounds	The possibility of electron injection in compounds based on (BBT) is greater than compounds based on anthracene, and therefore the first is better than the second in solar cell applications

Chapter Four

Conclusions and Future works

4.1 Conclusions

The electronic and optical properties of anthracene and benzobisthiadiazole (BBT) were studied with the subgroups (1-cyanoacrylic acid (CYN), 2-benzothiadiazole, 3-benzoxadiazole) and the following important points were obtained.:

1- Both anthracene and (BBT) compounds, their molecules are distributed in a three-dimensional space, depending on the length of the single and double bonds between the atoms and the angles formed by these bonds together, which gives each compound its own geometric shape.

2-The energy gap for anthracene compounds ranges between (0.8 - 2.9) eV, while the energy gap for (BBT) compounds ranges between (0.7-1.8) eV, so they are better in solar cell applications because they require less catalytic energy than the energy needed to catalyze anthracene compounds .

3-The ionization energy (IE) of anthracene compounds ranges between (3-5) eV, while that of (BBT) compounds ranges between (5-6) eV this means that (BBT) compounds are more stable than anthracene compounds.

4-The electron affinity (EA) for anthracene compounds ranges between (2-4) eV, while the affinity for (BBT) ranges between (3-4) eV this gives preference to (BBT) over anthracene compounds in solar cell applications.

5-The rate of interaction of anthracene compounds with the medium is relatively low, as the chemical hardness and softness data indicated that (BBT) compounds interact more easily than anthracene compounds, and this gives an impression on the feasibility of using (BBT) compounds in solar cell applications.

6-Electrophilic index for five anthracene compounds out of 12 compounds ranges from (10-13) eV and seven compounds range from (1-5) eV, while nine (BBT) compounds out of 12 compounds have an electrolyte index ranging from (10-14) eV and three compounds are (5) eV, (7) eV and (9) eV. Therefore, (BBT) have a higher electrophilic index than anthracene. they are the best in solar cell applications.

7- The light harvesting efficiency (LHE) of eight anthracene compounds out of 12 compounds ranges between (0.0006-0.04) and four compounds ranged between (0.2-0.3), while nine (BBT) ranged between (0.1-0.3)) and three compounds ranged between (0.02-0.09). From this we conclude that the light harvest in (BBT) compounds is higher than in anthracene compounds.

8- The electronegativity of the anthracene compounds ranged between (2.9-4.9), while the electronegativity of the proposed benzopaisthiadiazole compounds ranged between (4.5-5.6). Therefore, benzobethiadiazoles have a higher electronegativity than anthracene compounds.

9-In all compounds, the degeneracy of the occupied molecular orbitals is greater than that of the virtual molecular orbitals, indicating HOMO localization and LUMO delocalization. This is an indication that DOS has been distributed in the conduction band more than in the valence band.

10 -The visible and ultraviolet spectrum of anthracene compounds ranges between the ultraviolet and infrared regions. There are three anthracene compounds that do not have a spectrum within the UV-Vis region, and they are compounds (1,3,7), and the rest of the compounds have transitions, some within the intended region and others outside it (within the limits of the IR) the absorption spectrum of (BBT) compounds extends from the ultraviolet region to the infrared region, while only one compound does not have a spectrum within the limits of UV-Vis, which is compound No. (13), and the other compounds have direct and indirect transitions. The absorption spectrum of some of them within the visible and ultraviolet rays and some outside this region. From the foregoing, we conclude that the electronic transitions in (BBT) compounds record a greater absorption spectrum within the UV-Vis region than the transitions of anthracene.

11- The values of the open circuit voltage (V_{oc}) indicate the presence of electron transfer between the LUMO level and the conduction band of (TiO_2) (electron injection) for all compounds except compound No. (1), where the negative value of (V_{oc}) indicates the impossibility of electron injection, noting that the (V_{oc}) values for compounds based on the (BBT) compound is higher than that of anthracene-based compounds.

12-The electron injection values range between (-2 and +2), and most of the positive values belong to compounds based on the BBT molecule, which confirms that using this compound in solar cells is better than using anthracene.

4.2 The Future Works:

Based on the results of this Works, recommend conducting the following studies:

- 1- Constructing a chemical structure consisting of (BBT) as a basic compound with cyanoacrylic acid sub-group on one side and (BBT) on the other side.
- 2-Building a chemical structure consisting of (BBT) as a basic compound with the sub-group consisting of cyanoacrylic acid on one side and benzoxadiazoles on the other side.
- 3-Substitution of cyanoacrylic acid with any other acceptor compound such as benzoxazole ($N_2SeC_6H_{18}$) and study of all electronic, mechanical and optical properties.
- 4- Manufacturing a solar cell according to the best chemical composition that has been studied theoretically to know its efficiency.

References:

- [1] CHEN, C. Julian. " *Physics of solar energy*". John Wiley & Sons, 2011.
- [2] Enam Abbas S. AL-saadiy " *Electronic Structure for Dye Sensitized Organic of Solar Cells*"MSc. thesis, College of Science, University of Babylon, (2018).
- [3] Kirchartz, T. Rau, U. " *What makes a good solar cell?* ". *Advanced Energy Materials*, 8(28), 1703385.(2018).
- [4] Alharbi, F. H. Rashkeev, S. N. El-Mellouhi, F. Lüthi, H. P. Tabet, N. & Kais, S. " *An efficient descriptor model for designing materials for solar cells*". *npjComputationalMaterials*, 1(1), 1-9,(2015).
- [5] Vozel,K. " *Solar Cells*", University of Ljubljana Faculty of Mathematics and Physics,(2011).
- [6] Ranabhat, Patrikeev, K.L. Antal'evna-Revina, A. Andrianov, K. Lapshinsky, V.and Sofronova, E, **An introduction to solar cell technology**. *Journal of Applied Engineering Science*, 14(4), 481-491,(2016).
- [7] Tarsang, R., Promarak, V. Sudyoadsuk, T. Namuangruk, S. Kungwan, N. Khongpracha, P. and Jungsuttiwong, S," *Triple bond-modified anthracene sensitizers for dye-sensitized solar cells: a computational study*" . *RSC Advances*, 5(48), 38130-38140,(2015).
- [8] EFSA Panel on Food Additives and Nutrient Sources added to Food (ANS), Younes, M., Aggett, P., Aguilar, F., Crebelli, R., Filipič, M., ... and Wright, M, " *Safety of hydroxyanthracene derivatives for use in food*". *EFSA Journal*, 16(1), e05090,(2018).
- [9] Wu, T. Y., and Li, J. L,Electrochemical synthesis, optical, "*electrochemical and electrochromic characterizations of indene*" and 1, 2, 5-thiadiazole-based poly (2, 5-dithienylpyrrole) derivatives. *RSC advances*, 6(19), 15988-15998, . (2016).
- [10] Li, W., Guo, Y., Shi, J., Yu, H., and Meng, H, " *Solution-processable neutral green electrochromic polymer containing thieno [3, 2-b] thiophene derivative as unconventional donor units*". *Macromolecules*, 49(19), 7211-7219, (2016).

- [11] Pang, Y., Tao, Y., Zhang, C., and Cheng, H, " *Fast switching soluble electrochromic polymers obtained from a 4, 9-Dihydro-s-indaceno [1, 2-b: 5, 6-b'] dithiophene-embedded system*". *Synthetic Metals*, 242, 29-36,(2018).
- [12] Çelikkilek, Ö., İçli-Özkut, M., Algi, F., Önal, A. M., and Cihaner, A, Donor–acceptor polymer electrochromes with cyan color: " *Effect of alkyl chain length on doping processes*". *Organic Electronics*, 13(1), 206-213,(2012).
- [13] Arkadiusz Matwijczuk , Andrzej Górecki, Marcin Makowski, Katarzyna Pustuła, Alicja Skrzypek, Joanna Waś, Andrzej Niewiadomy, " *Spectroscopic and Theoretical Studies of Fluorescence Effects in 2-Methylamino-5-(2,4-dihydroxyphenyl)-1,3,4-thiadiazole Induced by Molecular Aggregation*" , *Journal of Fluorescence*, 28, 65-77,(2018).
- [14] Kayes, B. M. Atwater, H. A., & Lewis, N. S, " *Comparison of the device physics principles of planar and radial p-n junction nanorod solar cells*". *Journal of applied physics*, 97(11), 114302, (2005).
- [15] Kitai, A', " *Principles of Solar Cells*", *LEDs and Diodes: The role of the PN junction*. John Wiley & Sons, 2011.
- [16] Jampana, B. R., Melton, A. G., Jamil, M., Faleev, N. N., Opila, R. L., Ferguson, I. T., and Honsberg, C. B, Design and Realization of Wide-Band-Gap (~ 2.67 eV) InGaN pn " *Junction Solar Cell*". *IEEE Electron Device Letters*, 31(1), 32-34, 2009.
- [17] Carlson, D. E., and Wronski, C. R, " *Amorphous silicon solar cell*". *Applied Physics Letters*, 28(11), 671-673,(1976).

- [18] Sharma, S., Jain, K. K., and Sharma, A, "**Solar cells: in research and applications—a review**". *Materials Sciences and Applications*, 6(12), 1145, (2015).
- [19] Benanti, T. L., and Venkataraman, D, Organic solar cells: "**An overview focusing on active layer morphology**". *Photosynthesis research*, 87, 73-81, (2006).
- [20] Daram, B., Al-Rawi, K. R., and Al-Shaikh Hussin, S, "**Improve the performance efficiency of solar cell by using epoxy plates doped with Rhodamine 6G dye**". *Indian Journal of Science and Technology*, 4(12), 1726-1731, (2011).
- [21] Myrvold, W. C, "**What is a wavefunction?**". *Synthese*, 192(10), 3247-3274, (2015).
- [22] Taghreed Najah Jamil "**Improvement Solar Cells Efficiency By Using Organic Dye Concentrator**", MSc. thesis, Faculty of Science, University of Kufa, (2023).
- [23] Nielsen, C. B., Holliday, S., Chen, H. Y., Cryer, S. J., & McCulloch, "**Non-fullerene electron acceptors for use in organic solar cells**". *Accounts of chemical research*, 48(11), 2803-2812, I. (2015).
- [24] Zhao, J., Li, Y., Yang, G., Jiang, K., Lin, H., Ade, H., ... and Yan, Efficient organic solar cells processed from hydrocarbon solvents. *Nature Energy*, 1(2), 1-7, H. (2016).
- [25] Zhao, W., Li, S., Yao, H., Zhang, S., Zhang, Y., Yang, B., and Hou, "**Molecular optimization enables over 13% efficiency in organic solar cells**". *Journal of the American Chemical Society*, 139(21), 7148-7151, J. (2017).
- [26] Li, W., Ye, L., Li, S., Yao, H., Ade, H., and Hou, J, "**A highefficiency organic solar cell enabled by the strong intramolecular electron push–pull effect of the nonfullerene acceptor**". *Advanced Materials*, 30(16), 1707170, (2018).
- [27] Delgado-Montiel, T., Baldenebro-López, J., Soto-Rojo, R., and Glossman-Mitnik, D, "**Theoretical study of the effect of π -bridge on optical and electronic properties of carbazole-based sensitizers for DSSCs**". *Molecules*, 25(16), 3670, (2020).

- [28] Bhatnagar, A., Singh, A. R., Amrit, A., Saxena, A., and Singh, H. R, "*Study on some aspects of solar photo voltaic thermal storage: A review*". *Materials Today: Proceedings*, 47, 3198-320, (2021).
- [29] Wang, T., Hao, X., Han, L., Li, Y., Ye, Q., & Cui, Y, DA- π -"*A carbazole dyes bearing fluorenone acceptor for dye sensitized solar cells*". *Journal of Molecular Structure*, 1226, 129367, (2021).
- [30] Noor Abdul Ameer Hameed H., "*Study of the Solar Cell Systems Constructed by Carbon Nanotube and Organic Dyes Using First Principle Calculations*", MSc thesis, College of Science, University of Babylon,(2022).
- [31] Sun, R., Wang, T., Fan, Q., Wu, M., Yang, X., Wu, X., ... and Min, 18.2%-"*efficient ternary all-polymer organic solar cells with improved stability enabled by a chlorinated guest polymer acceptor*". *Joule*, 7(1), 221-237, J. (2023).
- [33] Tuckerman, M, "*Statistical mechanics: theory and molecular simulation*". Oxford university press, (2010).
- [34] Schwabl, F, "*Quantum mechanics*". Springer Science and Business Media,(2007).
- [35] Busch, P., Heinonen, T., and Lahti, P, "*Heisenberg's uncertainty principle*". *Physics reports*, 452(6), 155-176,(2007).
- [36] Fitts, D. D, "*Principles of quantum mechanics: as applied to chemistry and chemical physics*". Cambridge University Press,(1999).
- [37] Lepage, G. P, "*How to renormalize the Schrodinger equation*". *Nuclear Physics (ed. by CA Bertulani et al.)*, 135,(1997).
- [38] Blohm, J. D, "*Thermally-induced chemical transformations and self-assembly of short peptides on metal surfaces*" (Doctoral dissertation, University of Warwick),(2020).
- [39] Rabinowitz, P. H. "*On a class of nonlinear Schrödinger equations*". *Zeitschrift Angewandte Mathematik und Physik*, 43(2), 270-291, (1992).

- [40] Fibich, G, " *The nonlinear Schrödinger equation: singular solutions and optical collapse* "(Vol. 192). Springer,(2015).
- [41] Sharma, H., Wang, Z., & Kramer, B, "*Hamiltonian operator inference: Physics-preserving learning of reduced-order models for canonical Hamiltonian systems*". *Physica D: Nonlinear Phenomena*, 431, 133122, (2022).
- [42]Choukroun, Y., Shtern, A., Bronstein, A., & Kimmel, R, "*Hamiltonian operator for spectral shape analysis*". *IEEE transactions on visualization and computer graphics*, 26(2), 1320-1331,(2018).
- [43] Myrvold, W. C, "*What is a wavefunction?* ". *Synthese*, 192(10), 3247-3274, (2015).
- [44] Libisch, F., Huang, C., & Carter, E. A, "*Embedded correlated wavefunction schemes: Theory and applications*". *Accounts of chemical research*, 47(9), 2768-2775,(2014).
- [45] Valeev, E. F., & Sherrill, C. D, "*The diagonal Born–Oppenheimer correction beyond the Hartree–Fock approximation*". *The Journal of chemical physics*, 118(9), 3921-392, (2003).
- [46] Hanna, C. B., Laughlin, R. B., & Fetter, A. L, "*Quantum mechanics of the fractional-statistics gas: Hartree-Fock approximation*". *Physical Review B*, 40(13), 8745,(1989).
- [47] Epperlein, F., Schreiber, M., & Vojta, T, " *Quantum Coulomb glass within a Hartree-Fock approximation.* " *Physical Review B*, 56(10), 5890,(1997).
- [48] Schulze, H. J., Lejeune, A., Cugnon, J., Baldo, M., & Lombardo, U, " *Hypernuclear matter in the Brueckner-Hartree-Fock approximation*". *Physics Letters B*, 355(1-2), 21-26 , (1995).
- [49]Zakutayev A, Woods-Robinson R, Han Y, Zhang H, Khan I, Persson K and Ablekim T , "*Wide band gap chalcogenide semiconductors*"*Chemical Reviews***120**, (2020).

- [50] M. H. N. Assadi and D. A. H. Hanaor, "*Theoretical study on copper's energetics and magnetism in TiO₂ polymorphs*", Journal of Applied Physics, 113, 23, 1-13,(2013).
- [51] PetersilkaM., U. J. Gossmann, and E. K. U. Gross, "*Excitation Energies from Time-Dependent Density-Functional Theory*", Physical Review Letters, 76, 8, 1212-1215,(1996).
- [52]PetersilkaM., U. J. Gossmann, and E. K. U. Gross, "*Excitation Energies from Time-Dependent Density-Functional Theory*", Physical Review Letters, 76, 8, 1212-1215,(1996).
- [53] FiolhaisC., F. Nogueira and M. Marques, "*A Primer in Density Functional Theory*", Springer-Verlag Berlin Heidelberg New York,(2003).
- [54] MarquesA. L. M., C. A. Ullrich, F. Nogueira, A. Rubio and K. B. K.U. Eberhard, "*Time-Dependent Density Functional Theory*", Springer, Berlin Heidelberg,(2006).
- [55] Botti,S. "*Applications of Time-Dependent Density Functional Theory*", PhysicaScripta, T109, 54-60,(2004).
- [56] Fiolhais,C. F. Nogueira and M. Marques, "*A Primer in Density Functional Theory*", Springer-Verlag Berlin Heidelberg New York,(2003).
- [57] SamalP., "*Studies in Excited-State Density-Functional Theory*", Ph.D. Thesis, Indian Institute of Technology, India,(2006).
- [58] Ullrich,Y. Li and C. A. "*Time-dependent V-representability on lattice systems*", The Journal of Chemical Physics, 129, 1-9,(2008).
- [59] Gerber and I. C. J. G. Angyan, "*Hybrid functional with separated range*", Chemical Physics Letters, 415, 100-105,(2005).
- [60] JonesR. O., "*Density functional theory: Its origins, rise to prominence, and future*", Reviews of Modern Physics, 87, 897-923, 2015.

- [61] Sahni V., "*Quantal Density Functional Theory II: Approximation Methods and Applications*", Springer Verlag, Berlin Heidelberg, (2010).
- [62] Stephens P. J., F. J. Devlin, C. F. Chabalowski and M. J. Frisch, "*Ab Initio Calculation of Vibrational Absorption and Circular Dichroism Spectra Using Density Functional Force Fields*", The Journal of Physical Chemistry, 98, 43, 11624-11627, (1994).
- [63] Szabo A. and N. S. Ostlund, "*Modern quantum chemistry: Introduction to advanced electronic structure theory*", Dover Publication, Inc. Mineola, New York, (1997).
- [64] Silver D. M., "*Energy Internals Involving Both Slater-Type and Gaussian Atomic Orbitals*", Journal De Physique, 32, 129-133, (1971).
- [65] Young D. C., "*Computational Chemistry: A Practical Guide for Applying Techniques to Real-World Problems*", NY: John Wiley & Sons, Inc., New York, (2001).
- [66] Bach, R. D. G. J. Wolber and H. B. Schlege, "*The Origin of the Barriers to Thermally Allowed, Six-Electron, Pericyclic Reactions: The Effect of HOMO-HOMO Interactions on the Trimerization of Acetylene*", Journal American Chemical Society, 107, 10, 2838-2841, (1985).
- [67] Rogers D. W., "*Computational Chemistry Using the PC*", Third Edition, John Wiley and Sons, Inc., Hoboken, New Jersey, (2003).
- [68] Buendia E., F. J. Galvez and A. Sarsa, "*Hartree-Fock Wave Functions with a Modified GTO Basis for Atoms*", International Journal of Quantum Chemistry, 65, 1, 59-64, (1997).
- [69] Wang Y., "*Theoretical Studies on Water Splitting Using Transition Metal Complexes*", Ph.D. Thesis, Royal Institute of Technology Stockholm, Sweden, (2014).

- [70] Fitts D. D., *"Principles of Quantum Mechanics as Applied to Chemistry and Chemical Physics"*, Published by Cambridge University Press, New York, 2002.
- [71] Godbout N., D. R. Salahub, J. Andzelm and E. Wimme, *"Optimization of Gaussian-type basis sets for local spin density functional calculations. Part I. Boron through neon, optimization technique and validation"*, Journal of Chemistry and Physics, 70, 561-571, (1992).
- [72] Koch W. and M. C. Holthausen, *"A Chemist's Guide to Density Functional Theory"*, Second Edition, Wiley-VCH Verlag GmbH, Weinheim, (2001).
- [73] Mueller M., *"Fundamentals of Quantum Chemistry: Molecular Spectroscopy and Modern Electronic Structure Computations"*, Kluwer Academic/Plenum Publishers, New York, (2001).
- [74] Jensen F., *"Introduction to Computational Chemistry"*, Second Edition, John Wiley & Sons, Ltd, Denmark, (2007).
- [75] Tsipis C. A., *"DFT flavor of coordination chemistry"*, Coordination Chemistry Reviews, 272, 1-29, (2014).
- [76] Nagarajan V. and R. Chandiramouli, *"Quantum Chemical Studies on ZrN Nanostructures"*, International Journal of Chem. Tech. Research, 6, 1, 21-30, (2014).
- [77] Zhuo L. G., W. Liao and Z. X. Yu, *"A Frontier Molecular Orbital Theory Approach to Understanding the Mayr Equation and to Quantifying Nucleophilicity and Electrophilicity by Using HOMO and LUMO Energies"*, Asian Journal of Organic Chemistry, 1, 336-345, (2012).
- [78] Zarkadoula E. N., S. Sharma, J. K. Dewhurst, E. K. U. Gross and N. N. Lathiotakis, *"Ionization potentials and electron affinities from reduced-density-matrix functional theory"*, Physical Review A, 85, 1-7, (2012).
- [79] Zhan C., J. A. Nichols and D. A. Dixon, *"Ionization Potential, Electron Affinity, Electronegativity, Hardness, and Electron Excitation Energy: Molecular*

- Properties from Density Functional Theory Orbital Energies*", Journal Physical and Chemistry A, 107, 4184-4195,(2003).
- [80] Hinchliffe A., "*Molecular Modelling*", John Wiley & Sons Ltd, England, (2003).
- [81] York D. M. and W. Yang, "A *chemical potential equalization method for molecular simulations*", The Journal of Chemical Physics, 4, 1, 159-172, 1996.
- [82] Pearson R. G., "*Chemical hardness and density functional theory*", Journal Chemical Sciences, 117, 5, 369-377,(2005).
- [83] Reyes R. V. and A. Aria, "*Evaluation of group electronegativities and hardness (softness) of group 14 elements and containing functional groups through density functional theory and correlation with NMR spectra data*", Journal Ecl. Quim., Sao Paulo, 33, 3, 69-76, (2008).
- [84] A. Aizman, R. Contreras and P. Perez, "*Relationship between local electrophilicity and rate coefficients for the hydrolysis of carbenium ions*", Journal Am. Chem. Soc., 125, 1-7,(2003).
- [85] R. V.Reyes and A. Aria, "*Evaluation of group electronegativities and hardness (softness) of group 14 elements and containing functional groups through density functional theory and correlation with NMR spectra data*", Journal Ecl. Quim., Sao Paulo, 33, 3, 69-76,(2008).
- [86] R. Parthasarathi, J. Padmanabhan, U. Sarkar, B. Maiti, V. Subramanian and P. K. Chattaraj, "*Toxicity Analysis of Benzidine Through Chemical Reactivity and Selectivity Profiles: A DFT Approach*", Internet Electronic Journal of Molecular Design, 2, 12, 798-813,(2003).
- [87] J.Prashanth, G. Ramesh, J. L. Naik, J. K. Ojha, B. V Reddy and G. R.Rao, "*Molecular Structure, Vibrational Analysis and First Order Hyperpolarizability of 4-Methyl-3-Nitrobenzoic Acid Using Density Functional Theory*", Optics and Photonics Journal, 5, 91-107,(2015).

- [88] A. Hinchliffe, "*Molecular Modelling*", John Wiley & Sons Ltd, England, (2003).
- [89] Yang W. and Robert G. Parr, "*Chemistry Hardness, softness, and the Fukui function in the electronic theory of metals and catalysis*", Vol. 82, P. 6723-6726, October (1985) .
- [90] Schuchardt K L, Didier B T, Elsethagen T, Sun L, Gurumoorthi V, Chase J, Li J and Windus T L , "*Basis set exchange: a community database for computational sciences*", Journal of chemical information and modeling **47** 1045–52,(2007).
- [91] Lee, M. H, "*Identifying correlation between the open-circuit voltage and the frontier orbital energies of non-fullerene organic solar cells based on interpretable machine-learning approaches*", *Solar Energy*, **234**, 360-367. (2022).
- [92] Elumalai, N. K., & Uddin, A. "*Open circuit voltage of organic solar cells*", an in-depth review. *Energy & Environmental Science*, **9**(2), 391-410, (2016).
- [93] Katoh, R., & Furube, A, " *Electron injection efficiency in dye-sensitized solar cells. Journal of Photochemistry and Photobiology*" *C: Photochemistry Reviews*, **20**, 1-16,(2014).
- [94] Portillo-Cortez K and Martínez , "*Different anchoring ligands for Ru complexes dyes and the effect on the performance of ZnO-based Dye-Sensitized Solar Cell*"(DSSC): A computational study *Computational and Theoretical Chemistry* **1209** 113627, A(2022).
- [95] Abdulzahra]R. A. "*Density Functional Theory Calculations of donor- σ -bridge - acceptor Molecules*", (2013).
- [96] ourdarJ. L. and D. S. Chemla, "*Hyperpolarizabilities of the nitroanilines and their relations to the excited state dipole moment*" *J. Chem. Phys.*, **66**, 2664, (1977).

- [97] Erickson C B, Ankenman B E and Sanchez S M , "*Comparison of Gaussian process modeling software*" *European Journal of Operational Research* **266** 179–92,(2018).
- [98] Patterson, M. A., & Rao, GPOPS-II: A MATLAB, "*software for solving multiple-phase optimal control problems using hp-adaptive Gaussian quadrature collocation methods and sparse nonlinear programming*". *ACM Transactions on Mathematical Software (TOMS)*, *41*(1), 1-37, A. V. (2014).
- [99] M. J. Frisch, G. W. Trucks, H. B. Schlegel, G. E. Scuseria, M. A. Robb, J. R. Cheeseman, G. Scalmani, V. Barone, B. Mennucci, G. A. Petersson, H. Nakatsuji, M. Caricato, X. Li, H. P. Hratchian, A. F. Izmaylov, J. Bloino, G. Zheng, J. L. Sonnenberg, M. Hada, M. Ehara, K. Toyota, R. Fukuda, J. Hasegawa, M. Ishida, T. Nakajima, Y. Honda, O. Kitao, H. Nakai, T. Vreven, J. A. Montgomery, Jr., J. E. Peralta, F. Ogliaro, M. Bearpark, J. J. Heyd, E. Brothers, K. N. Kudin, V. N. Staroverov, R. Kobayashi, J. Normand, K. Raghavachari, A. Rendell, J. C. Burant, S. S. Iyengar, J. Tomasi, M. Cossi, N. Rega, J. M. Millam, M. Klene, J. E. Knox, J. B. Cross, V. Bakken, C. Adamo, J. Jaramillo, R. Gomperts, R. E. Stratmann, O. Yazyev, A. J. Austin, R. Cammi, C. Pomelli, J. W. Ochterski, R. L. Martin, K. Morokuma, V. G. Zakrzewski, G. A. Voth, P. Salvador, J. J. Dannenberg, S. Dapprich, A. D. Daniels, O. Farkas, J. B. Foresman, J. V. Ortiz, J. Cioslowski and D. J. Fox, "*Gaussian 09, revision A. 02 Gaussian, Inc*", Wallingford CT. (2009).
- [100] Pacheco, A. B. "*Electronic Structure Calculations in Quantum Chemistry*", HPC Training Louisiana State University, (2011).
- [101] Kinney, W. M. "*Python for Data Analysis*", O'Reilly Media, Inc. United States of America, (2013).
- [102] Hanwell, M. D., Curtis, D. E., Lonie, D. C., Vandermeersch, T., Zurek, E., and Hutchison, G. R. "*Avogadro: an advanced semantic chemical editor*", visualization, and analysis platform. *Journal of cheminformatics*, *4*(1), 1-17. (2012).

- [103] Williams, T., & Kelley, GNU PLOT: An Interactive Plotting Program, Version 3.7 organized by: David Denholm. *R. Alfieri et al. / "Parameter Estimation for Cell Cycle Ordinary Differential Equation Models"*, 101, C. (1998).
- [104] Pauling, L. "*The nature of the chemical bond*". II. The one-electron bond and the three-electron bond. *Journal of the American Chemical Society*, 53(9), 3225-3237, (1931).
- [105] Bouachrine, M. A. Echchary, S. M. Bouzzine, M. Amine, M. Hamidi, A. Amine and T. Zair, "*Oligothiophenes bridged by silicon groups, DFT study of structural and electronic properties*", *Phys. Chem. News*, 58, 61-66, (2011).
- [106] Constantin, L. A., Snyder, J. C., Perdew, J. P., & Burke, K. Communication: "*Ionization potentials in the limit of large atomic number*". *The Journal of chemical physics*, 133(24), 241103. (2010).
- [107] كتاب الكيمياء العامة (نظري – مسائل محلولة). محي الدين البكوش – نوري بسيسو – ياسر حورية – نبيل شيخ قروش، الطبعة الثانية (2003م) / شركة الجا للنشر العلمي – طرابلس.
- [108] Makov, G. "*Chemical hardness in density functional theory*". *The Journal of Physical Chemistry*, 99(23), 9337-9339. (1995).
- [109] Vanin, M. "*Electronic and chemical properties of graphene-based structures: A density functional theory study*" Kgs. Lyngby, Denmark: Technical University of Denmark (DTU), (2011).
- [110] Mazhir, S. N., Abbood, H. I., & Abdulridha, H. A. "*Electron Transport in Graphene-B/P compound Heterojunction Using LDA/SZ*". *International Journal of Advanced Engineering Research and Science*, 3(6), 236762. (2016).
- [111] Andrew S. Leathers, David A. Micha, Dmitri S. Kilin, "*Direct and indirect electron transfer at a semiconductor surface with an adsorbate : Theory and*

- application to Ag₃Si(111)*" ,the Journal of Chemical Physics , Reserch Article , March 16.(2010).
- [112]Galen L. Eakins, Matthew W. Cooper, Nikolay N. Gerasimchuk, Terry J. Phillips, Bryan E. Breyfogle, and Chad J. Stearman , "***Structural influences impacting the role of the 9-ylidene bond in the electronic tuning of structures built upon 9-fluorenylidene scaffolds***",Article in Canadian Journal of Chemistry · November,(2013).
- [113]Liu, X., Fan, X., Wang, L., Sun, J., Wei, Q., Zhou, Y., & Huang, W. "***Competitive adsorption between sulfur-and nitrogen-containing compounds over NiMoS nanocluster: The correlations of electronegativity, morphology and molecular orbital with adsorption strength***". *Chemical Engineering Science*, 231, 116313.(2021).
- [114]Manzoor, T., Niaz, S., & Pandith, A. H. "***Exploring the effect of different coumarin donors on the optical and photovoltaic properties of azobridged pushpull systems: A theoretical approach***". *International Journal of Quantum Chemistry*, 119(18), e25979. (2019).
- [115] Mehmood, U., Hussein, I. A., Harrabi, K., & Ahmed, S. "***Density functional theory study on the electronic structures of oxadiazole based dyes as photosensitizer for dye sensitized solar cells***" , *Advances in Materials Science and Engineering*,(2015).
- [116] Islam, A., Sugihara, H., & Arakawa, H. " ***Molecular design of ruthenium (II) polypyridyl photosensitizers for efficient nanocrystalline TiO₂ solar cells***", *Journal of Photochemistry and Photobiology A: Chemistry*, 158(2-3), 131.(2003).

الخلاصة:

تتعامل دراستنا الحالية مع التراكيب النانوية (24) مركباً كيميائياً مقترحاً استخدامها في التطبيقات الكهروضوئية. تتكون الدراسة من جزئين يعتمدان على نفس مبدأ العمل، الجزء الأول يتعامل مع (11) مركب يقوم على أساس جزيء الانثراسين، و الجزء الثاني يتعامل مع (13) مركب يقوم على أساس جزيء البنزوبايزثياديازول (BBT)، مع مركبات فرعية مكون من ثلاثة مركبات (مركب واحد مستقبل و مركبين مانحين لغرض إنشاء مستويات طاقة بين نطاقي التكافؤ و التوصيل للمركبين الرئيسيين لتسهيل الانتقالات الالكترونية .

من خلال هذا العمل قمنا بفحص الخصائص البصرية والالكترونية للمركبات الناتجة وقد حصلنا على نتائج افضل من بعض الدراسات السابقة .

تم بناء المركبات ابتداءً باستخدام برنامج (Gauss View 5.0.8) ثم تم تطبيق الدالة الهجينة B3LYP من نظرية دالية الكثافة DFT مع دوال الأساس (6-31G) في حزمة (Gaussian) لدراسة و تحليل خصائص الحالة الأرضية للمركبات المقترحة، و من ثم تم استخدام برنامج (Gauss Sum) بعد استخدام نظرية دالية الكثافة المعتمدة على الزمن (TD-DFT) لمعرفة خصائص الحالة المثارة و أطيف الامتصاص للمركبات قيد الدراسة.

باستخدام برنامج (Gauss View 5.0.8) تم حساب أطوال الأواصر بين الذرات و الزوايا بين الأواصر ومنها تمت معرفة الشكل الهندسي لكل مركب .

بواسطة نظرية (DFT) تم حساب فجوة الطاقة لكل مركب وذلك من معرفة فرق الطاقة بين (LUMO - HOMO) وقد حصلنا على فجوة طاقة صغيرة نسبياً تتفق مع الدراسات السابقة .

أيضا من الحسابات المهمة التي حصلنا عليها من دراسة الحالة المستقرة هو حساب التقارب الالكتروني و كذلك الصلابة و النعومة الكيميائية و كذلك مؤشر الالكتروفليك وان كل هذه الخصائص تعتمد على معرفة مستوى طاقة (HOMO و LUMO) وقد تم الحصول على أدنى فجوة طاقة في المركبين 12 و 13 حيث اعتمد المركبان المذكوران على جزيء بنزوبايزثياديازول (BBT) بينما كانت اقل فجوة طاقة للمركبات التي تعتمد على جزيء الانثراسين ، إن هذه النتائج أفضل من العديد من الدراسات السابقة .

وباستخدام نظرية دالية الكثافة المعتمدة على الزمن (TD-DFT) و برنامج (Gauss Sum) تمت دراسة أطيف الامتصاص لكل مركب و تم تحديد الانتقالات الالكترونية حيث كان لكل مركب انتقالات مباشرة وغير مباشرة وحدث كل انتقال عند طول موجي محدد ، ومن معرفة الطول الموجي هذا تمكنا من حساب عملية الحقن الالكتروني و الحصاد الضوئي لكل مركب من خلال دراسة خصائص الحالة المثيجة .



جمهورية العراق
وزارة التعليم العالي
والبحث العلمي
جامعة بابل
كلية العلوم
قسم الفيزياء

التحقيق في بعض الصبغات العضوية لتطبيقات الخلايا الشمسية
رسالة مقدمة إلى قسم الفيزياء / كلية العلوم كجزء من متطلبات نيل درجة الماجستير
علوم في الفيزياء

من قبل

صادق عباس صبح فيحان

بكالوريوس علوم فيزياء 2007

بإشراف

أ.م.د. نضال محمد عبيد الشريف
أ.م.د. محسن كاظم عبد الخيكاني

1445 هـ

2023 م